Astro/Phys 224 Spring 2012

Origin and Evolution of the Universe

Week 6

Galaxy Formation

Joel Primack

University of California, Santa Cruz

GRAVITY – The Ultimate Capitalist Principle

Astronomers say that a region of the universe with more matter is "richer." Gravity magnifies differences—if one region is slightly denser than average, it will expand slightly more slowly and grow relatively denser than its surroundings, while regions with less than average density will become increasingly less dense. The rich always get richer, and the poor poorer.

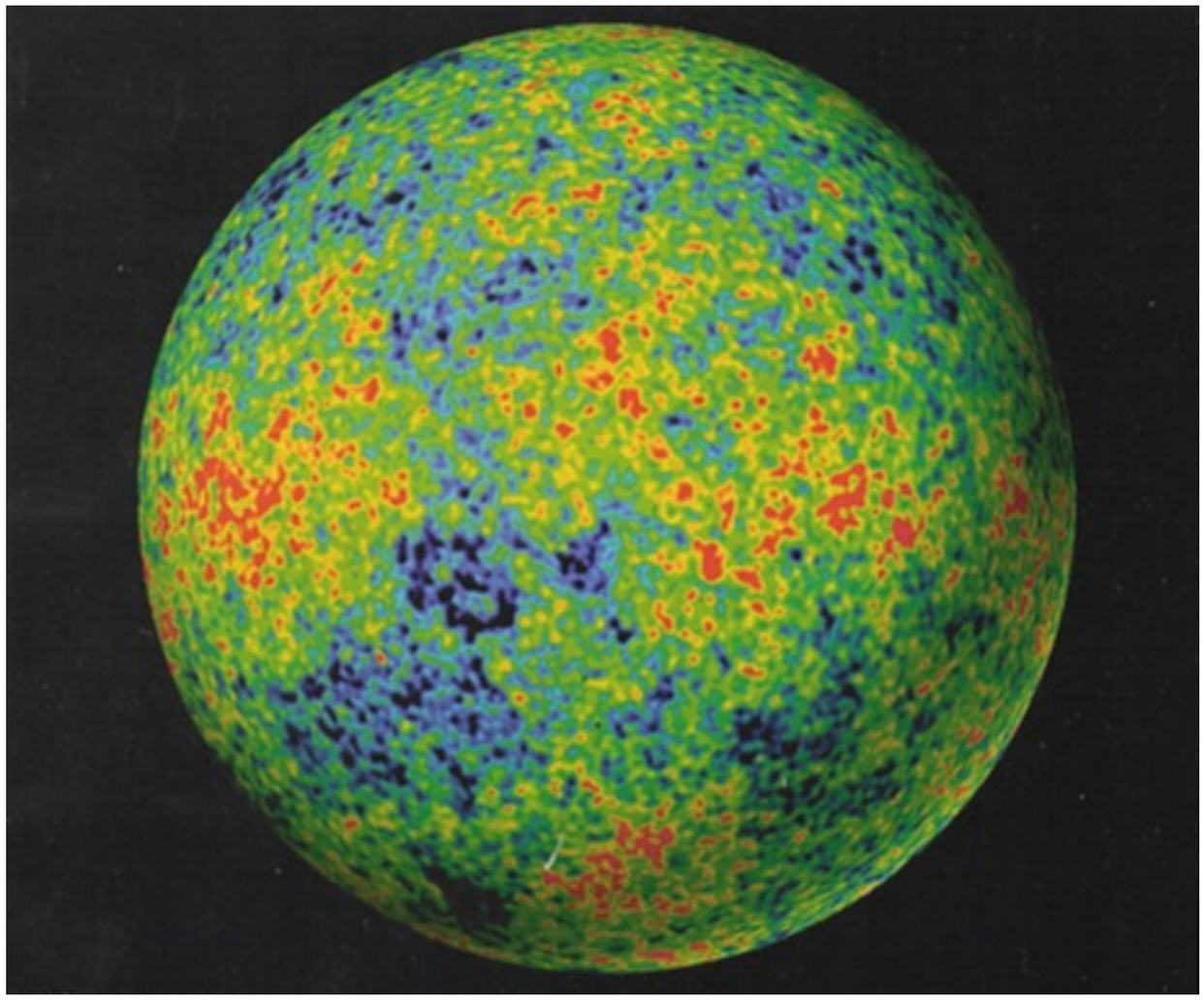

Temperature map at 380,000 years after the Big Bang. **Blue** (cooler) regions are slightly denser. From NASA's **WMAP** satellite, 2003.

The early universe expands ***almost*** perfectly uniformly. But there are small differences in density from place to place (about 30 parts per million). Because of gravity, denser regions expand more slowly, less dense regions more rapidly. Thus gravity amplifies the contrast between them, until…

Structure Formation by Gravitational Collapse

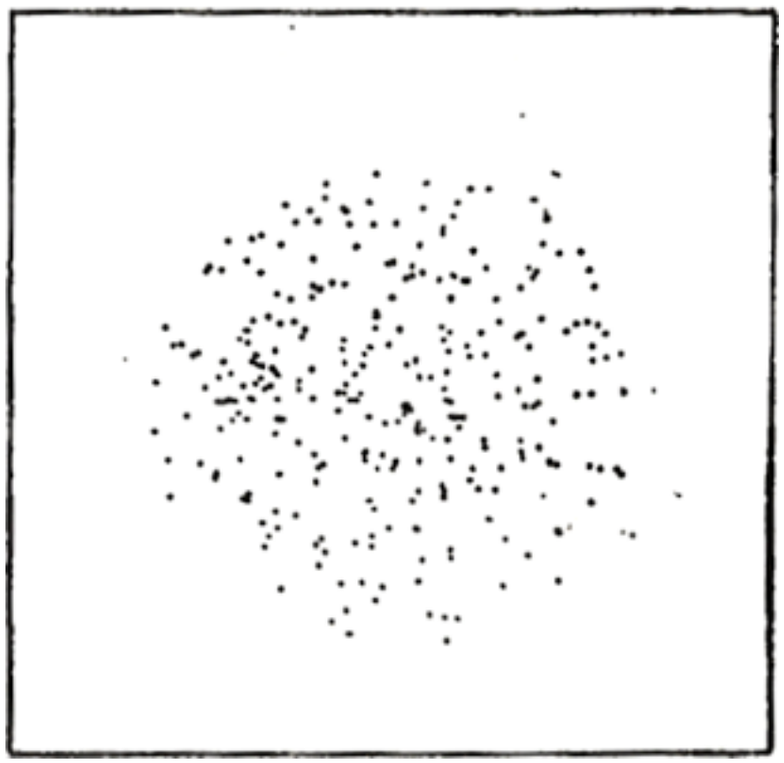

When any region becomes about twice as dense as typical regions its size, it reaches a maximum radius, ***stops expanding***,

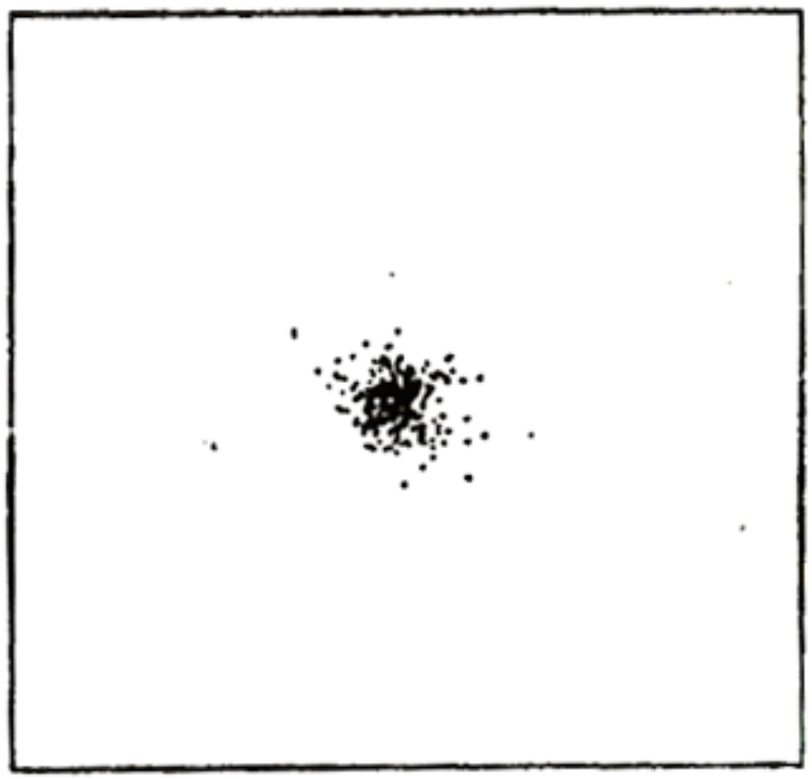

and starts falling together. The forces between the subregions generate velocities which ***prevent*** the material from ***all falling toward the center***.

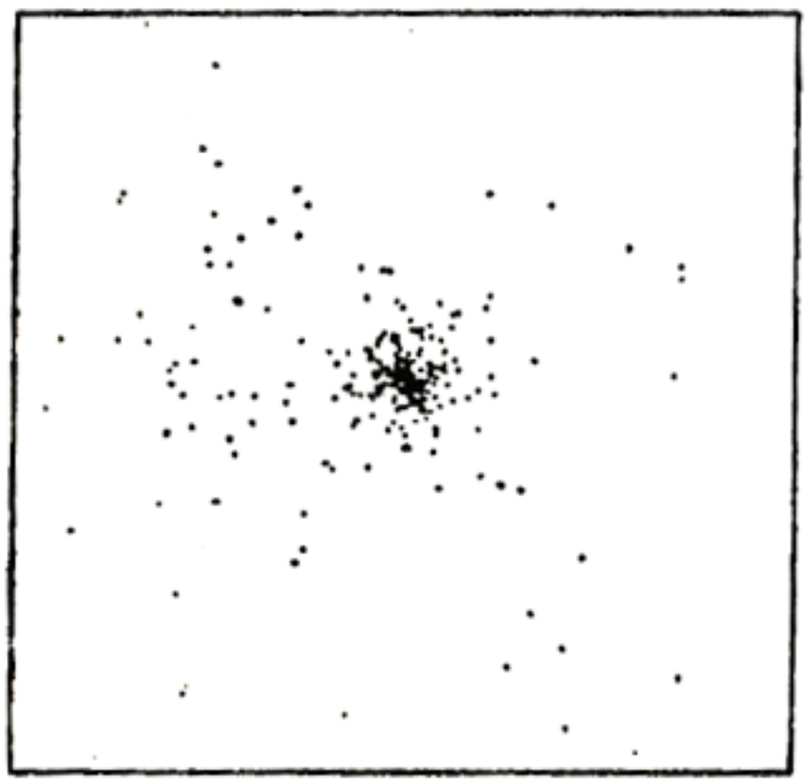

Through Violent Relaxation the dark matter quickly reaches a ***stable configuration*** that's about half the maximum radius but denser in the center.

Simulation of top-hat collapse:
P.J.E. Peebles 1970, ApJ, 75, 13.

Used in my 1984 summer school lectures "Dark matter, Galaxies, and Large Scale Structure," http://tinyurl.com/3bjknb3

TOP HAT
Max Expansion

VIOLENT RELAXATION

VIRIALIZED

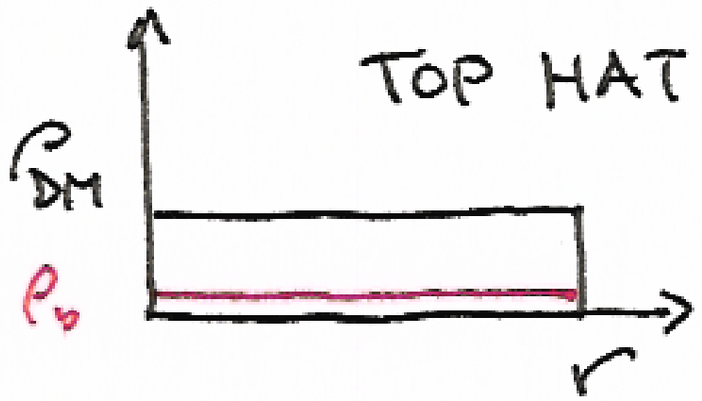

Virial Theorem: $\langle K \rangle = -\frac{1}{2}\langle W \rangle$

$-W_m = \frac{C}{r_m}$, so after virialization

$-\frac{C}{r_m} = E = W + K = \frac{1}{2}\langle W \rangle = -\frac{C}{2r_v}$

$\Rightarrow r_v = \frac{1}{2} r_m$, $\rho_v = 8\rho_m \approx 50\,\bar{\rho}(t_m)$

$\langle v^2 \rangle \approx \frac{GM}{r_v}$

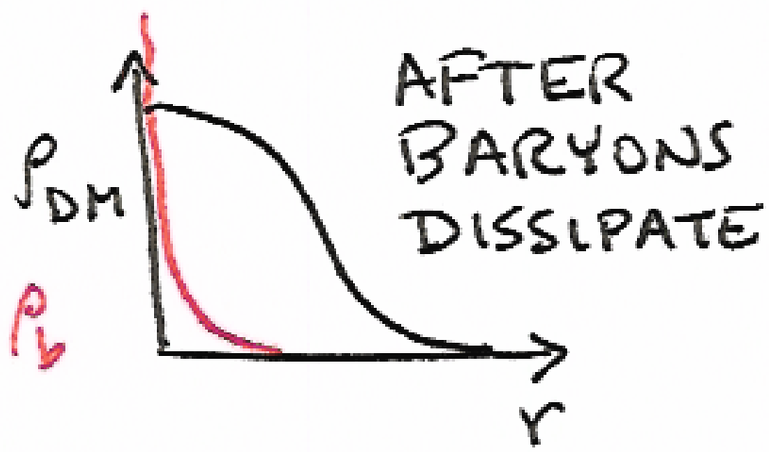

Growth and Collapse of Fluctuations

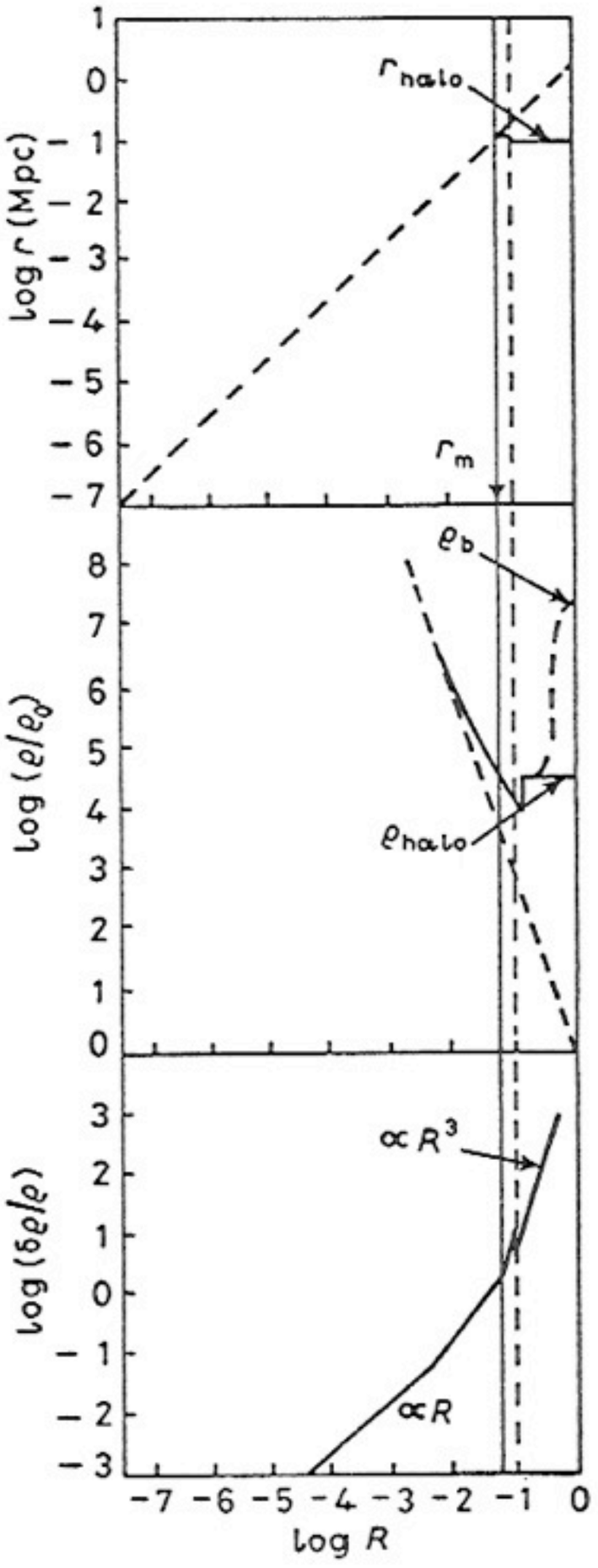

Schematic sketches of radius, density, and density contrast of an overdense fluctuation. It initially expands with the Hubble expansion, reaches a maximum radius (solid vertical line), and undergoes violent relaxation during collapse (dashed vertical line), which results in the dissipationless matter forming a stable halo. Meanwhile the ordinary matter ρ_b continues to dissipate kinetic energy and contract, thereby becoming more tightly bound, until dissipation is halted by star or disk formation, explaining the origin of galactic spheroids and disks.

(This was the simplified discussion of BFPR84; the figure is from my 1984 lectures at the Varenna school. Now we take into account halo growth by accretion, and the usual assumption is that spheroids form mostly as a result of galaxy mergers Toomre 1977. Also, we now know that most of the baryons in halos don't cool and fall to the center.)

Halo and Galaxy Merging and Spheroid Formation

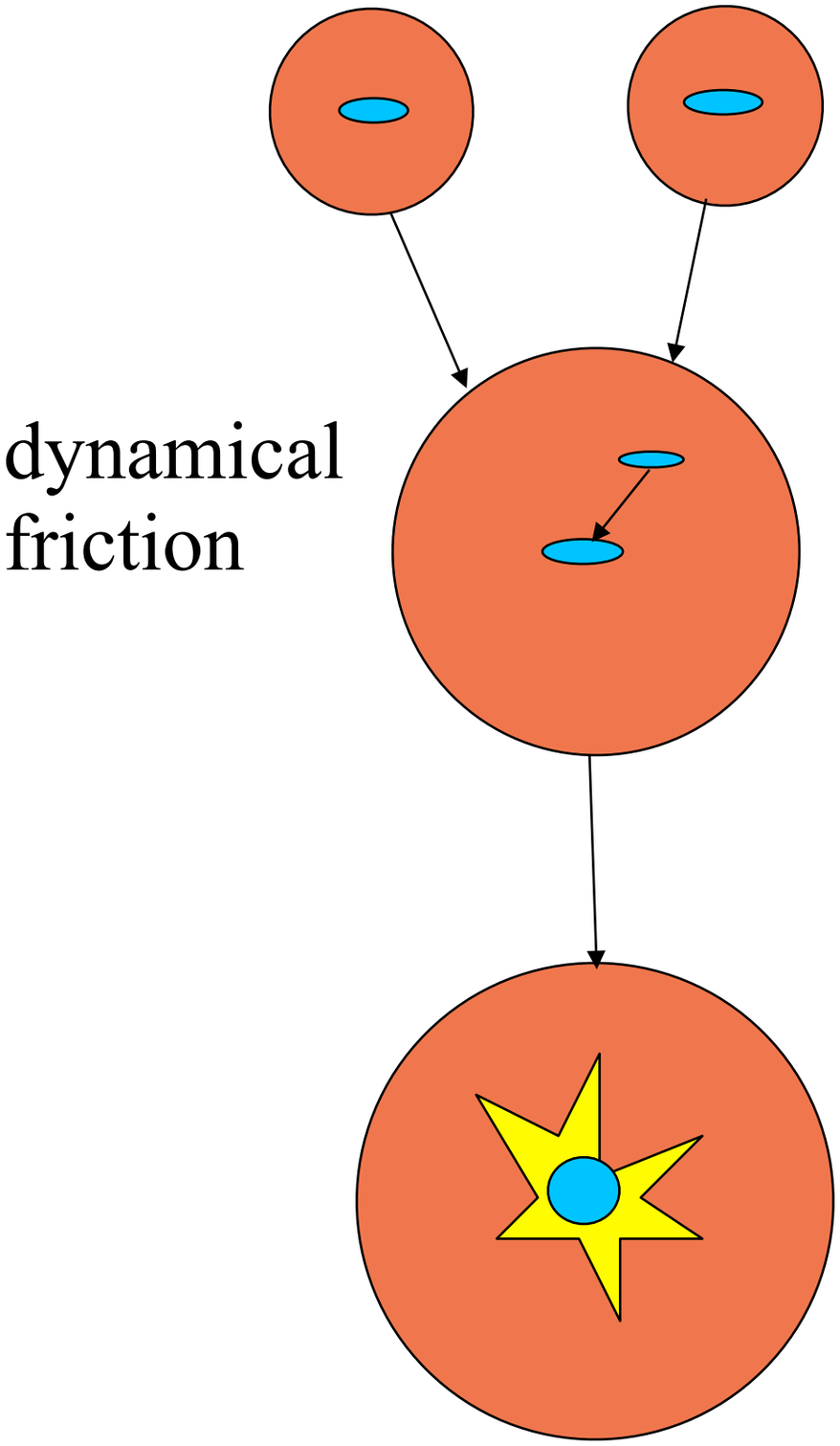

mergers can trigger starburst, forming spheroid

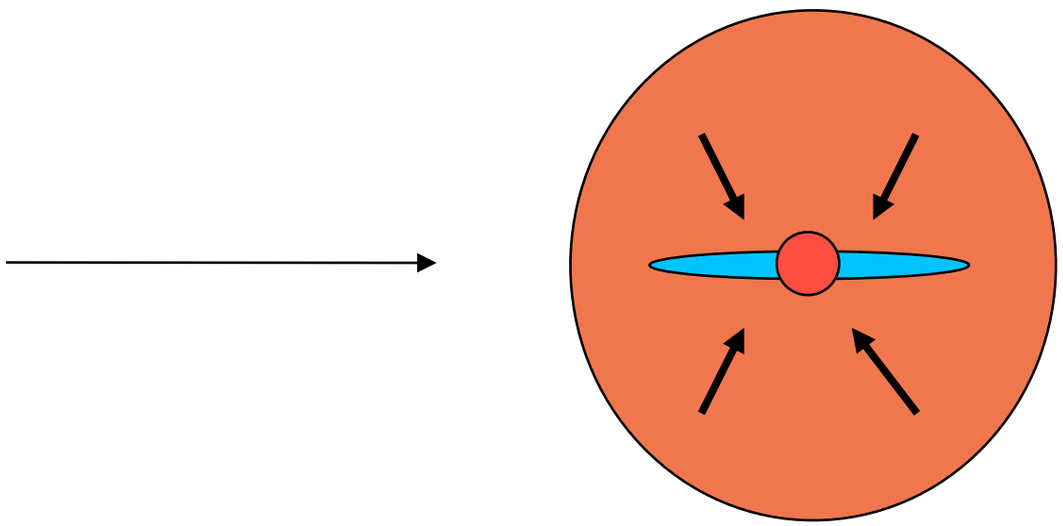

subsequent cooling forms disk

Spherical Collapse

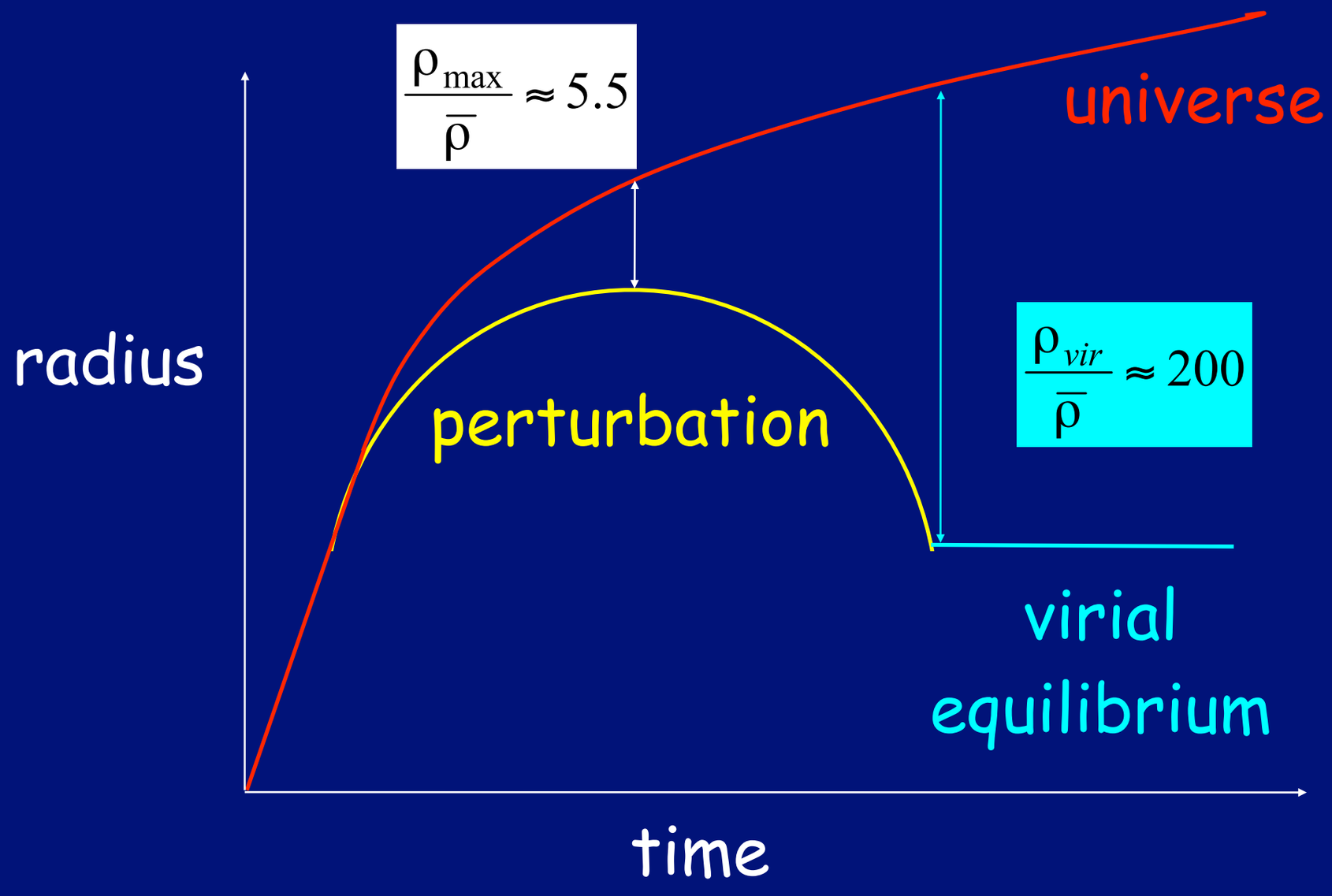

virial equilibrium: $E = -\frac{1}{2}\frac{GM}{R_{vir}} = -\frac{GM}{R_{\max}}$

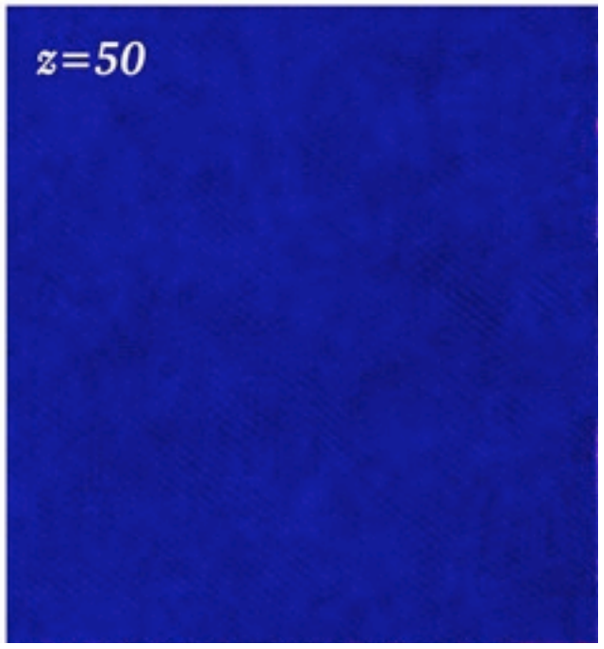

N-body simulation

ΛCDM

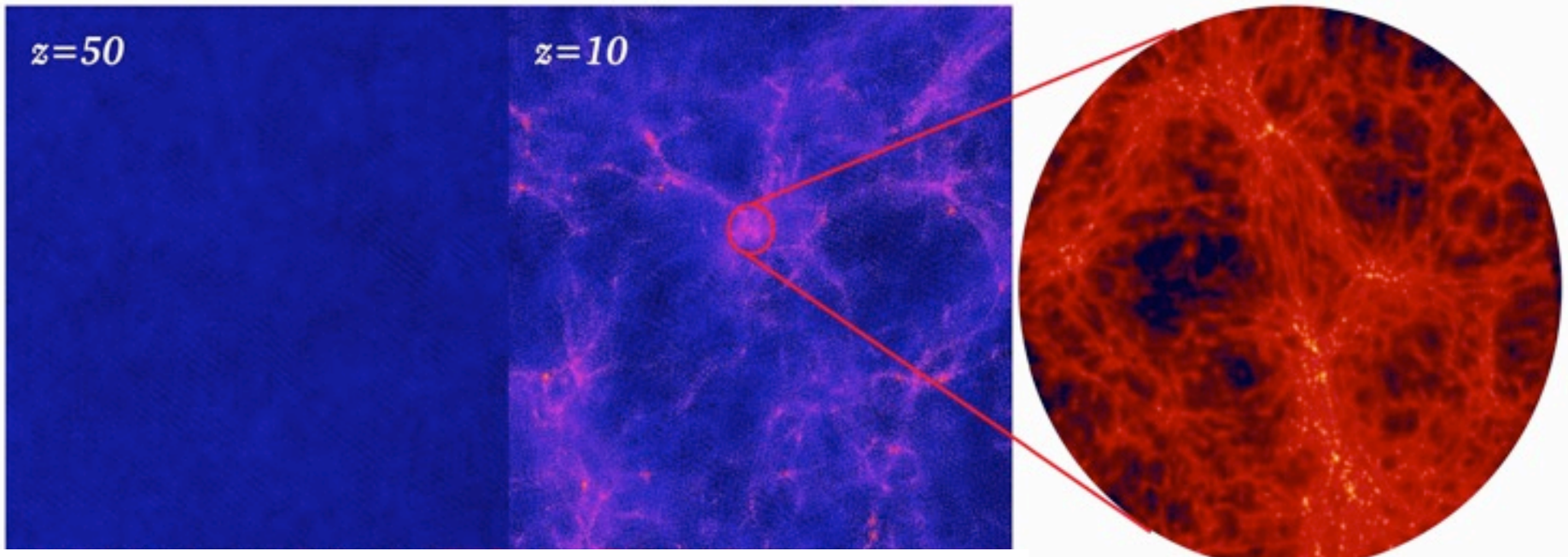
z=50
z=10

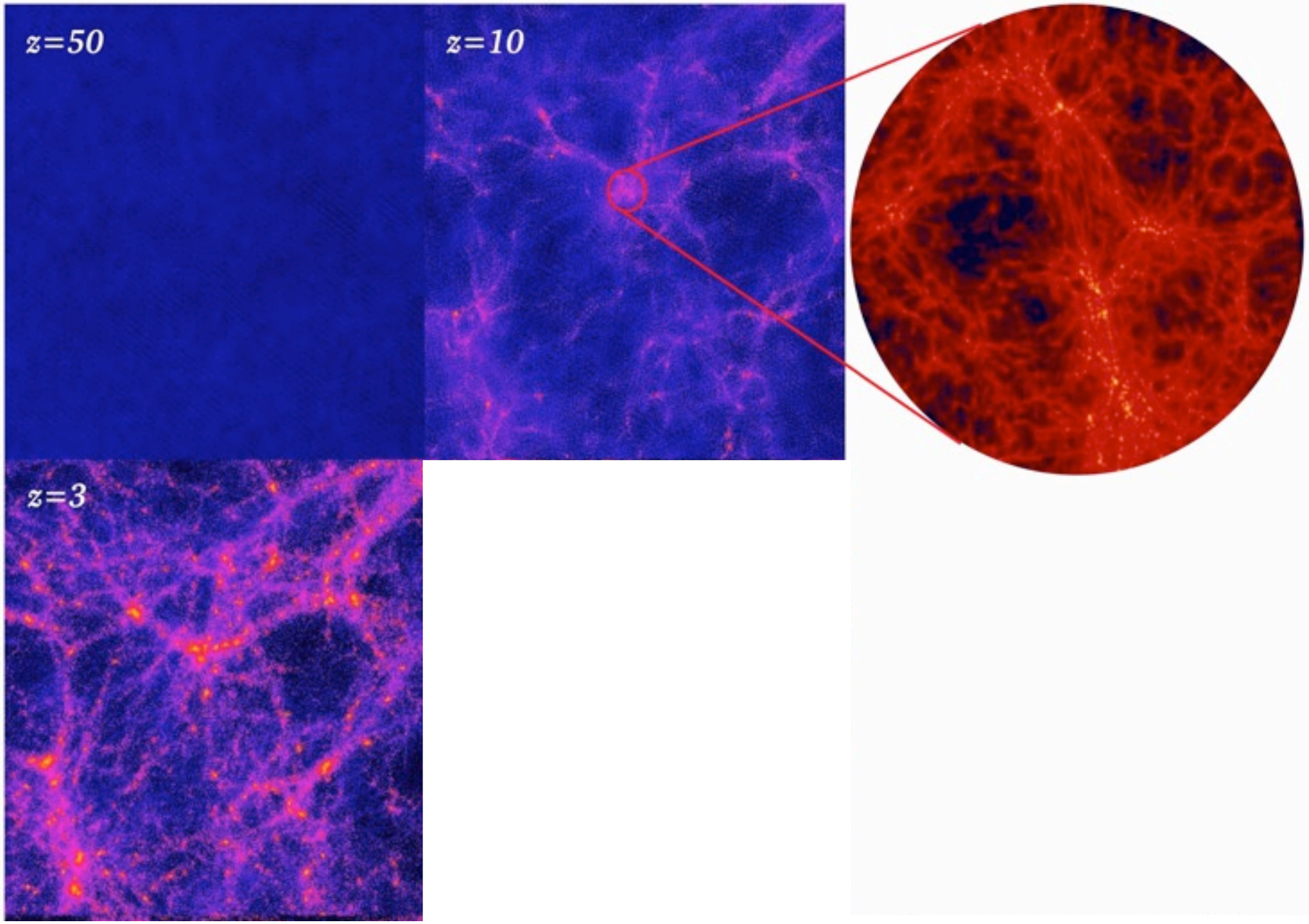
z=50
z=10
z=3

z=49.000

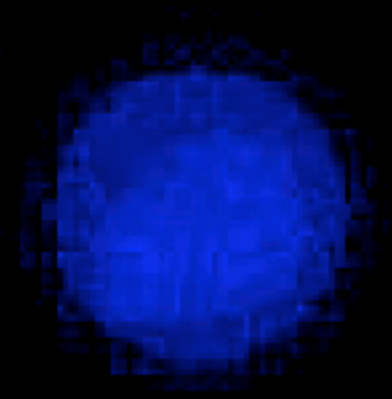

Expansion....

z=49.0t
=49 Myr

z=12.0
t=374Myr

z=2.95
t=2.23 Gyr

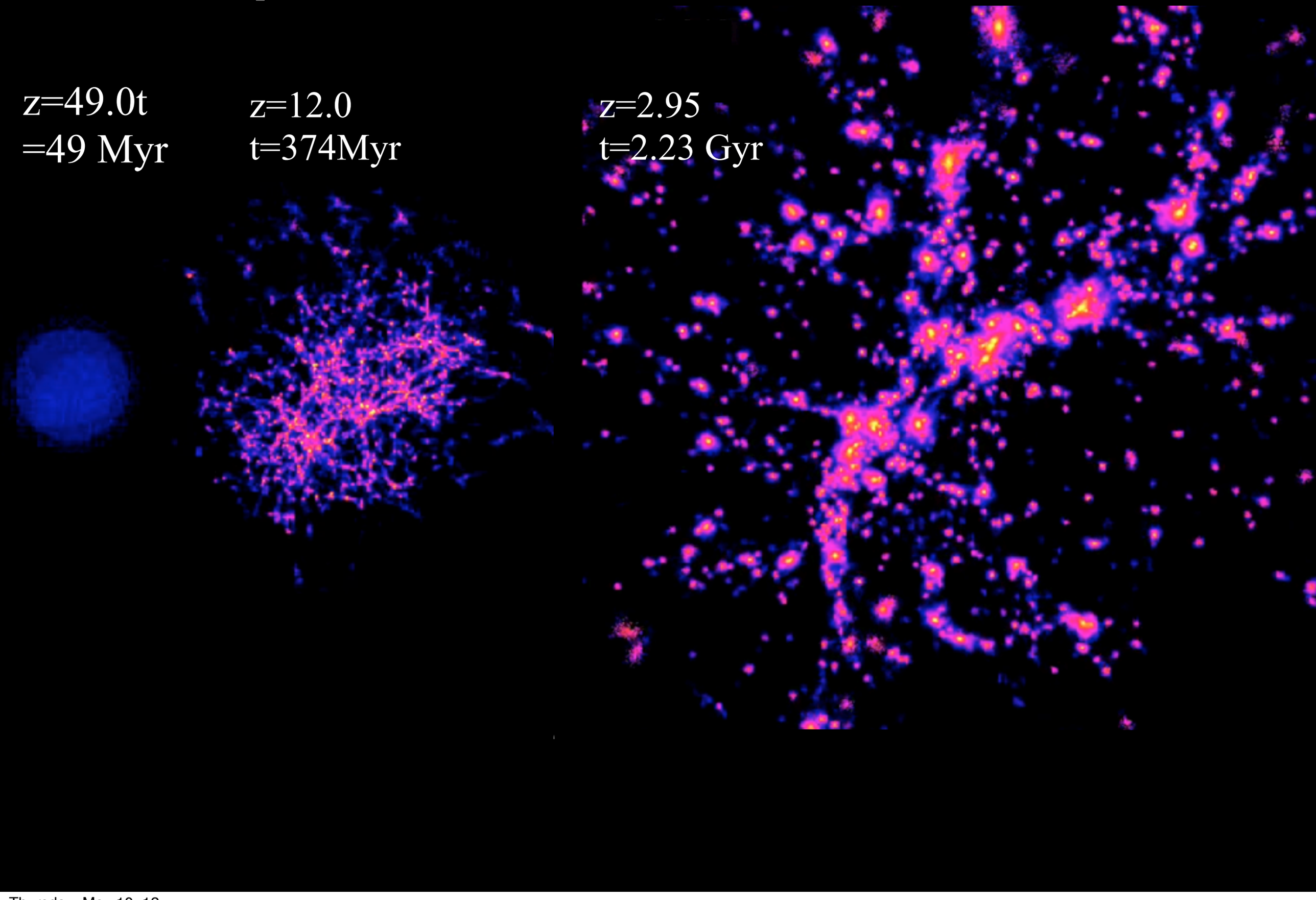

z= 0.837 t= 6.66 Gyr

End of expansion for this halo

z= 0.391 t= 9.48 Gyr

Wild Space

Tame Space

z= 0.391 t= 9.48 Gyr

Wild Space

Tame Space

z= 0.000 t= 13.7 Gyr (today)

Wild Space

Tame Space

Micro-Macro Connection

Cold Dark Matter

Hot Dark Matter

ν

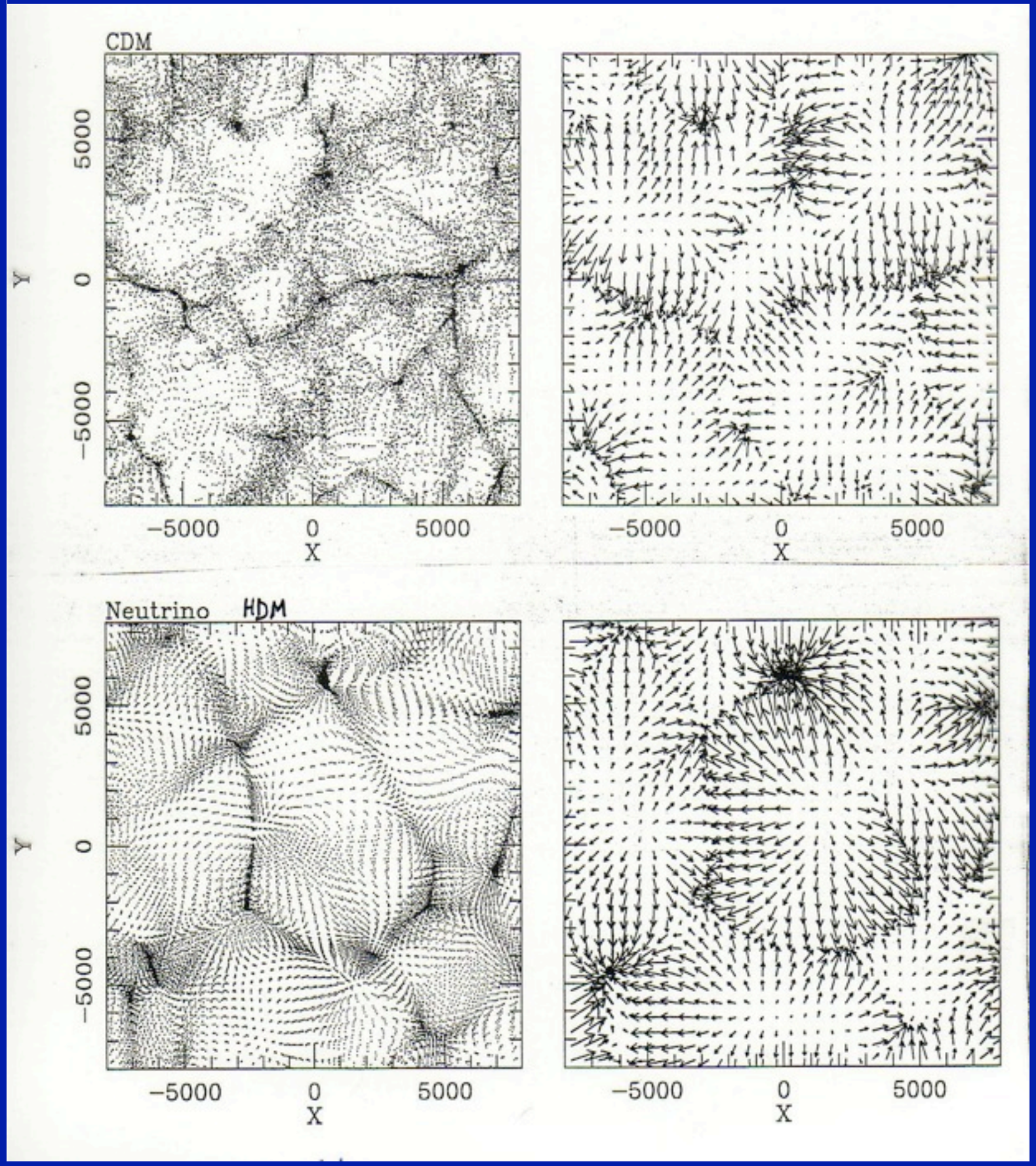

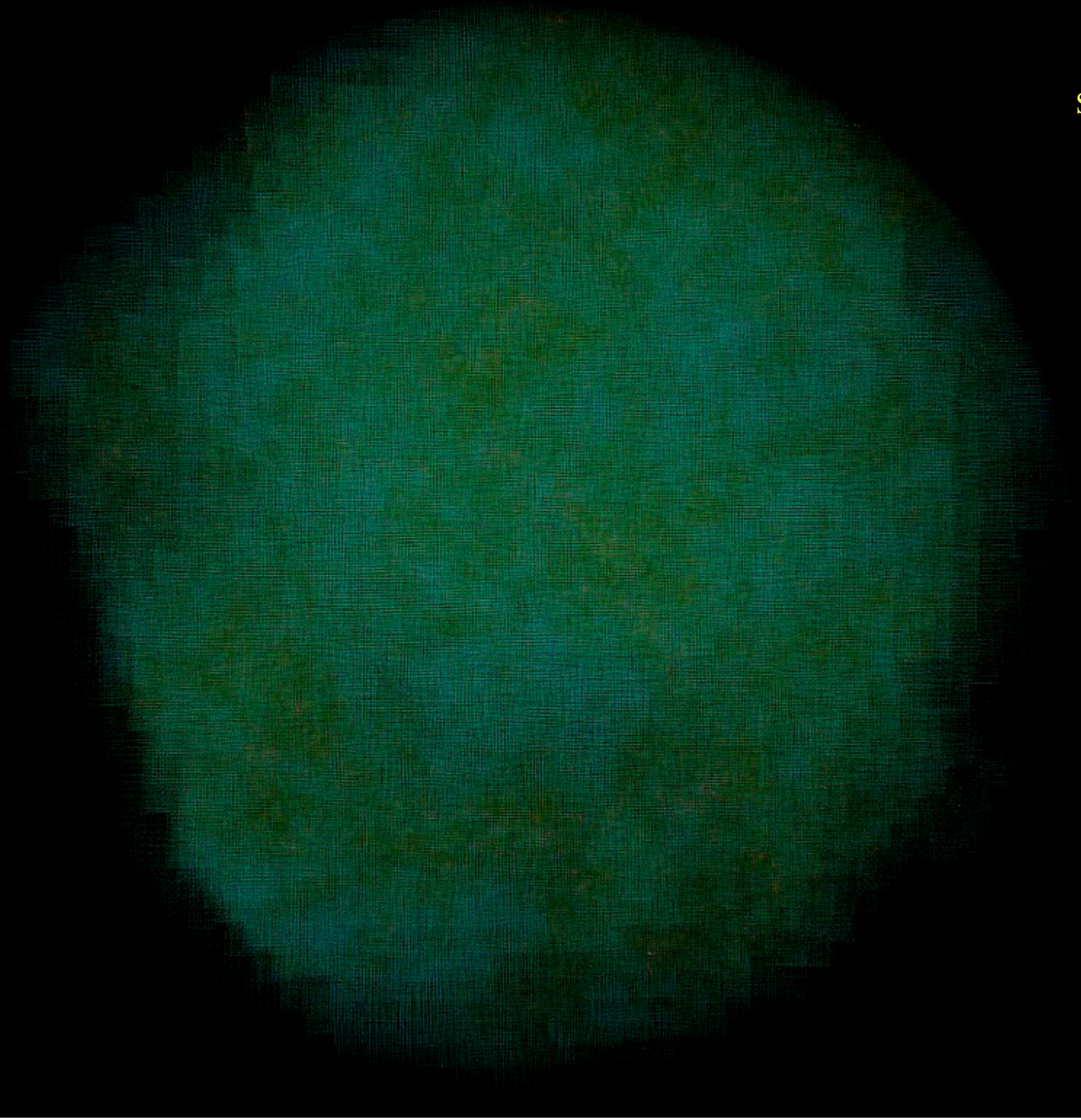

Columbia
Supercomputer
NASA Ames
2005

Simulation:
Brandon
Allgood &
Joel Primack

Visualization:
Chris Henze

(rotation to
show 3D)

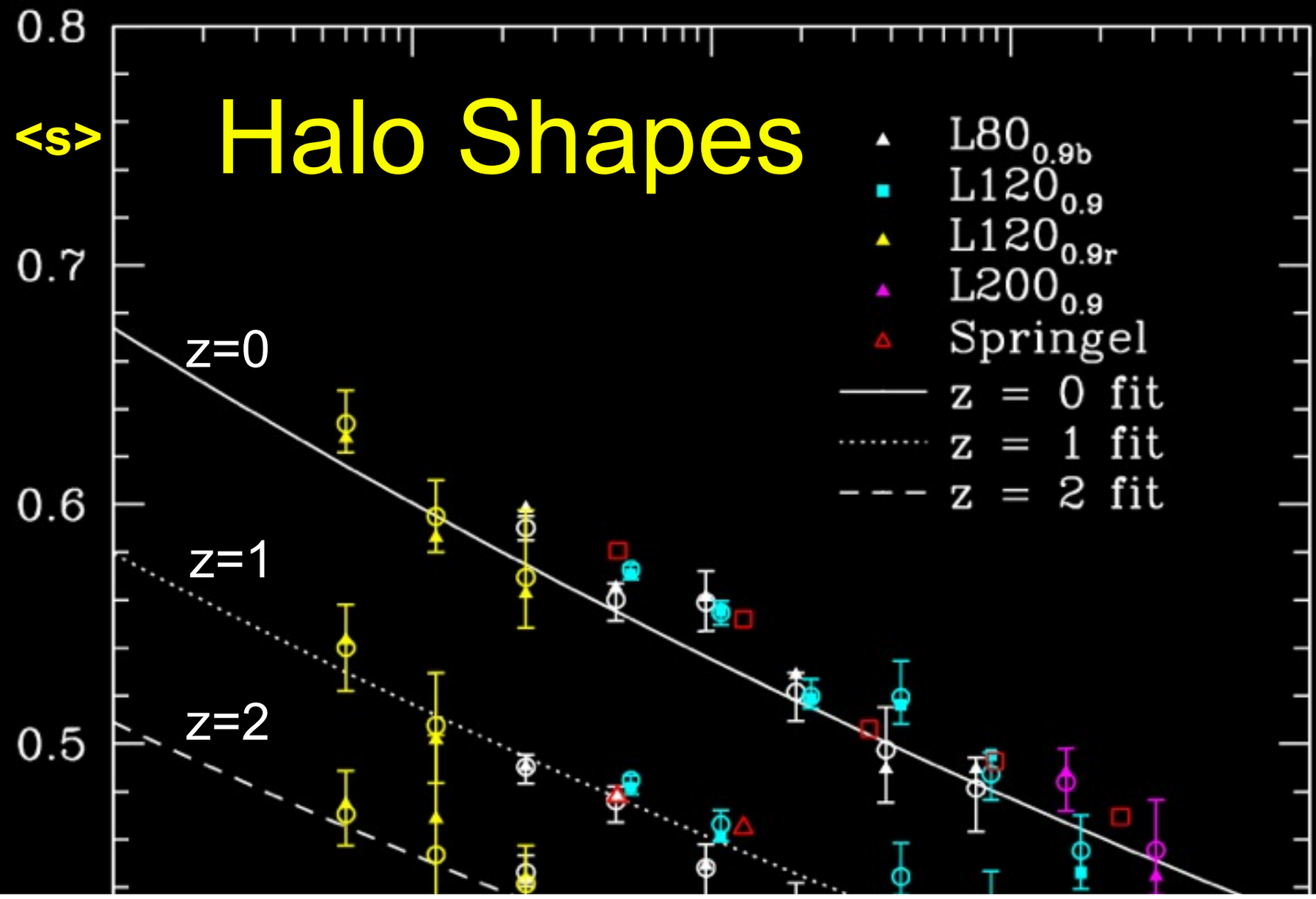

A simple formula describes these results, as well dependence on epoch and cosmological parameter σ_8 :

$$\langle s \rangle (M_{\rm vir}, z = 0) = \alpha \left(\frac{M_{\rm vir}}{M_*} \right)^{\beta}$$

with best fit values

$$\alpha = 0.54 \pm 0.03, \ \beta = -0.050 \pm 0.003.$$

<s> = short / long axis of dark halos vs. mass and redshift. Dark halos are more elongated the more massive they are and the earlier they form. We found that the halo <s> scales as a power-law in Mhalo/M*. Halo shape is also related to the Wechsler halo formation scale factor a_c.

Allgood+2006

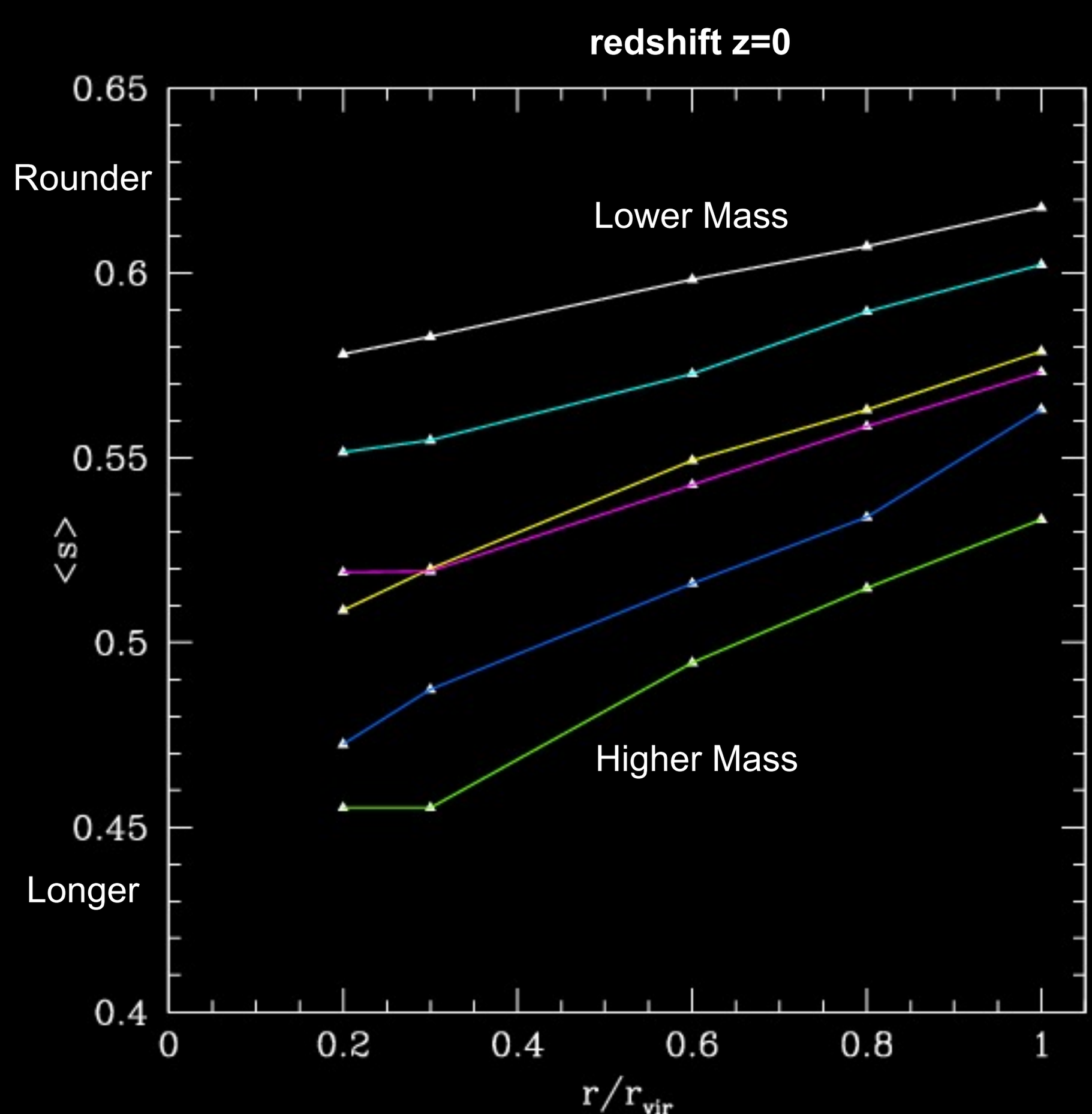

Halos become more spherical at larger radius and smaller mass. As before,

$$s = \frac{\text{short axis}}{\text{long axis}}$$

These predictions can be tested against cluster X-ray data and galaxy weak lensing data.

Allgood+2006

CONSTRAINED LOCAL UNIVERSE SIMULATION

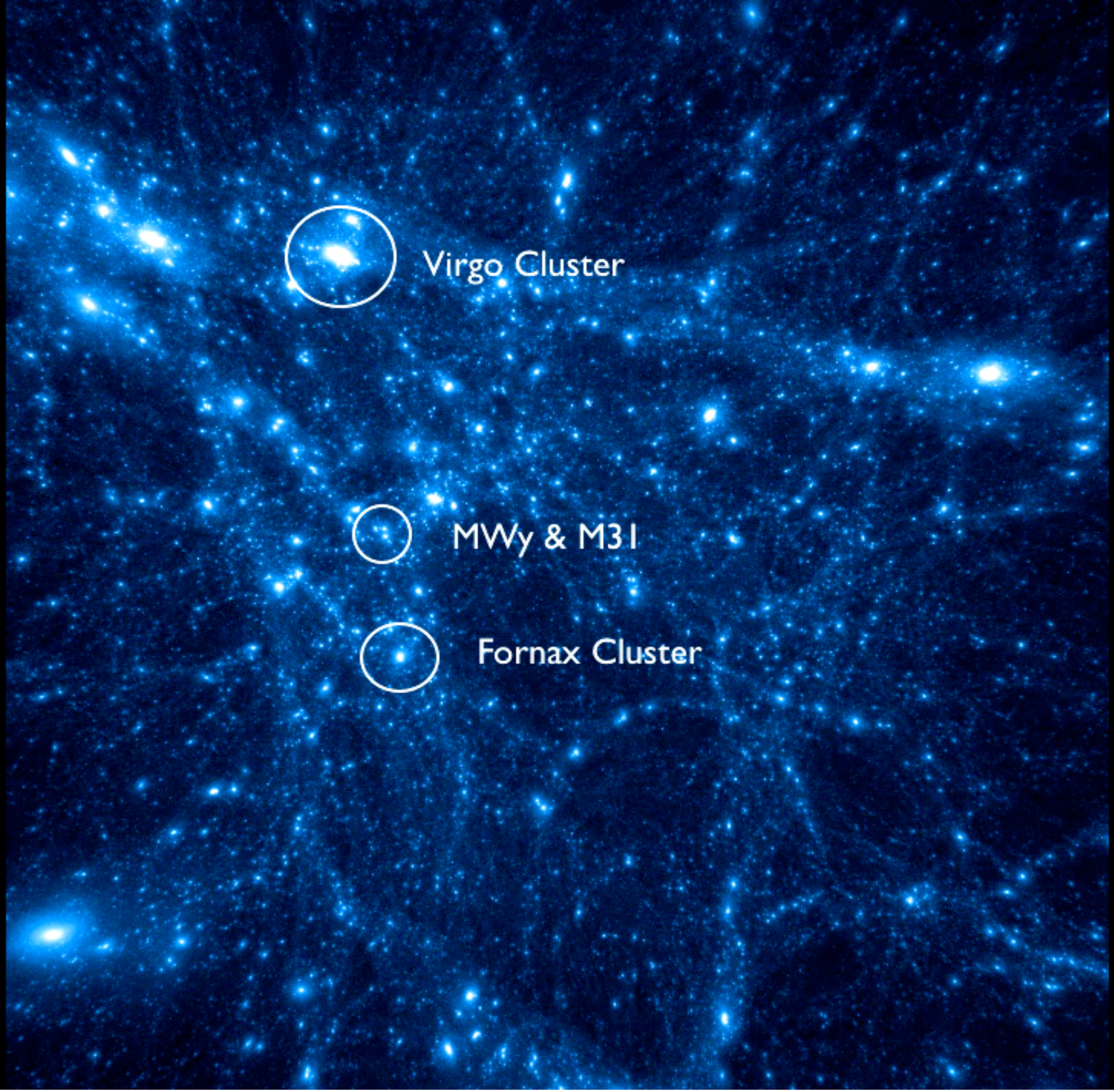
Virgo Cluster
MWy & M31
Fornax Cluster

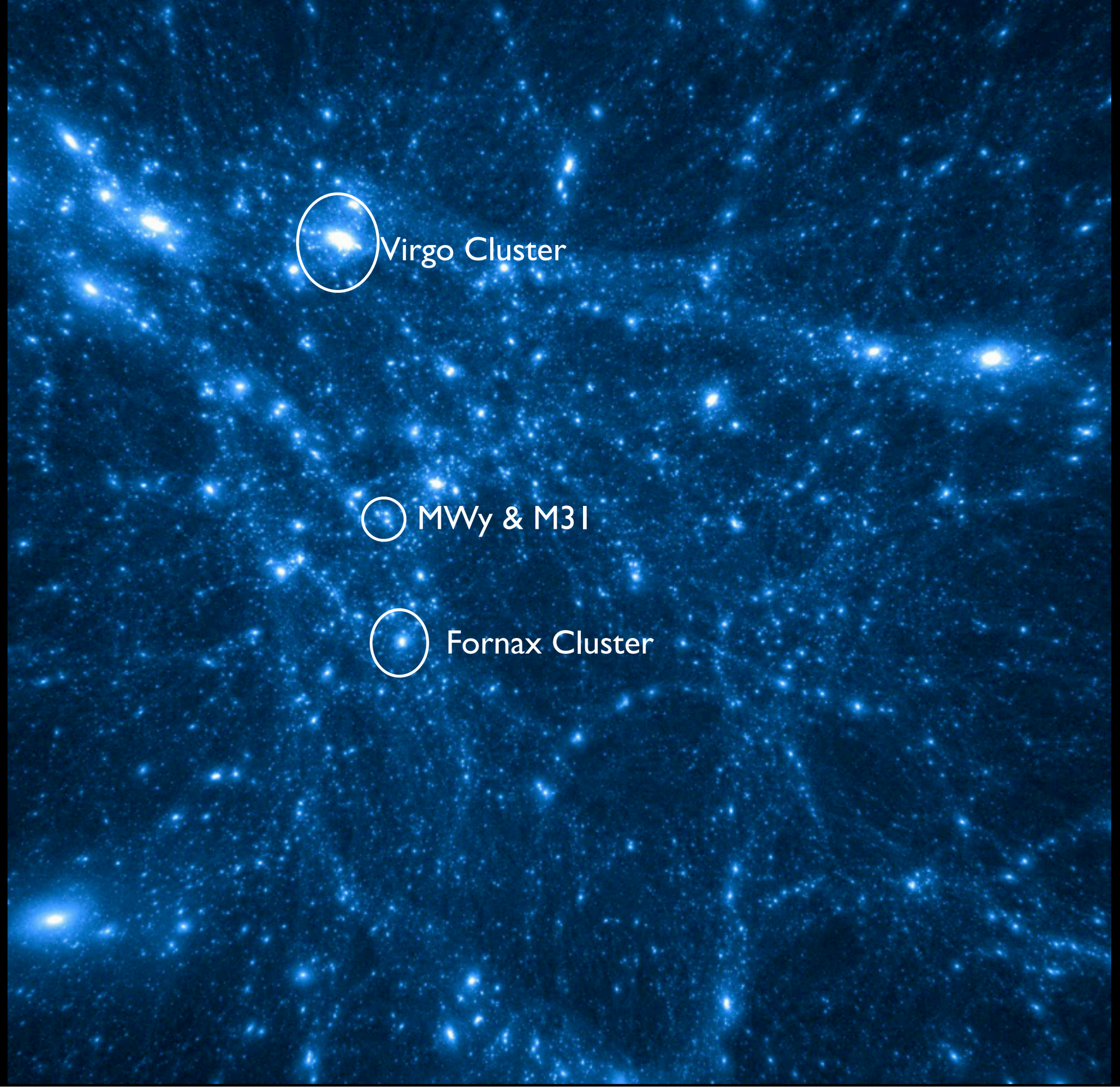
Virgo Cluster
MWy & M31
Fornax Cluster

Bolshoi Simulation
250x10 Mpc/h Slice

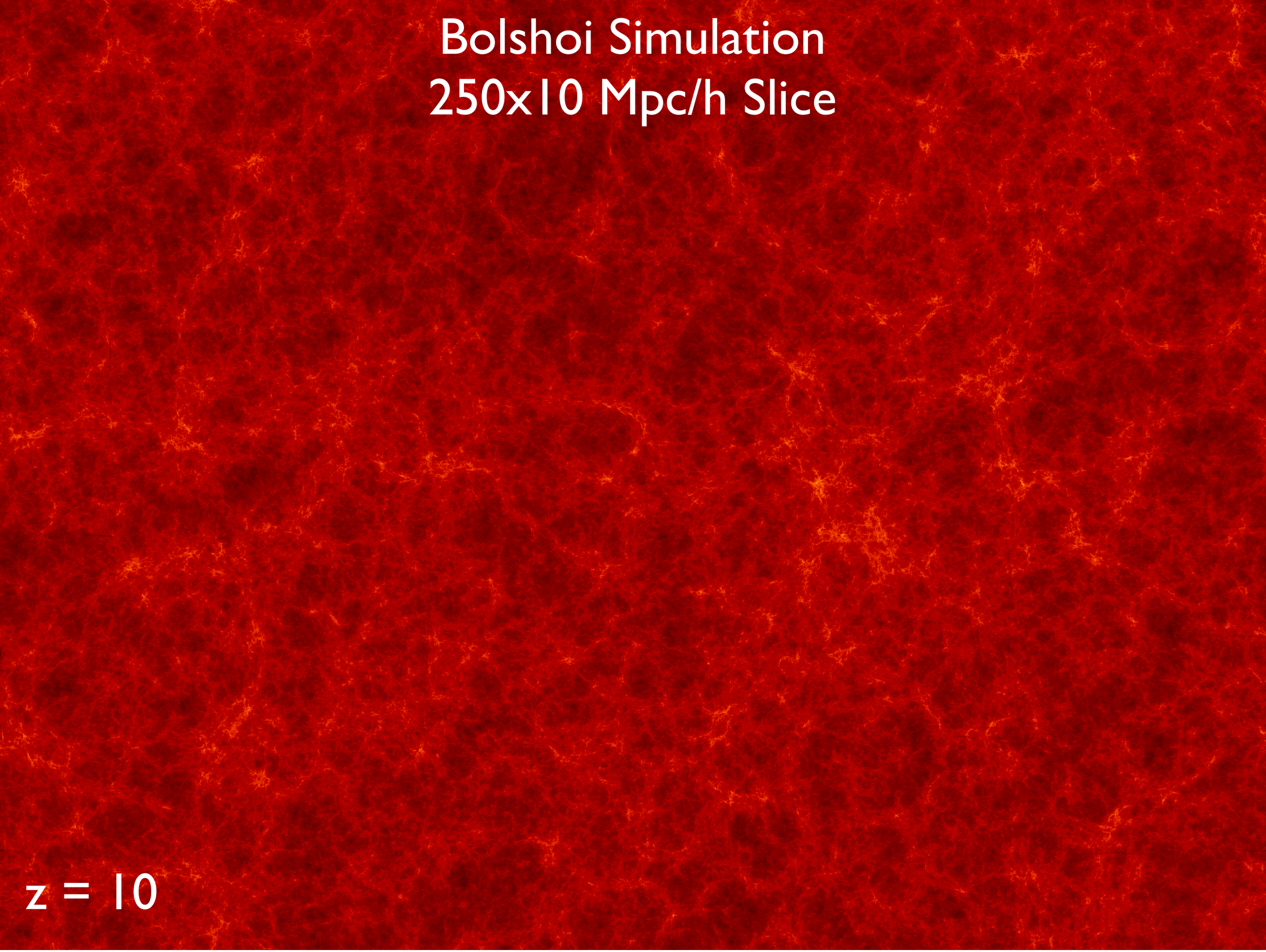

Bolshoi Simulation
250x10 Mpc/h Slice

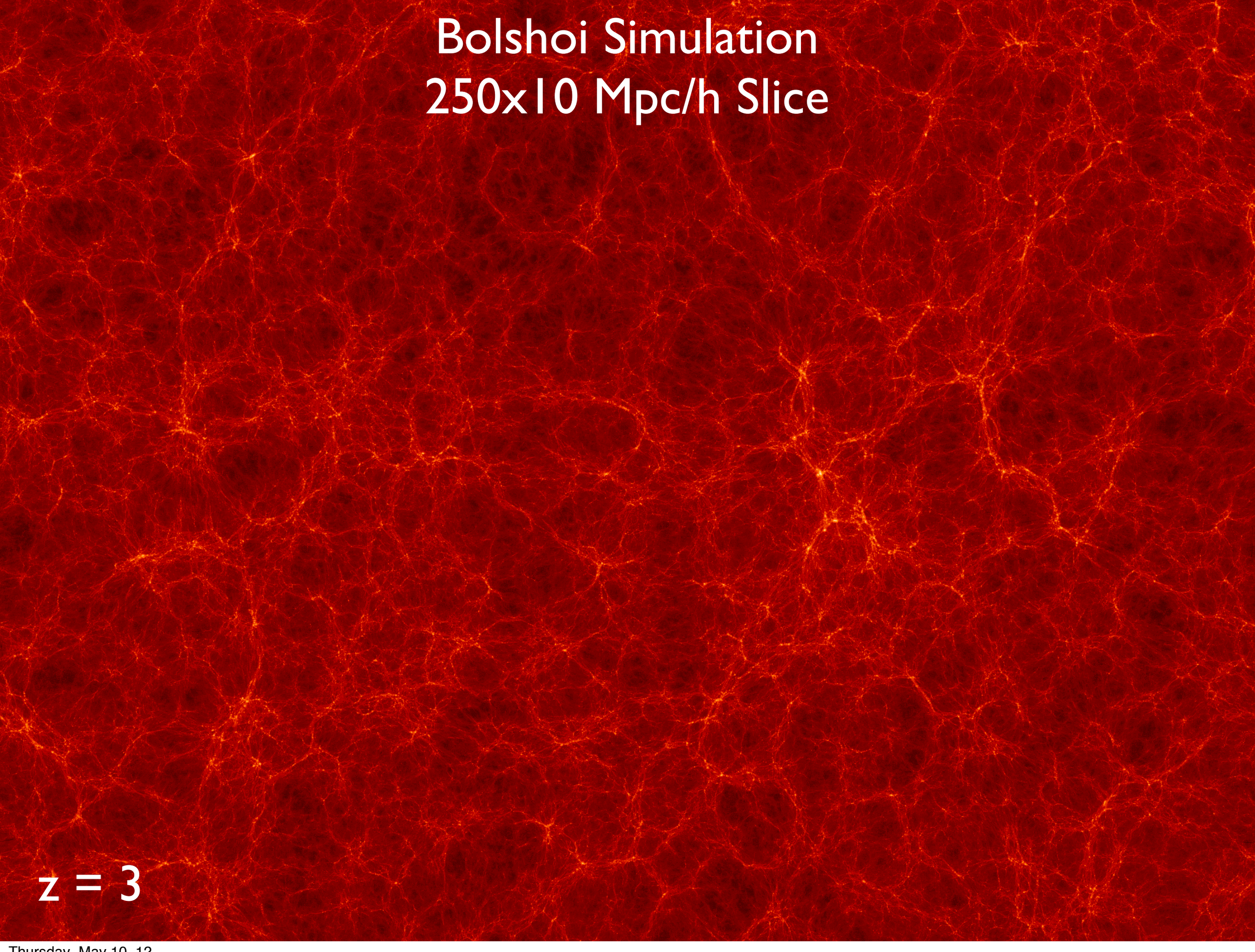

Bolshoi Simulation
250x10 Mpc/h Slice

z = 1

Bolshoi Simulation
250x10 Mpc/h Slice

z = 0

Bolshoi Simulation
125x10 Mpc/h Slice

z = 10

Bolshoi Simulation
125x10 Mpc/h Slice

z = 3

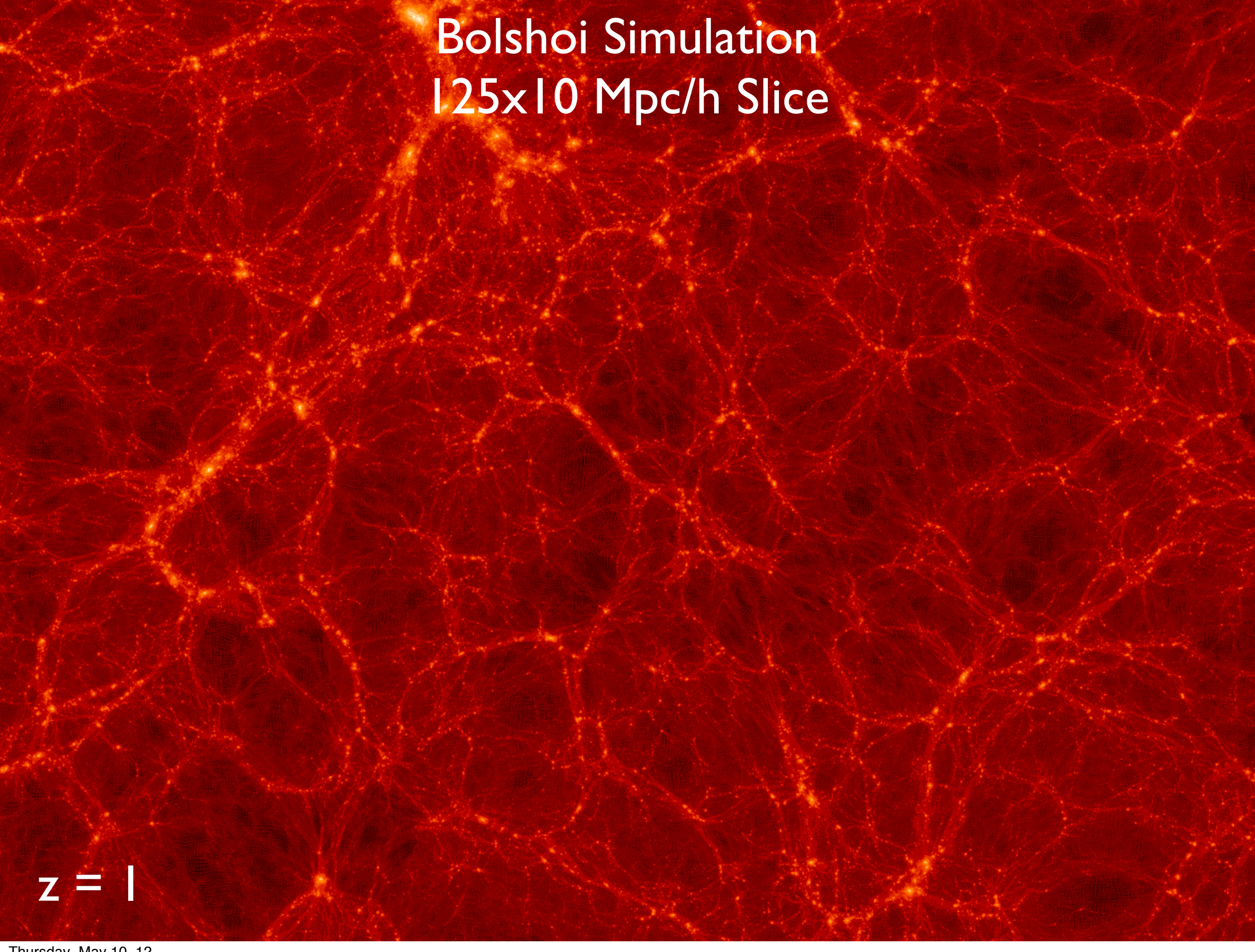
Bolshoi Simulation
125x10 Mpc/h Slice
z = 1

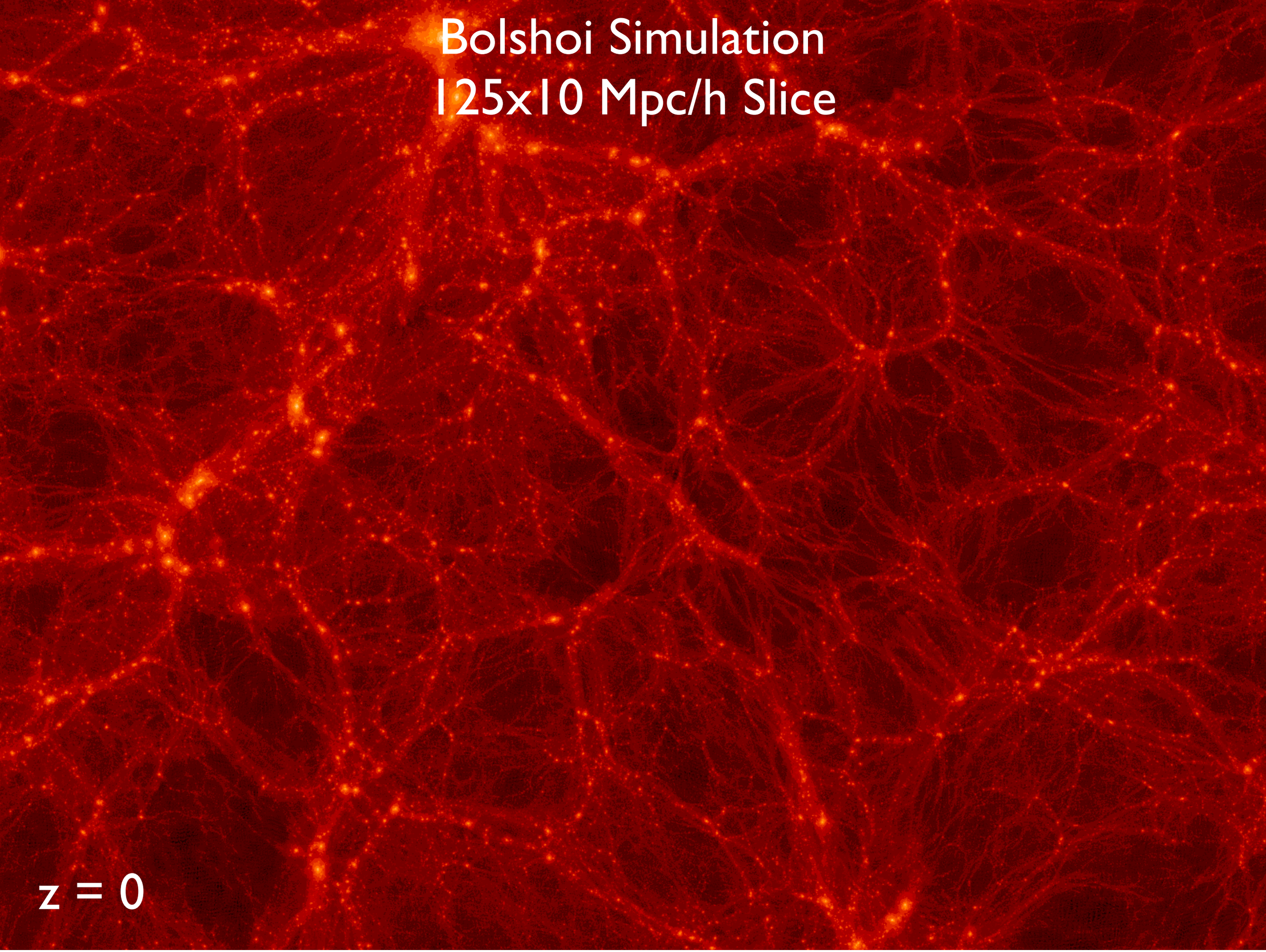
Bolshoi Simulation
125x10 Mpc/h Slice
z = 0

2dF redshift survey

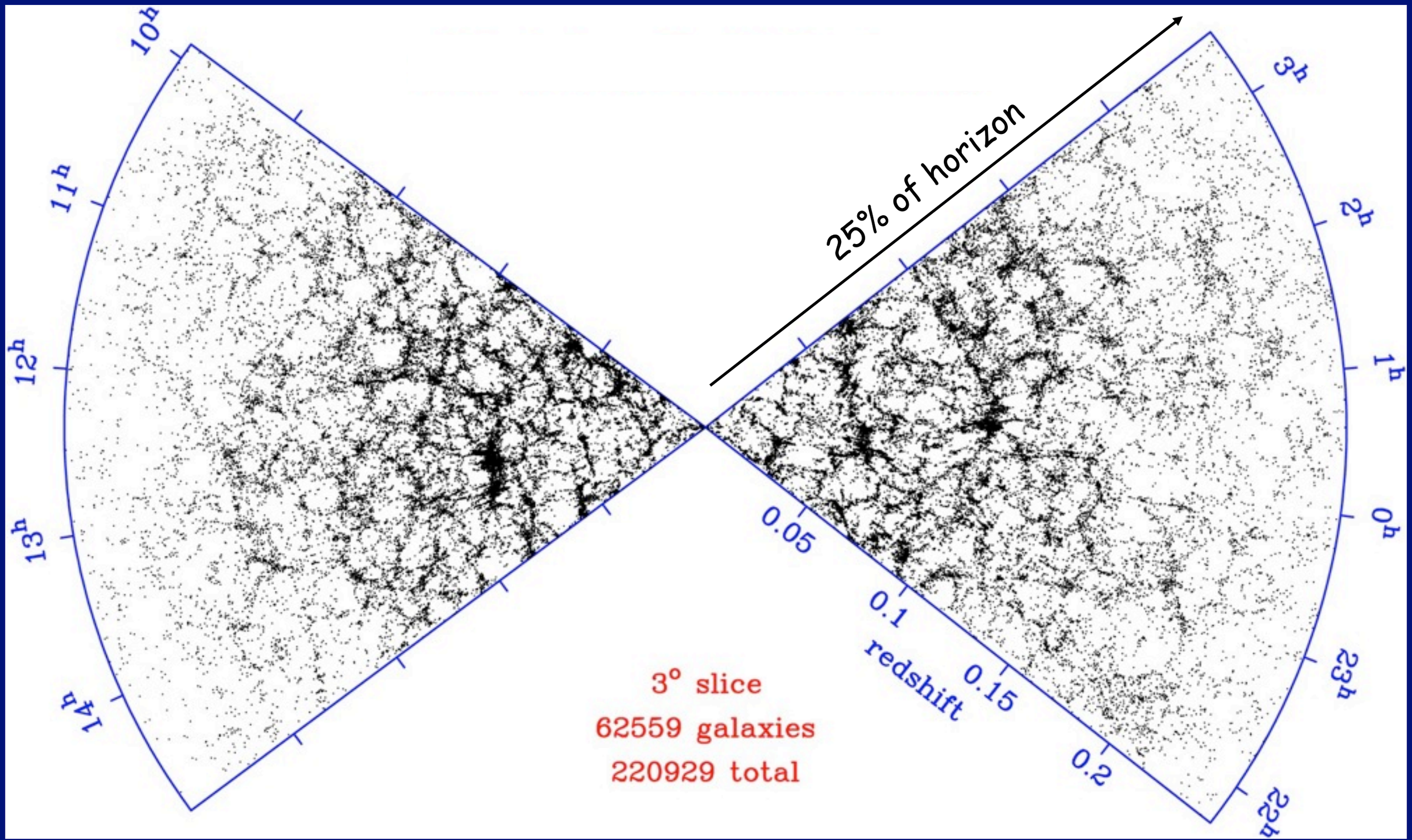

2dF and Mocks

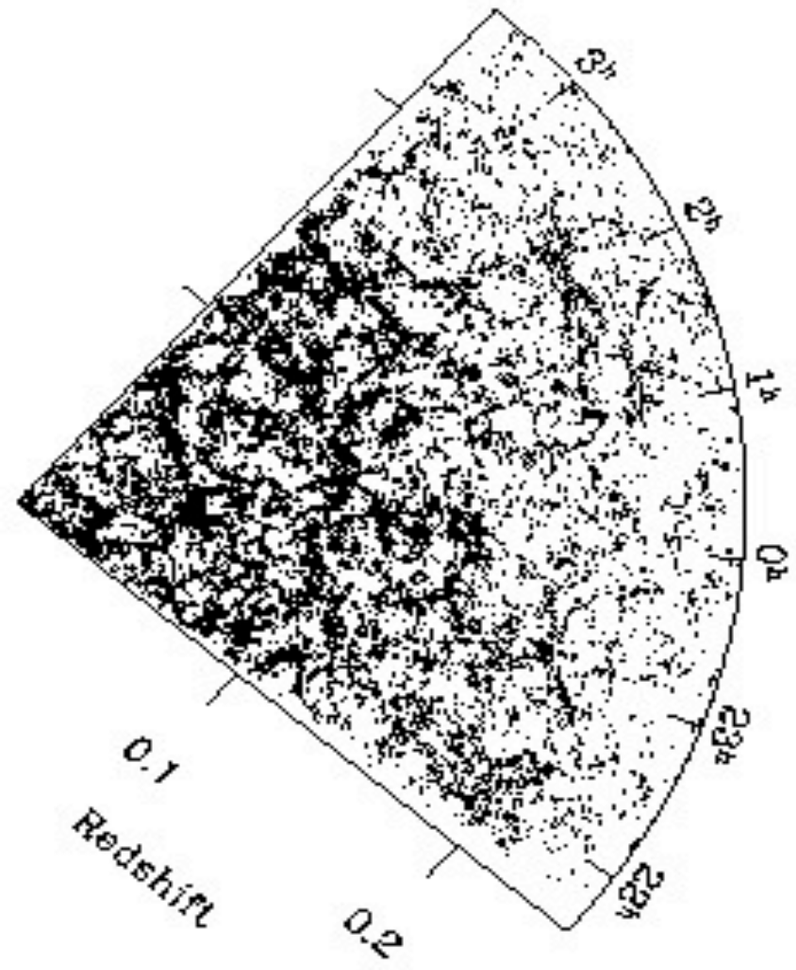

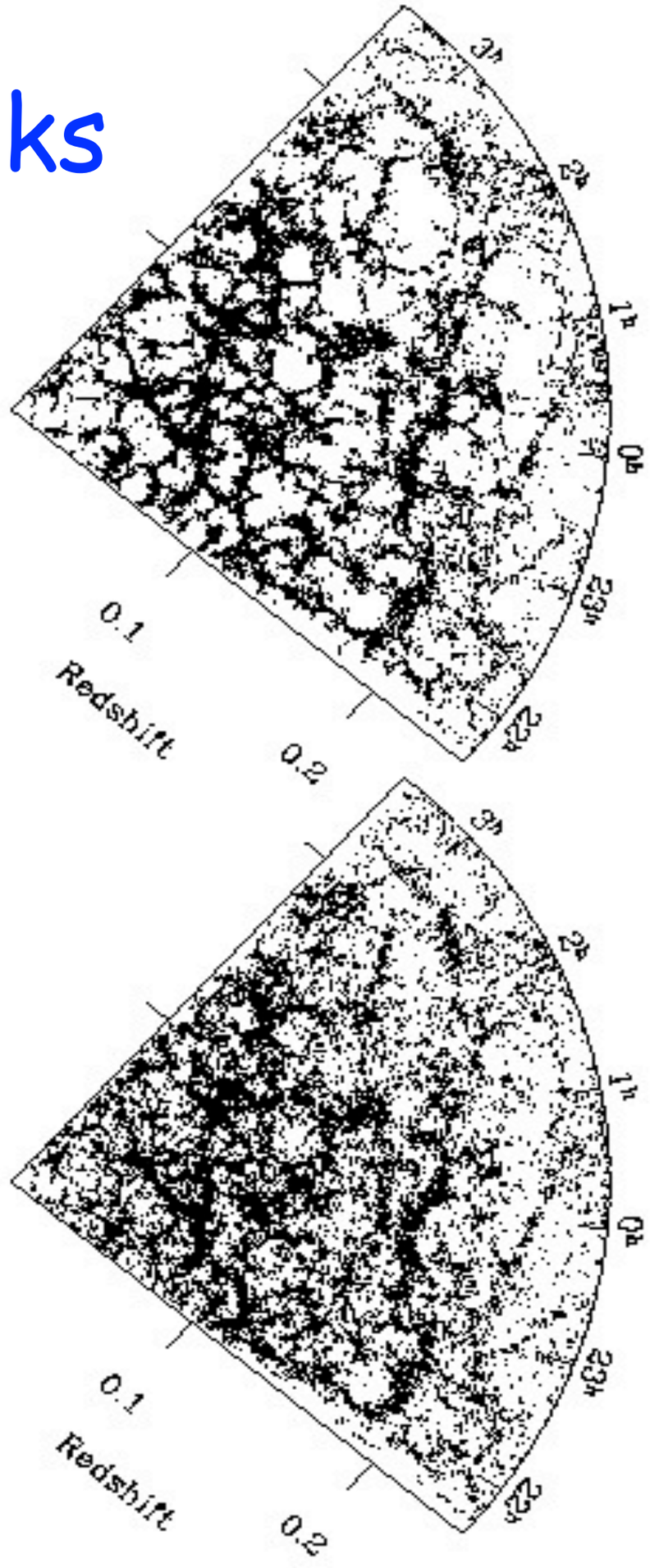

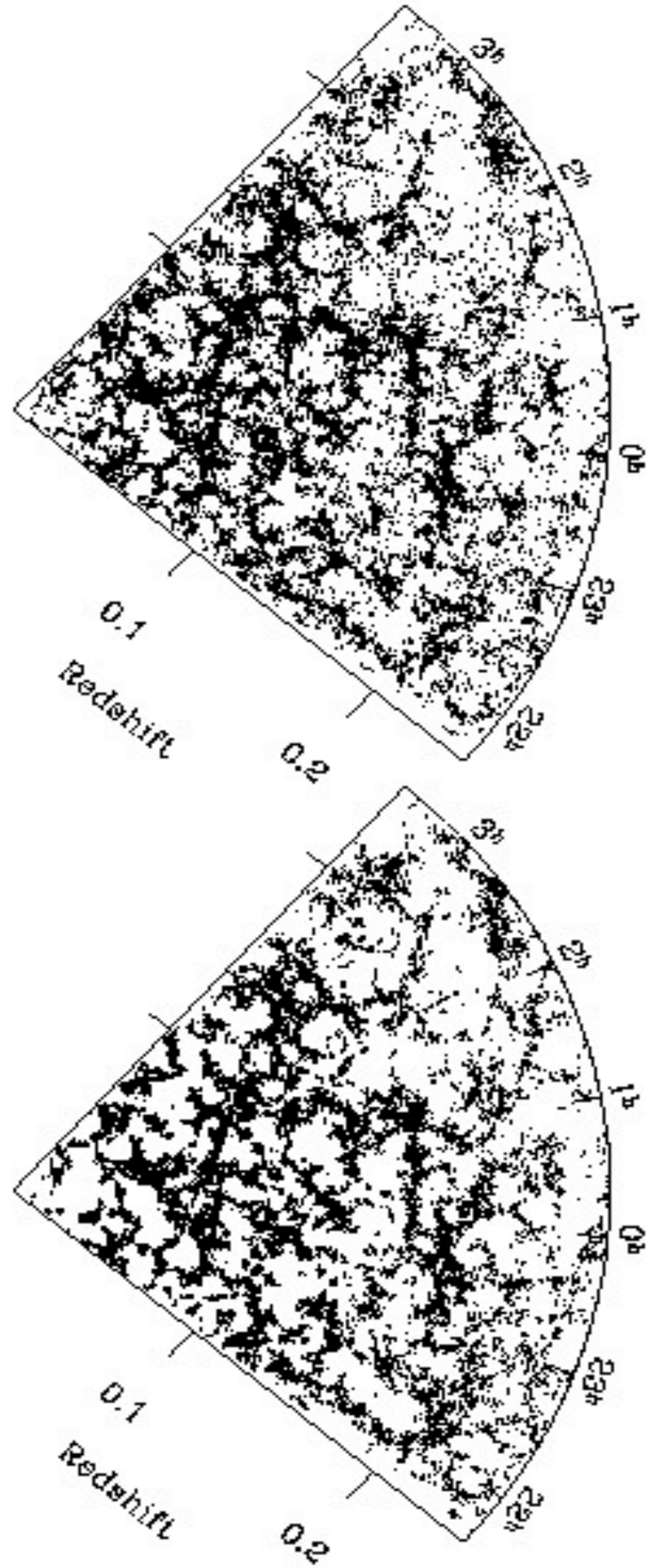

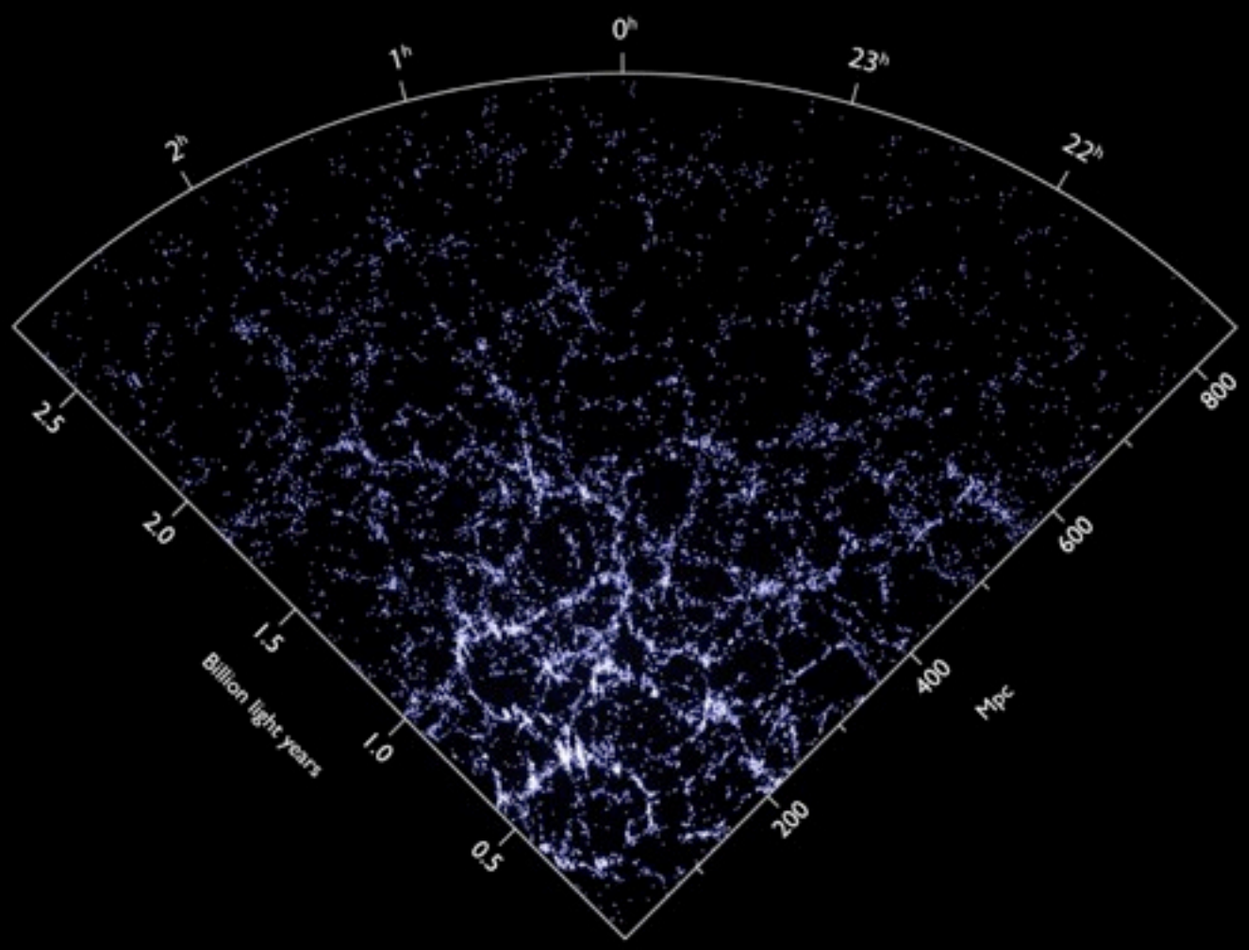
SDSS
0h
1h
23h
22h
2h
2.5
2.0
1.5
1.0
0.5
Billion light years
800
600
400
200
Mpc

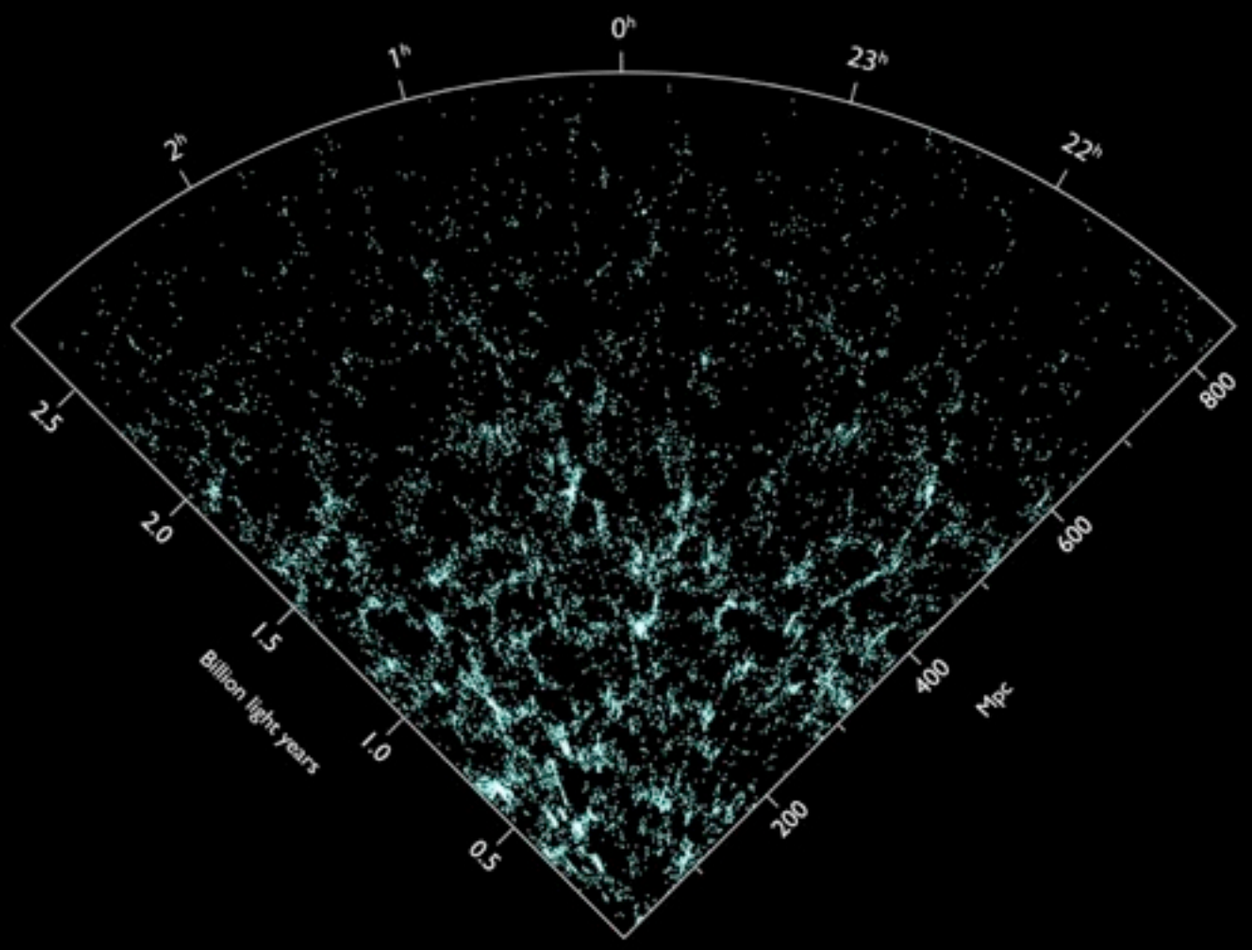
Bolshoi
0h
1h
23h
22h
2h
2.5
2.0
1.5
1.0
0.5
Billion light years
800
600
400
200
Mpc

ΛCDM Fluctuation Spectrum

Agrees with Observations!

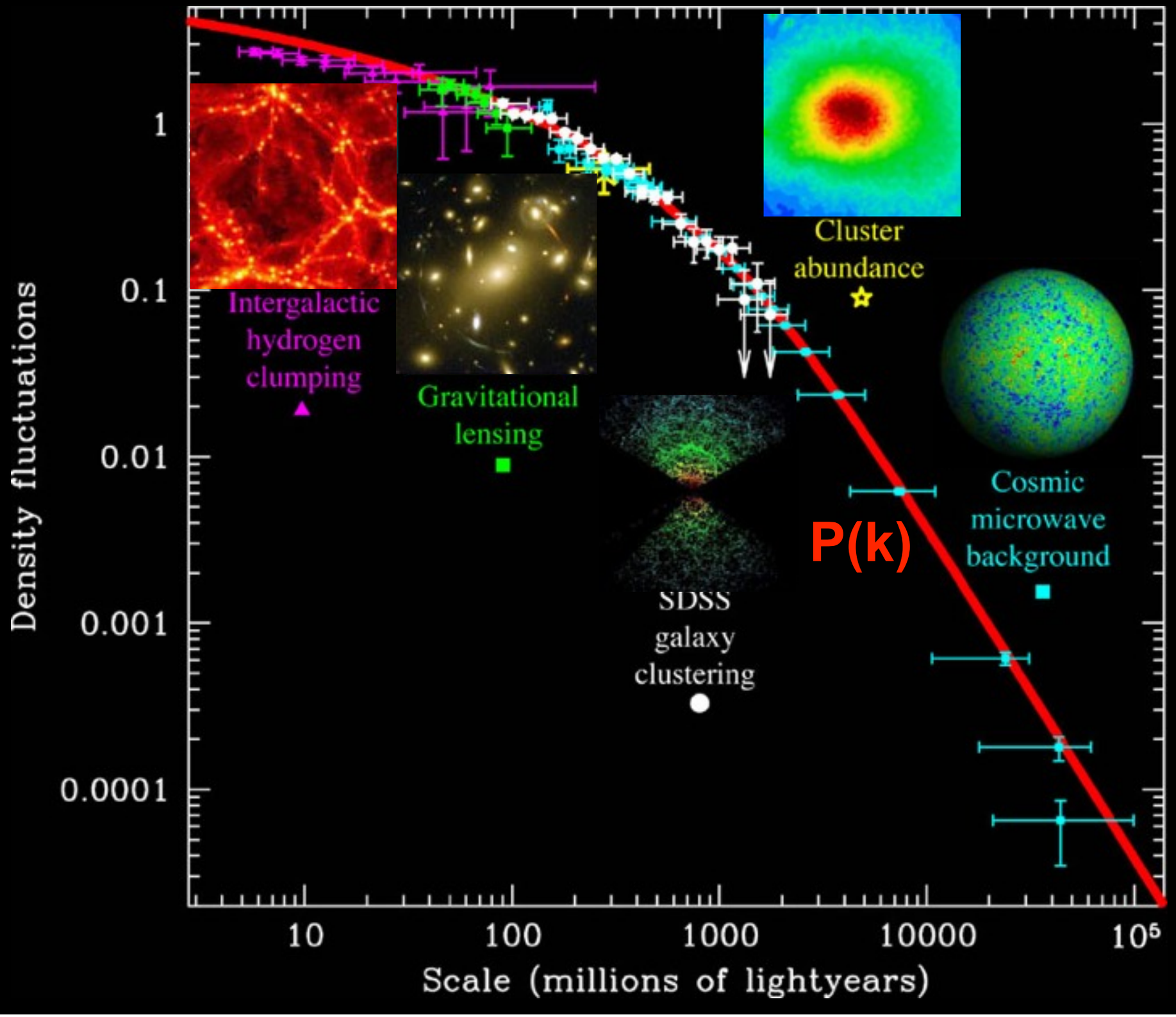

Max Tegmark

Filamentary Structure: Zel'dovich Approximation

displacement from initial position: $x(q,t) = q - D(t)\,\nabla\phi(q)$

Growth Factor

continuity: $\rho(x,t)\,d^3x = \rho_q d^3q \quad \rightarrow$

$$\rightarrow \rho(x,t) = \rho_q \,/\, \| \partial\vec{x} / \partial\vec{q} \|$$

$$= \frac{\rho_q}{(1-D(t)\lambda_1)(1-D(t)\lambda_2)(1-D(t)\lambda_3)}$$

eigenvalues of deformation tensor: $\lambda_i \equiv \frac{\partial^2\phi}{\partial^2 q_i}, \quad \lambda_1 \geq \lambda_2 \geq \lambda_3$

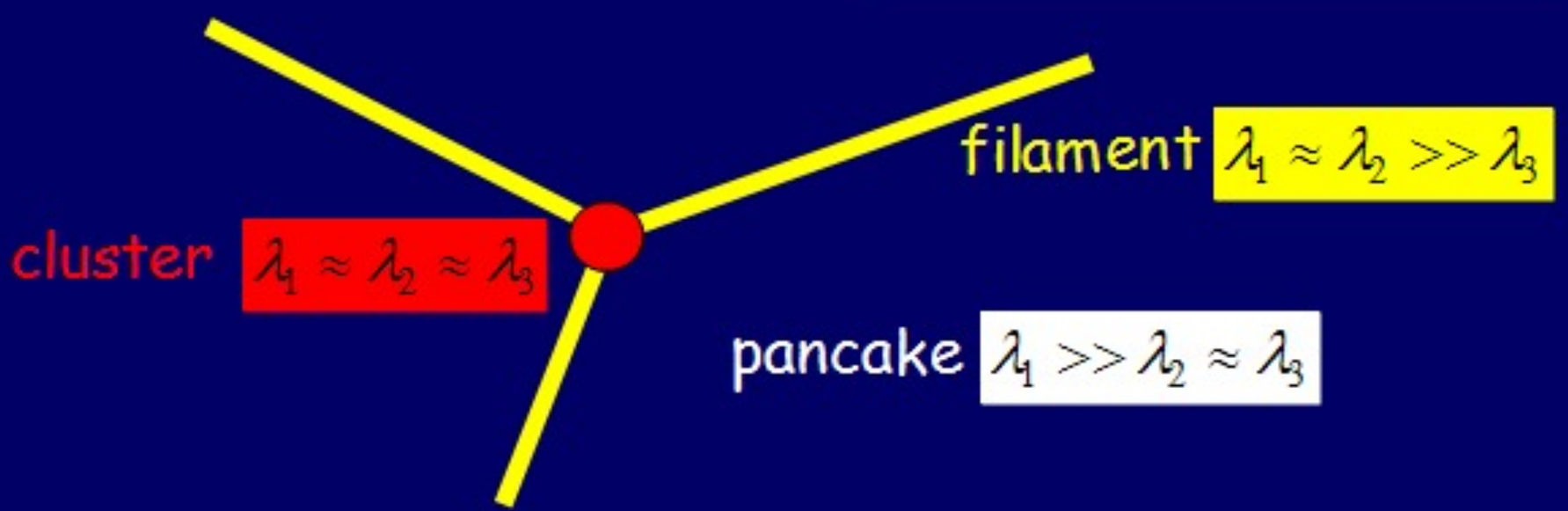

Mon. Not. R. Astron. Soc. **336,** 112–118 (2002)

The abundance and clustering of dark haloes in the standard ΛCDM cosmogony

H. J. Mo★ and S. D. M. White★

Max-Planck-Institute für Astrophysik, Karl-Schwarzschild-Strasse 1, 85740 Garching, Germany

Accepted 2002 May 27. Received 2002 May 27; in original form 2002 March 4

ABSTRACT

$\Omega_{\rm m,0}=0.3$, $\Omega_{\Lambda,0}=0.7$, $h=0.7$ and $\sigma_8=0.9$

Much evidence suggests that we live in a flat cold dark matter universe with a cosmological constant. Accurate analytic formulae are now available for many properties of the dark halo population in such a Universe. Assuming current 'concordance' values for the cosmological parameters, we plot halo abundance against redshift as a function of halo mass, halo temperature, the fraction of cosmic matter in haloes, halo clustering strength, and the clustering strength of the $z=0$ descendants of high-redshift haloes. These plots are useful for understanding how nonlinear structure grows in the model. They demonstrate a number of properties that may seem surprising, for example: 10^9 $M_\odot$ haloes are as abundant at $z=20$ as L_* galaxies are today; 10^6 K haloes are equally abundant at $z=8$ and at $z=0$; 10 per cent of all matter is currently in haloes hotter than 1 keV, while more than half is in haloes too cool to trap photo-ionized gas; 1 per cent of all matter at $z=15$ is in haloes hot enough to ionize hydrogen; haloes of given mass or temperature are more clustered at *higher* redshift; haloes with the abundance of present-day L_* galaxies are equally clustered at all $z<20$; the metals produced by star-formation at $z>10$ are more clustered at $z=0$ than are L_* galaxies.

H. J. Mo, S.D.M. White
MNRAS 336 (2002) 112

The abundance and clustering of dark haloes in the standard Lambda CDM cosmogony

We define the characteristic properties of a dark halo within a sphere of radius r_{200} chosen so that the mean enclosed density is 200 times the mean cosmic value. Then, with the Fourier transform of a radius R spherical top hat $\tilde{W}(x) = 3(\sin kR - kR\cos kR)/(kR)^3$

$$r_{200} = \left[\frac{GM}{100\Omega_{\rm m}(z)H^2(z)}\right]^{1/3}, \quad \text{and} \quad V_c = \left(\frac{GM}{r_{200}}\right)^{1/2}, R(M) \equiv \left(\frac{3M}{4\pi\bar{\rho}_0}\right)^{1/3}, \quad \sigma^2(R) = \frac{1}{2\pi^2}\int_0^\infty k^3 P(k)\tilde{W}^2(kR)\frac{{\rm d}k}{k},$$

According to the argument first given by Press & Schechter (1974, hereafter PS), the abundance of haloes as a function of mass and redshift, expressed as the number of haloes per unit comoving volume at redshift z with mass in the interval $(M, M + dM)$, may be written as

$$n(M,z){\rm d}M = \sqrt{\frac{2}{\pi}}\frac{\bar{\rho}_0}{M}\frac{{\rm d}\nu}{{\rm d}M}\exp\left(-\frac{\nu^2}{2}\right){\rm d}M\,. \tag{9}$$

Here $\nu \equiv \delta_c/[D(z)\sigma(M)]$, where $\delta_c \approx 1.69$ and the growth factor is $D(z) = g(z)/[g(0)(1+z)]$ with

$$g(z) \approx \frac{5}{2}\Omega_{\rm m}\left[\Omega_{\rm m}^{4/7} - \Omega_\Lambda + (1+\Omega_{\rm m}/2)(1+\Omega_\Lambda/70)\right]^{-1}, \ \Omega_{\rm m} \equiv \Omega_{\rm m}(z), \quad \Omega_\Lambda \equiv \Omega_\Lambda(z) = \frac{\Omega_{\Lambda,0}}{E^2(z)}.$$

$$E(z) = \left[\Omega_{\Lambda,0} + (1-\Omega_0)(1+z)^2 + \Omega_{{\rm m},0}(1+z)^3\right]^{\frac{1}{2}}.$$

Lahav, Lilje, Primack, & Rees 1991

Press & Schechter derived the above mass function from the *Ansatz* that the fraction F of all cosmic mass which at redshift z is in haloes with masses exceeding M is *twice* the fraction of randomly placed spheres of radius $R(M)$ which have linear overdensity at that time exceeding δ_c, the value at which a spherical perturbation collapses. Since the linear fluctuation distribution is gaussian this hypothesis implies

$$F(>M,z) = {\rm erfc}\left(\frac{\nu}{\sqrt{2}}\right), \tag{12}$$

and equation (9) then follows by differentiation.

The PS formula is $$n(M,z)\mathrm{d}M = \sqrt{\frac{2}{\pi}}\frac{\bar{\rho}_0}{M}\frac{\mathrm{d}\nu}{\mathrm{d}M}\exp\left(-\frac{\nu^2}{2}\right)\mathrm{d}M \quad (9)$$

Numerical simulations show that although the scaling properties implied by the PS argument hold remarkably well for a wide variety of hierarchical cosmogonies, substantially better fits to simulated mass functions are obtained if the error function in equation (12) is replaced by a function of slightly different shape. Sheth & Tormen (1999) suggested the following modification of equation (9)

$$n(M,z)\mathrm{d}M = A\left(1+\frac{1}{\nu'^{2q}}\right)\sqrt{\frac{2}{\pi}}\frac{\bar{\rho}}{M}\frac{\mathrm{d}\nu'}{\mathrm{d}M}\exp\left(-\frac{\nu'^2}{2}\right)\mathrm{d}M, \quad (14)$$

where $\nu' = \sqrt{a}\nu$, $a = 0.707$, $A \approx 0.322$ and $q = 0.3$.

[See Sheth, Mo & Tormen (2001) and Sheth & Tormen (2002) for a justification of this formula in terms of an ellipsoidal model for perturbation collapse.] The fraction of all matter in haloes with mass exceeding M can be obtained by integrating equation (14). To good approximation,

$$F(>M,z) \approx 0.4\left(1+\frac{0.4}{\nu^{0.4}}\right)\mathrm{erfc}\left(\frac{0.85\nu}{\sqrt{2}}\right)$$

In a detailed comparison with a wide range of simulations, Jenkins et al. (2001) confirmed that this model is indeed a good fit provided haloes are defined at the same density contrast relative to the mean in all cosmologies. This is for FOF halo finding -- but Klypin, Trujillo, Primack 2010 find that the more physical Bound Density Maximum (BDM) halo finder results in 10x lower halo number density at z=10.

Comoving Halo Number Density $n(M_{halo})$

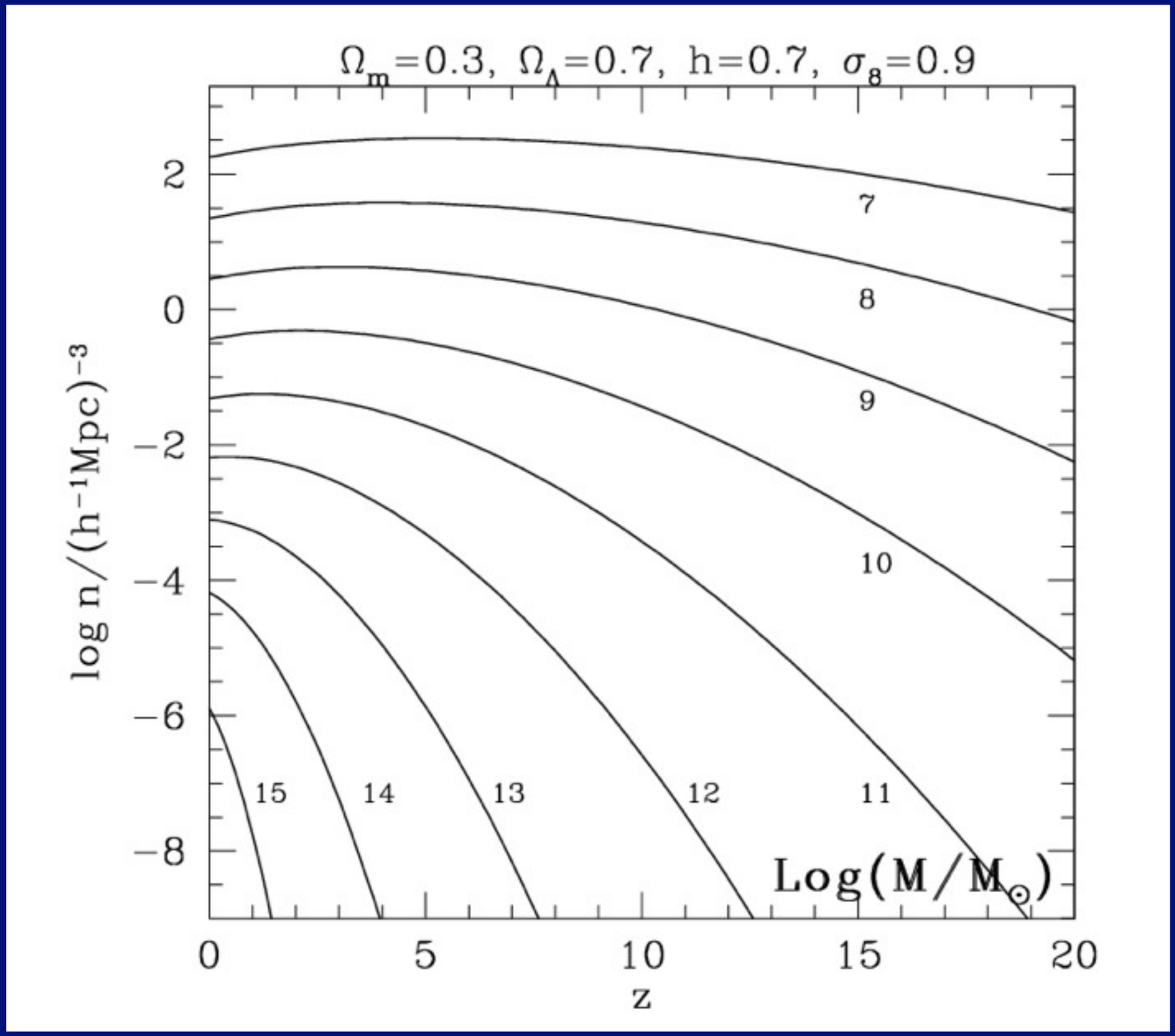

Mo & White 2002

Comoving Halo Number Density $n(M_{halo})$

Mo & White 2002

Standard LCDM

$\Omega_{m,0} = 0.3$, $\Omega_{\Lambda,0} = 0.7$, $h = 0.7$ and $\sigma_8 = 0.9$

About 1% of the mass is in halos with $M > 10^{15}\ M_\odot$ at $z = 0$, $M > 10^{12}\ M_\odot$ at $z = 5$, and $M > 10^{10}\ M_\odot$ at $z = 10$

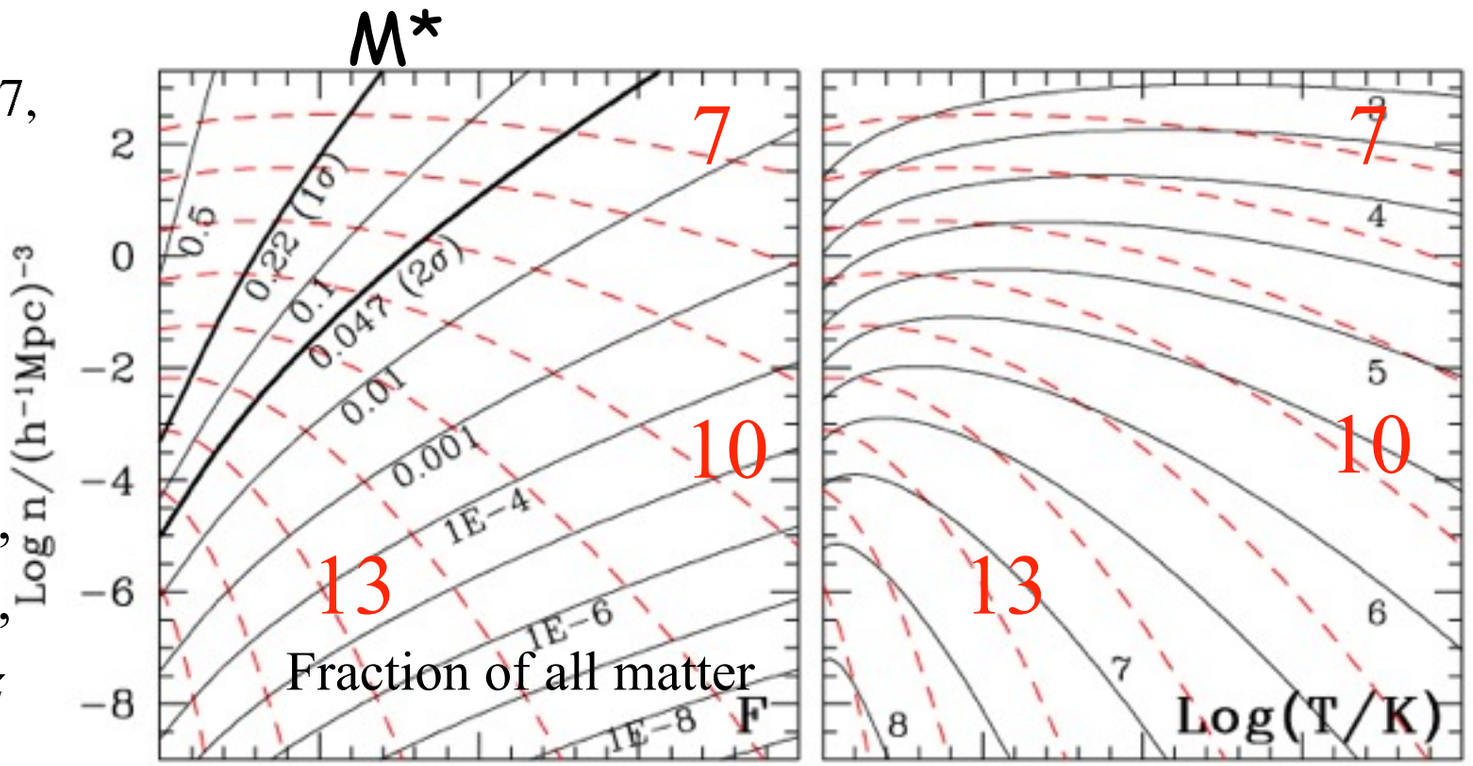

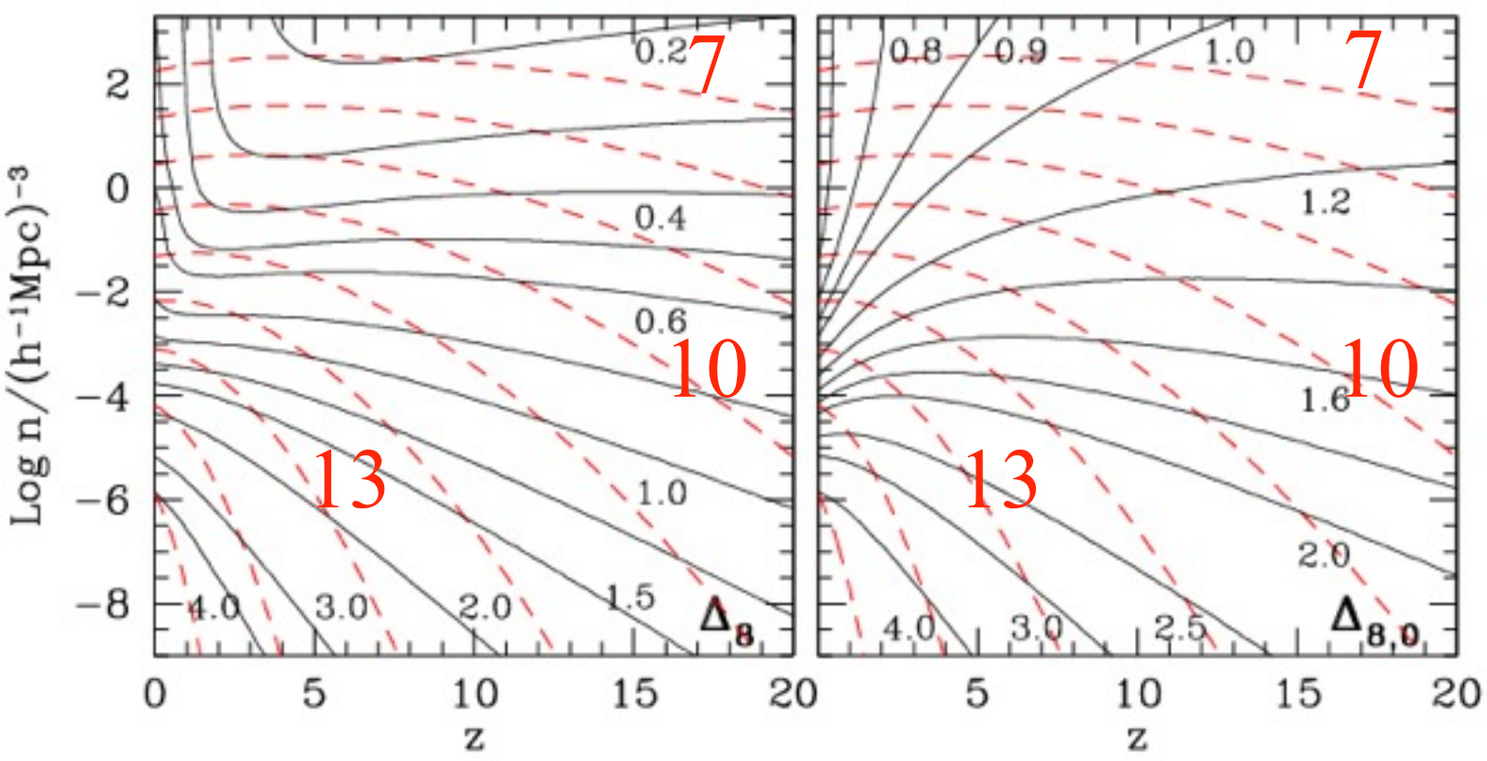

Δ_8 = "comoving clustering length of halos" = rms overdensity of halos > M at plotted redshift

A $10^{12}\ M_\odot$ halo now and a $2 \times 10^{10}\ M_\odot$ halo at $z = 20$ both have $T \sim 10^6$ K (i.e, $V_c \sim 200$ km/s)

T = virial temperature

$\Delta_{8,0}$ = comoving clustering length of halo descendants at $z = 0$

Dashed red curves: halo number density for log M/M_{sun}

Sheth-Tormen Fails at High Redshifts

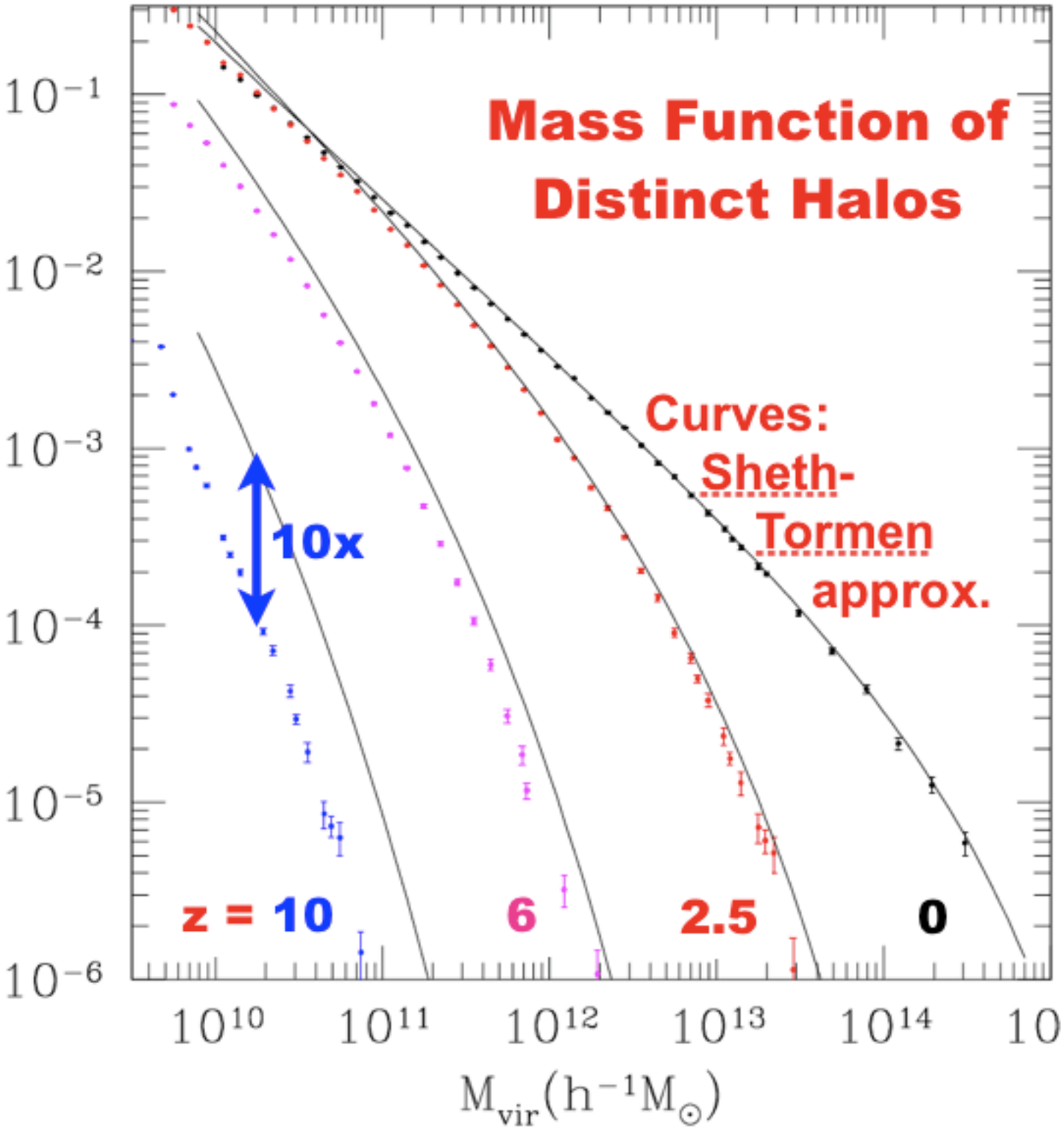

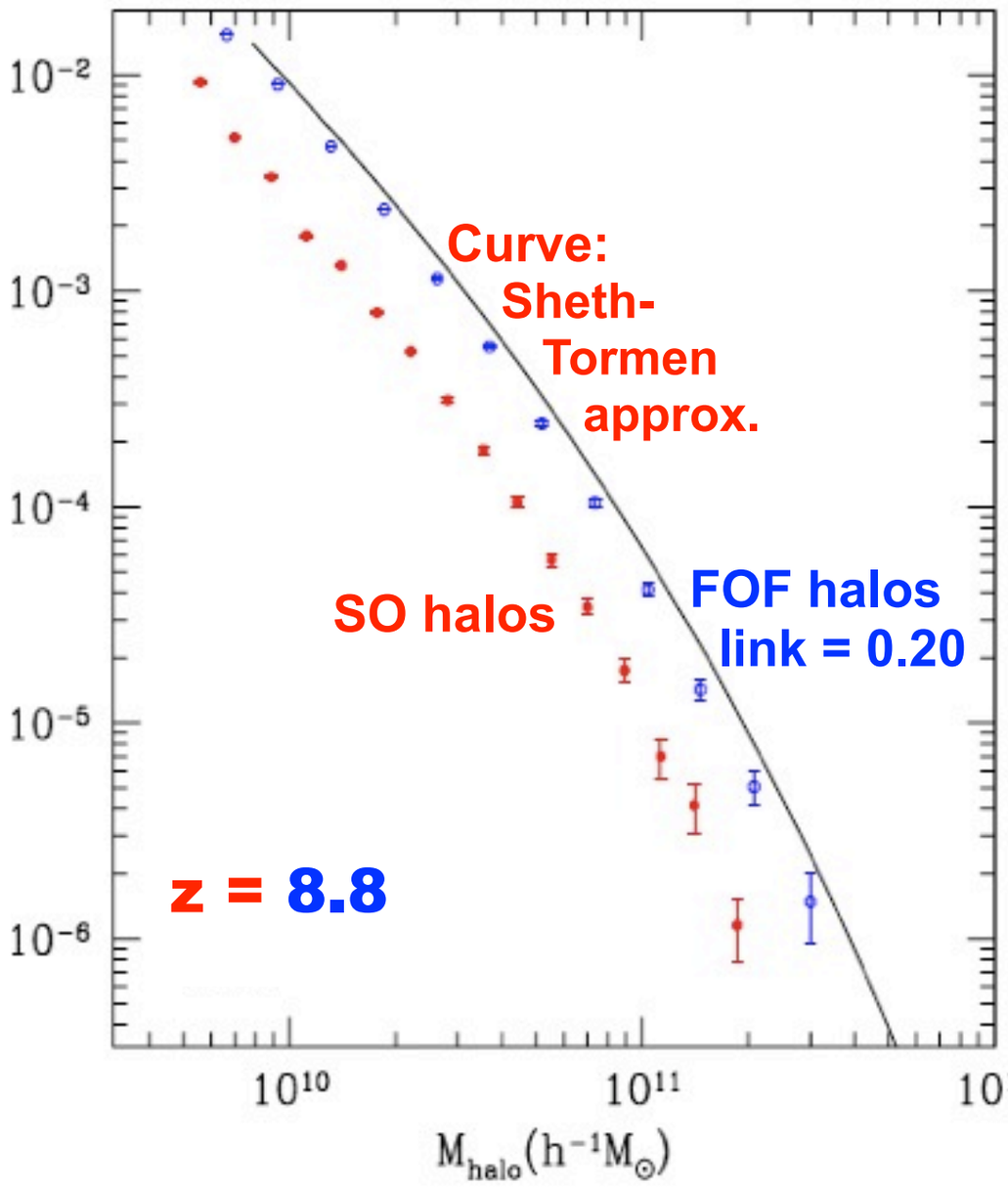

Sheth-Tormen approximation with the same WMAP5 parameters used for Bolshoi simulation very accurately agrees with abundance of halos at low redshifts, but increasingly overpredicts bound spherical overdensity halo abundance at higher redshifts.

Klypin, Trujillo, & Primack, arXiv: 1002.3660v3

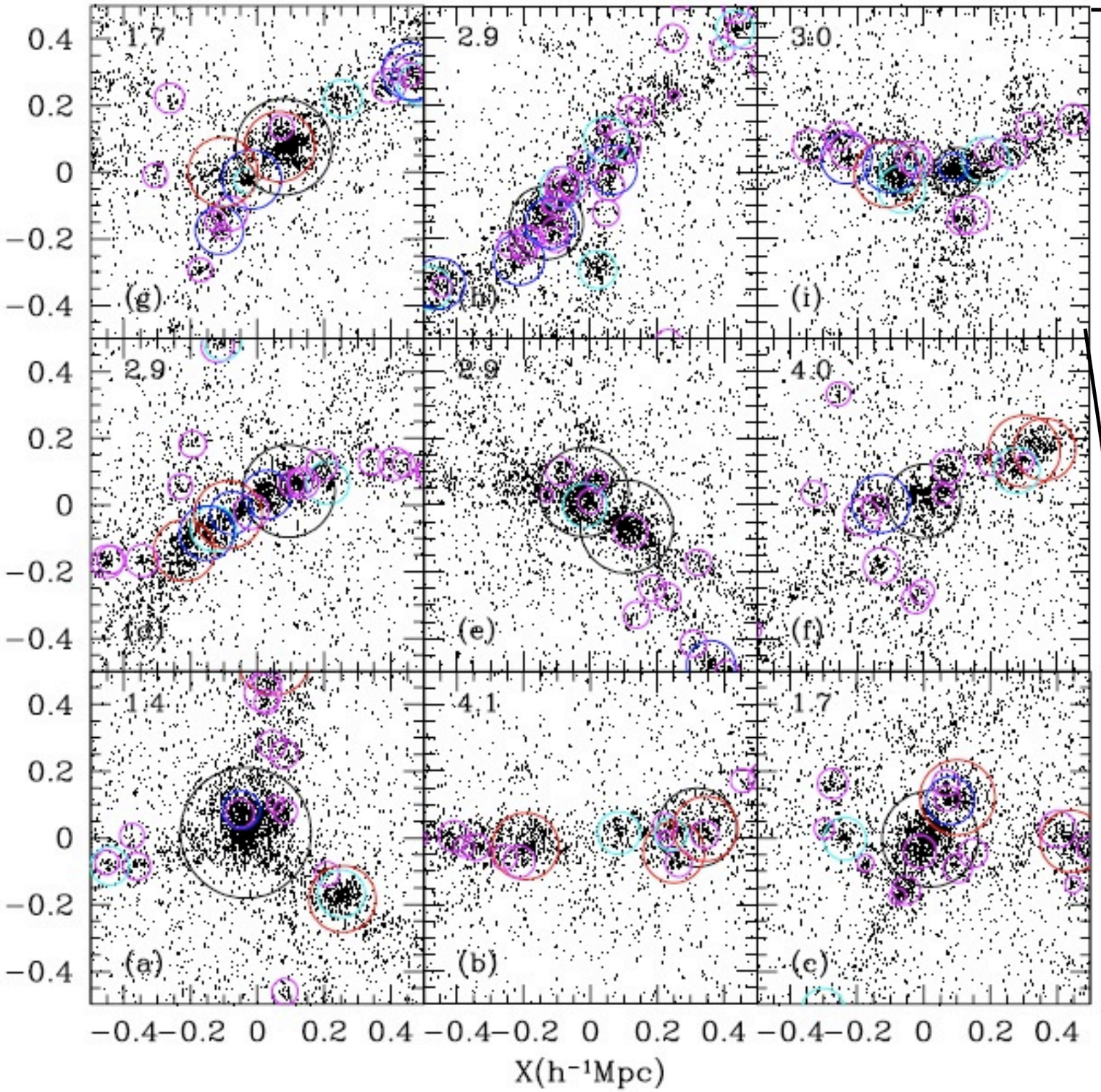

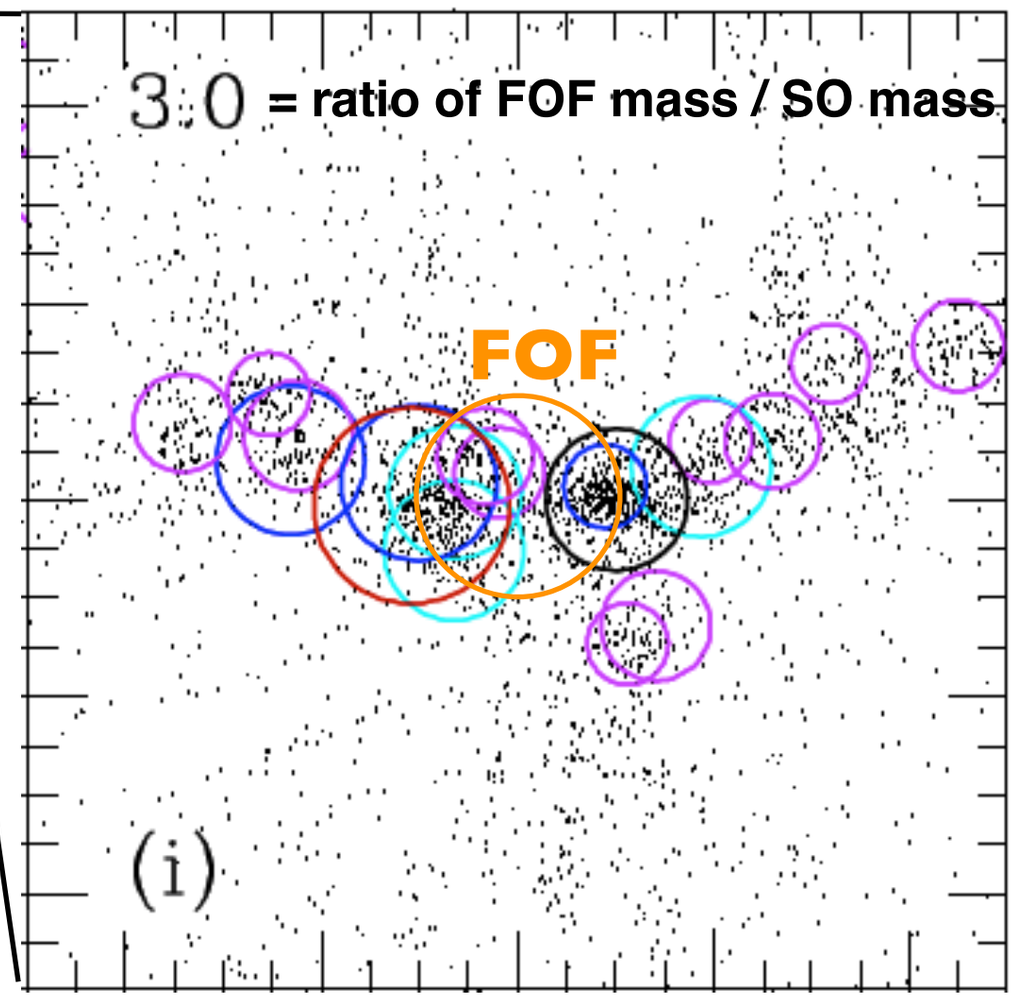

FOF linked together a chain of halos that formed in long and dense filaments (also in panels b, d, f, h; e = major merger)

Each panel shows 1/2 of the dark matter particles in cubes of $1h^{-1}$ Mpc size. The center of each cube is the exact position of the center of mass of the corresponding FOF halo. The effective radius of each FOF halo in the plots is 150 – 200 h^{-1} kpc. Circles indicate virial radii of distinct halos and subhalos identified by the spherical overdensity algorithm BDM.

Klypin, Trujillo, & Primack, arXiv: 1002.3660v3

Cosmological Simulation Methods

Dissipationless Simulations

Particle-Particle (PP) - Aarseth NbodyN, N=1,...,6
Particle Mesh (PM) - see Klypin & Holtzman 1997
Adaptive PM (P3M) - Efstathiou et al.
Tree - Barnes & Hut 1986, PKDGRAV Stadel
TreePM - GADGET2, Springel 2005
Adaptive Mesh Refinement (AMR) - Klypin (ART)

Hydrodynamical Simulations

Fixed grid - Cen & Ostriker
Smooth Particle Hydrodynamics (SPH) - GADGET2, Springel 2005
- Gasoline, Wadsley, Stadel, & Quinn
Adaptive grid - ART+hydro - Klypin & Kravtsov; ENZO - Norman et al.;
- RAMSES - Teyssier

Initial Conditions

Standard: Gaussian P(k) realized uniformly, Zel'dovich displacement
Multimass - put lower mass particles in a small part of sim volume
Constrained realization - small scale: simulate individual halos (NFW)
large scale: simulate particular region

Reviews

Bertschinger ARAA 1998; Klypin lectures 2002; U Washington website http://www-hpcc.astro.washington.edu/; UC-HiPACC 2010 summer school at UCSC http://hipacc.ucsc.edu/html/2010SummerSchool_archive.html

Structure of Dark Matter Halos

Navarro, Frenk, White

1996 1997 →

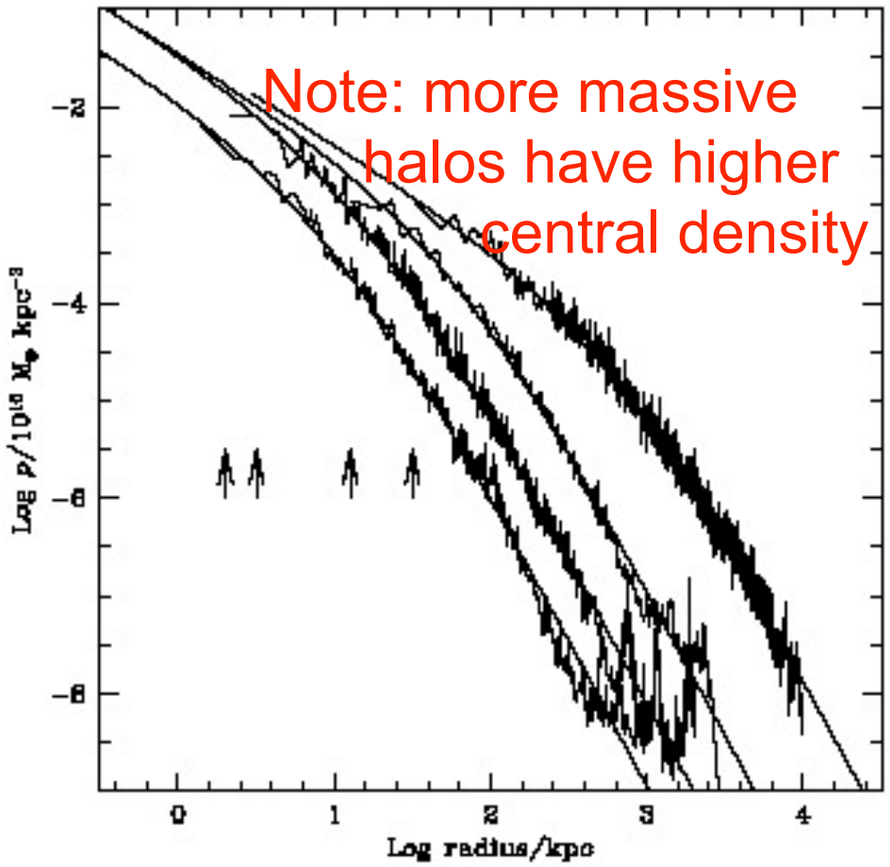

Fig. 3.— Density profiles of four halos spanning four orders of magnitude in mass. The arrows indicate the gravitational softening, h_g, of each simulation. Also shown are fits from eq.3. The fits are good over two decades in radius, approximately from h_g out to the virial radius of each system.

$$\frac{\rho(r)}{\rho_{crit}} = \frac{\delta_c}{(r/r_s)(1+r/r_s)^2}, \qquad (3)$$

NFW is a good approximation for all models

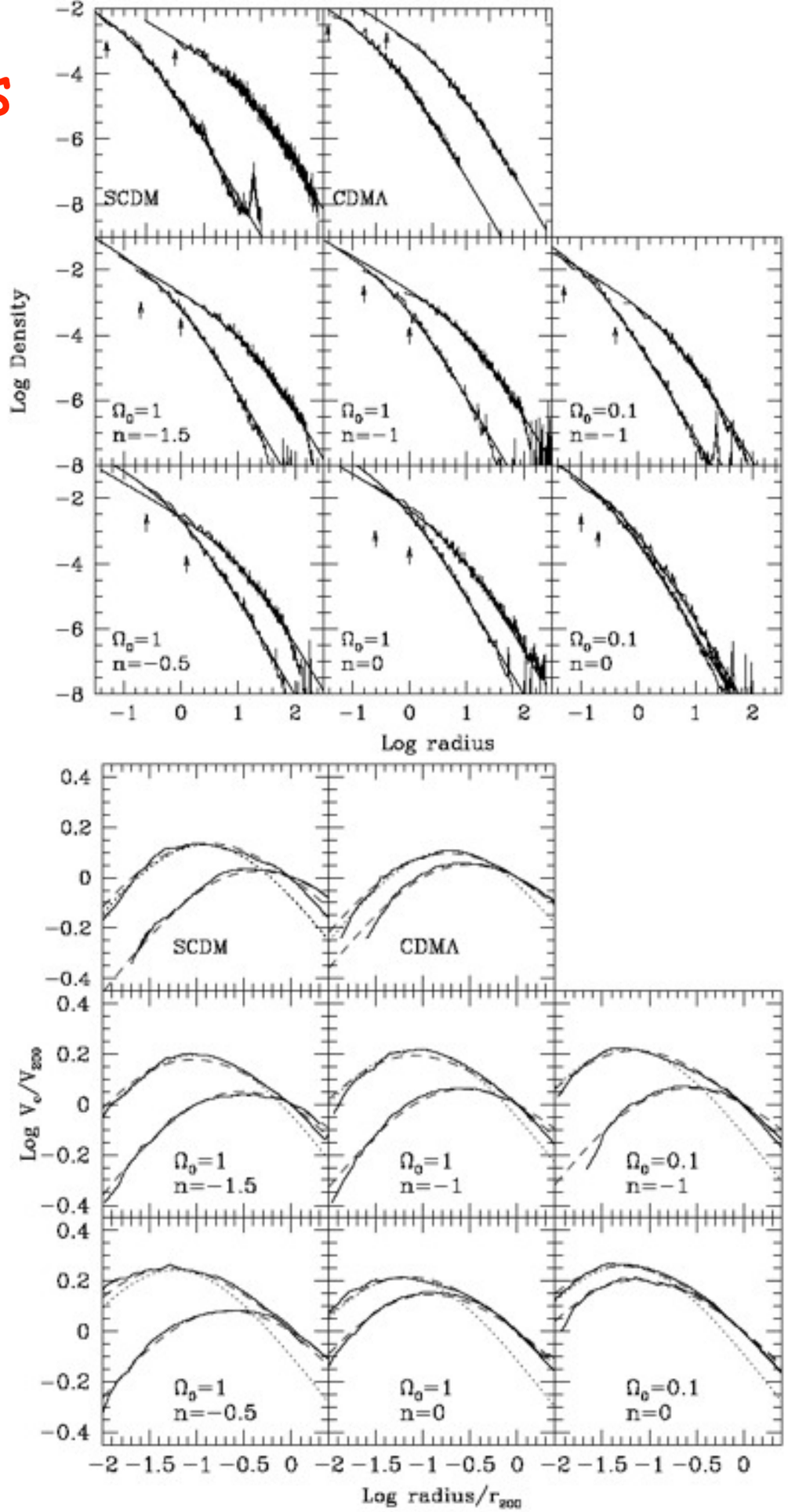

Dark Matter Halo Radial Profile

Comparison of NFW and Moore et al. profiles

Parameter	NFW	Moore et al.
Density $x = r/r_s$	$\rho = \frac{\rho_s}{x(1+x)^2}$ $\rho \propto x^{-3}$ for $x \gg 1$ $\rho \propto x^{-1}$ for $x \ll 1$ $\rho/\rho_s = 1/4$ at $x = 1$	$\rho = \frac{\rho_s}{x^{1.5}(1+x)^{1.5}}$ $\rho \propto x^{-3}$ for $x \gg 1$ $\rho \propto x^{-1.5}$ for $x \ll 1$ $\rho/\rho_s = 1/2$ at $x = 1$
Mass $M = 4\pi\rho_s r_s^3 f(x)$ $= M_{\rm vir} f(x)/f(C)$ $M_{\rm vir} = \frac{4\pi}{3}\rho_{\rm cr}\Omega_0\delta_{\rm top-hat} r_{\rm vir}^3$	$f(x) = \ln(1+x) - \frac{x}{1+x}$	$f(x) = \frac{2}{3}\ln(1+x^{3/2})$
Concentration $C = r_{\rm vir}/r_s$	$C_{\rm NFW} = 1.72 C_{\rm Moore}$ for halos with the same $M_{\rm vir}$ and $r_{\rm max}$ $C_{1/5} \approx \frac{C_{\rm NFW}}{0.86 f(C_{\rm NFW}) + 0.1363}$ error less than 3% for $C_{\rm NFW}$ =5-30 $C_{\gamma=-2} = C_{\rm NFW}$	$C_{\rm Moore} = C_{\rm NFW}/1.72$ $C_{1/5} = \frac{C_{\rm Moore}}{[(1+C_{\rm Moore}^{3/2})^{1/5} - 1]^{2/3}}$ $\approx \frac{C_{\rm Moore}}{[C_{\rm Moore}^{3/10} - 1]^{2/3}}$ $C_{\gamma=-2} = 2^{3/2} C_{\rm Moore}$ $\approx 2.83 C_{\rm Moore}$
Circular Velocity $v_{\rm circ}^2 = \frac{GM_{\rm vir}}{r_{\rm vir}}\frac{C}{x}\frac{f(x)}{f(C)}$ $= v_{\rm max}^2 \frac{x_{\rm max}}{x}\frac{f(x)}{f(x_{\rm max})}$ $v_{\rm vir}^2 = \frac{GM_{\rm vir}}{r_{\rm vir}}$	$x_{\rm max} \approx 2.15$ $v_{\rm max}^2 \approx 0.216 v_{\rm vir}^2 \frac{C}{f(C)}$ $\rho/\rho_s \approx 1/21.3$ at $x = 2.15$	$x_{\rm max} \approx 1.25$ $v_{\rm max}^2 \approx 0.466 v_{\rm vir}^2 \frac{C}{f(C)}$ $\rho/\rho_s \approx 1/3.35$ at $x = 1.25$

Klypin, Kravtsov, Bullock & Primack 2001

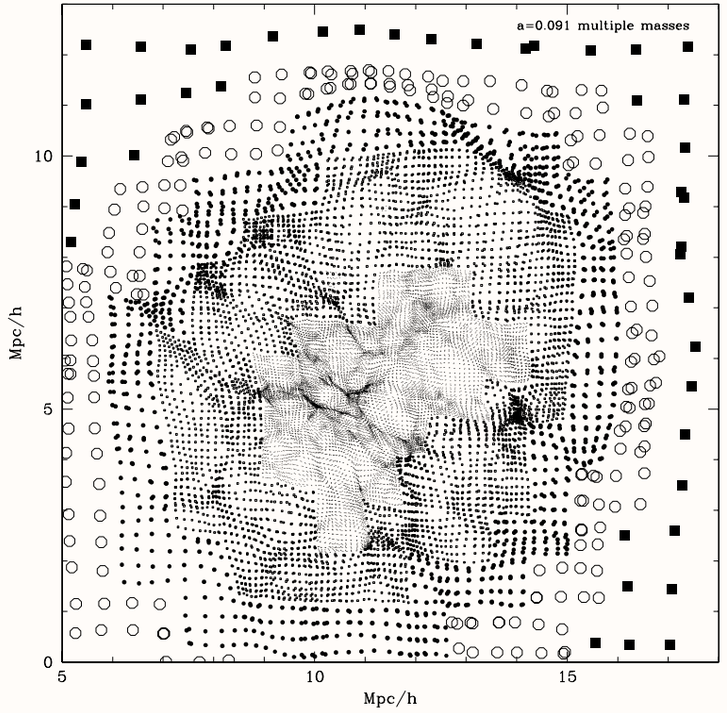

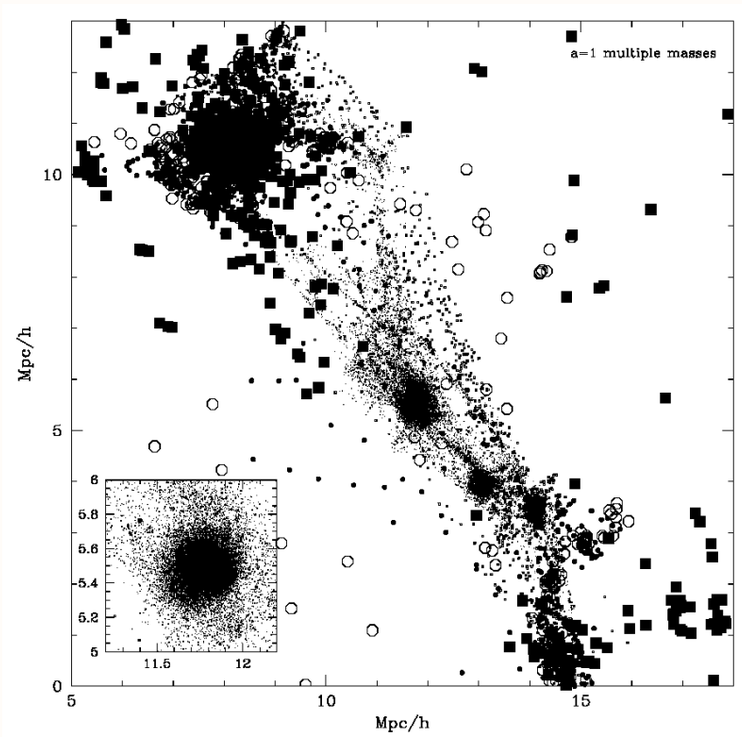

Fig. 2.— Distribution of particles of different masses in a thin slice through the center of halo A_1 (see Table 1) at $z = 10$ (top panel) and at $z = 0$ (bottom panel). To avoid crowding of points the thickness of the slice is made smaller in the center (about $30h^{-1}$kpc) and larger ($1h^{-1}$Mpc) in the outer parts of the forming halo. Particles of different mass are shown with different symbols: tiny dots, dots, large dots, squares, and open circles.

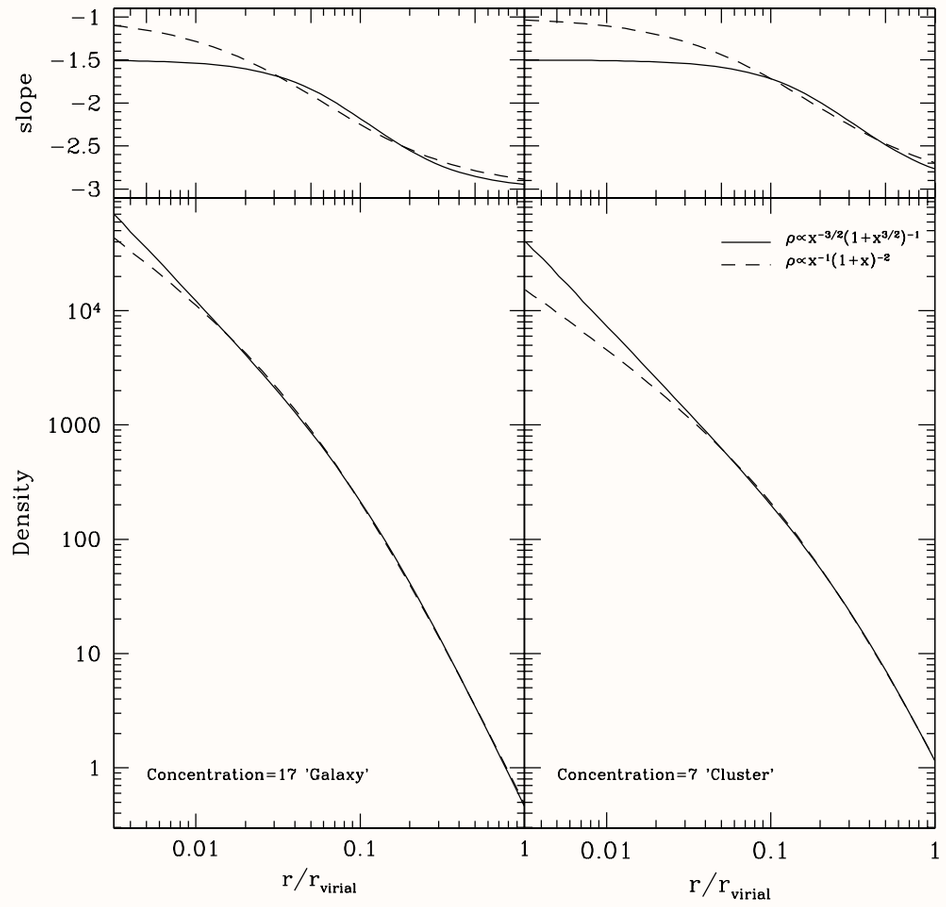

Fig. 3.— Comparison of the Moore et al. and the NFW profiles. Each profile is normalized to have the same virial mass and the same radius of the maximum circular velocity. *Left panels:* High-concentration halo typical of small galaxy-size halos $C_{\rm NFW} = 17$. *Right panels:* Low-concentration halo typical of cluster-size halos. The deviations are very small ($< 3\%$) for radii $r > r_s/2$. Top panels show the local logarithmic slope of the profiles. Note that for the high concentration halo the slope of the profile is significantly larger than the asymptotic value -1 even at very small radii $r \approx 0.01 r_{\rm vir}$.

Klypin, Kravtsov, Bullock & Primack 2001

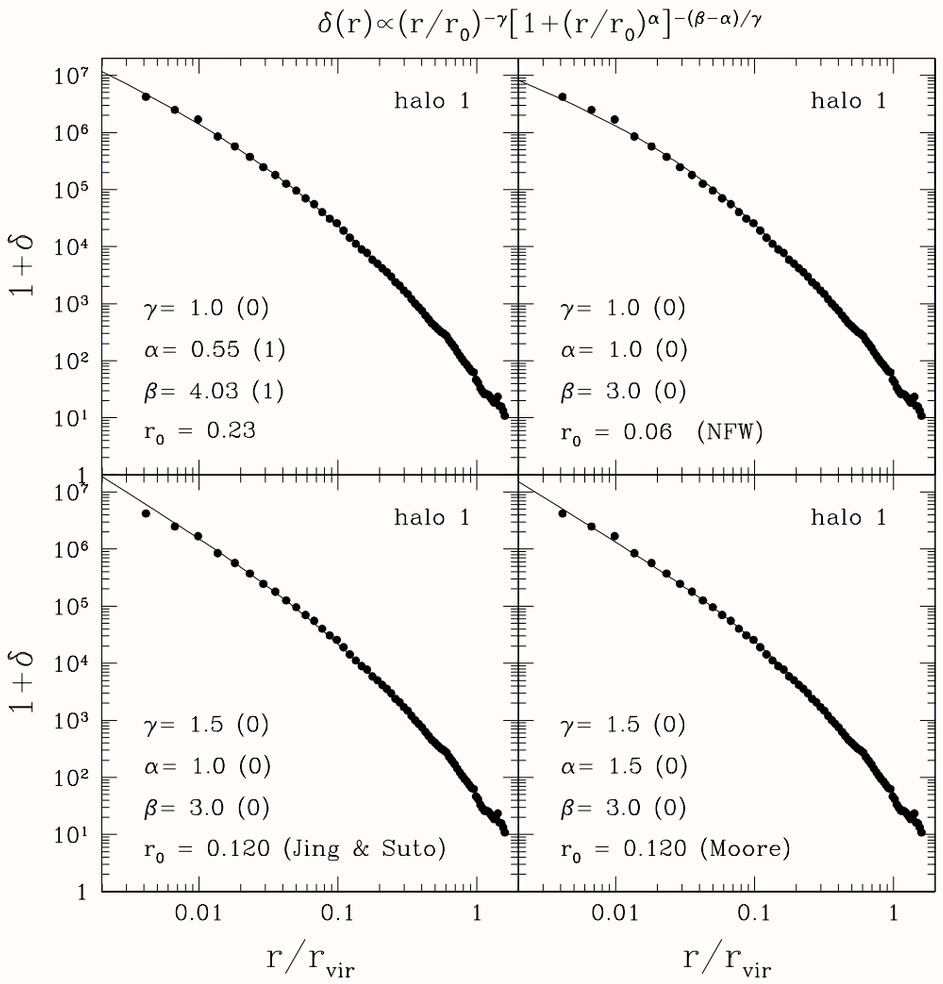

Fig. 8.— Analytic fits to the density profile of the halo A_1 from our set of simulations. The fits are of the form $\rho(r) \propto (r/r_0)^{-\gamma}[1+(r/r_0)^{\alpha}]^{-(\beta-\alpha)/\gamma}$. The legend in each panel indicates the corresponding values of α, β, and γ of the fit; the digit in parenthesis indicates whether the parameter was kept fixed (0) or not (1) during the fit. Note that various sets of parameters α, β, γ provide equally good fits to the simulated halo profile in the whole range resolved range of scales $\approx 0.005 - 1 r_{\rm vir}$. This indicates a large degree of degeneracy in parameters α, β, and γ

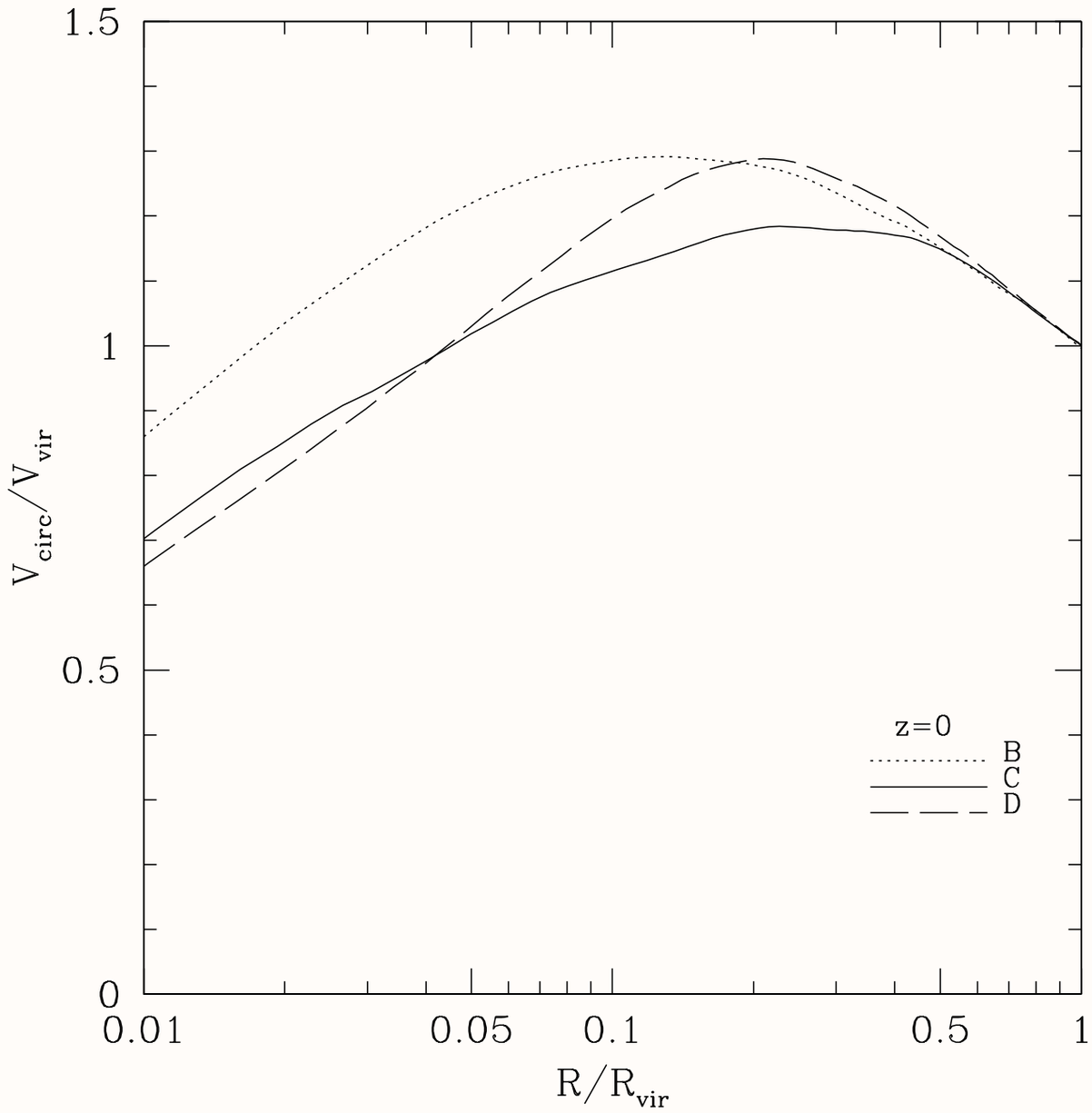

Fig. 9.— Circular velocity profiles for the halos B_1, C_1, and D_1 normalized to halo's virial velocity. Halos are well resolved on all shown scales. Although the halos have very similar masses, the profiles are very different; the differences are due to real differences in the concentration parameters.

Klypin, Kravtsov, Bullock & Primack 2001

Empirical Models for Dark Matter Halos. II. Inner profile slopes, dynamical profiles, and ρ/σ^3

Alister Graham, David Merritt, Ben Moore, Jürg Diemand, Balša Terzić 2006

Einasto's model is given by the equation

$$\rho(r) = \rho_{\rm e} \exp\left\{-d_n\left[(r/r_{\rm e})^{1/n} - 1\right]\right\}.$$

Data on log slopes from innermost resolved radius of observed galaxies, not corrected for observational effects -- adapted from de Blok (2004).

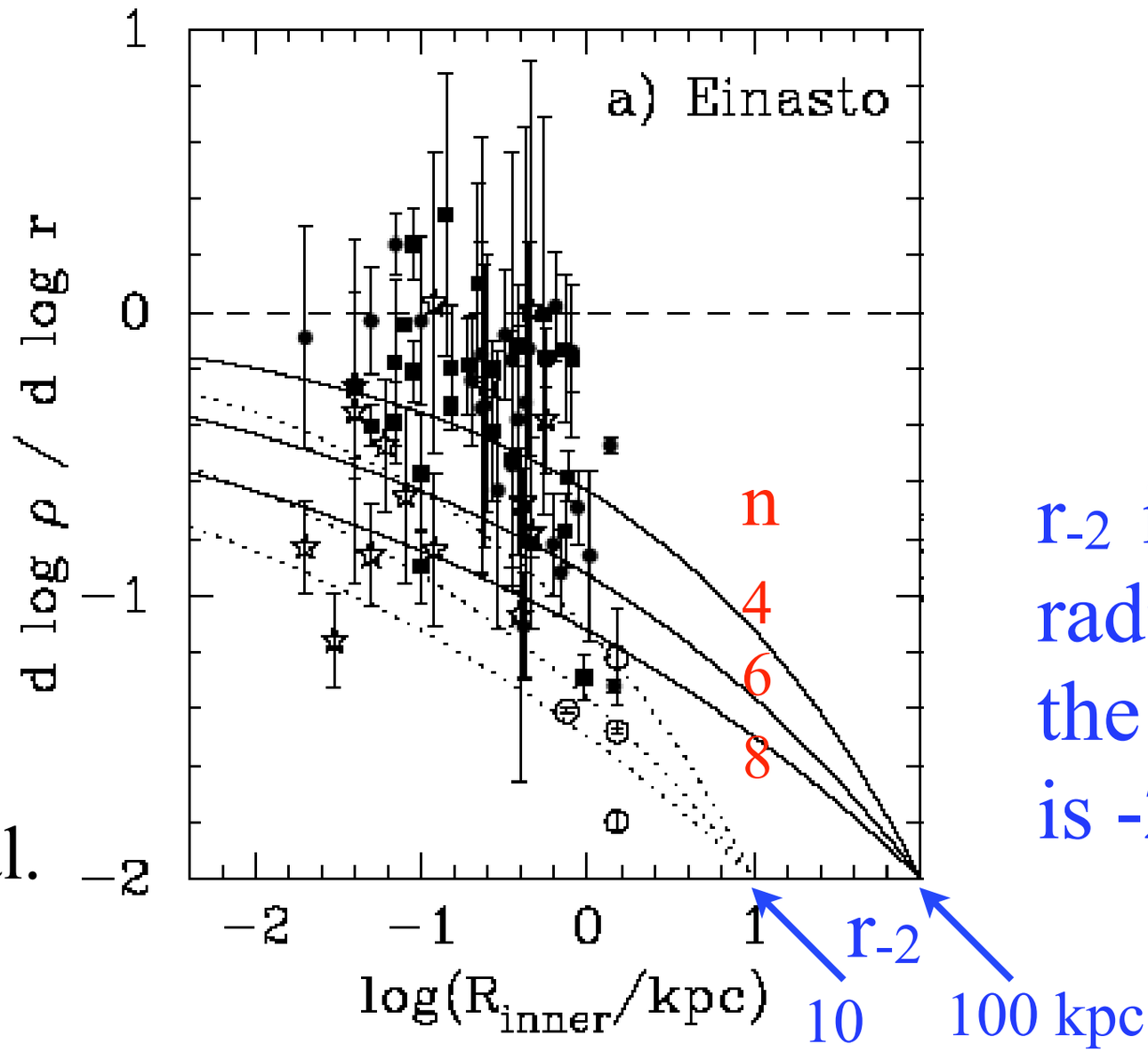

r_{-2} is the radius where the log-slope is -2

See also Navarro et al. Aquarius simulations arXiv:0810.1522

Aquarius Simulation: Formation of a Milky-Way-size Dark Matter Halo

Diameter of Milky Way Dark Matter Halo
1.6 million light years

Diameter of visible Milky Way
30 kpc = 100,000 light years

Diameter of Milky Way Dark Matter Halo
1.6 million light years

500 kpc

Volker Springel
Max-Planck-Institute
for Astrophysics

Diameter of visible Milky Way
30 kpc = 100,000 light years

Diameter of Milky Way Dark Matter Halo
1.6 million light years

500 kpc

Volker Springel
Max-Planck-Institute
for Astrophysics

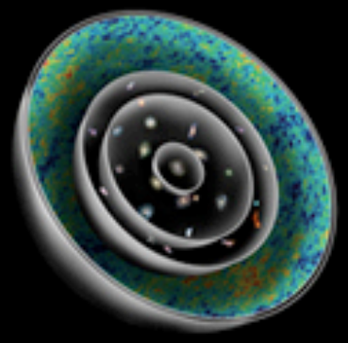

The New Universe and the Human Future

How a Shared Cosmology Could Transform the World

Nancy Ellen Abrams and Joel R. Primack

Click to view videos

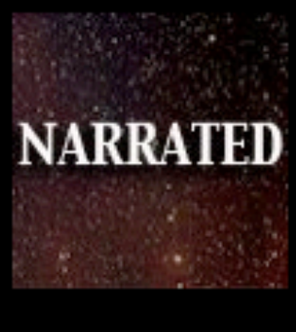

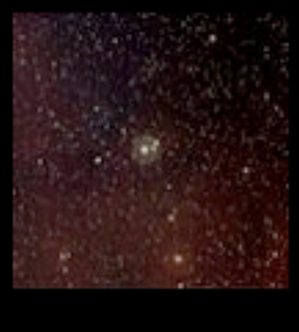

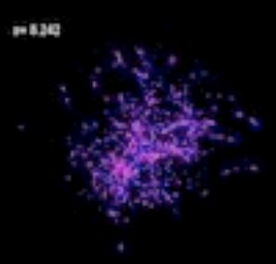

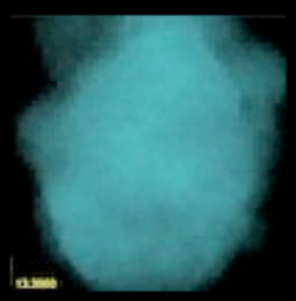

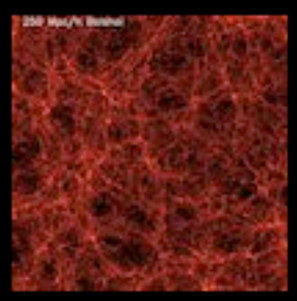

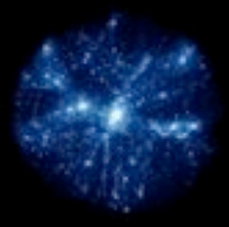

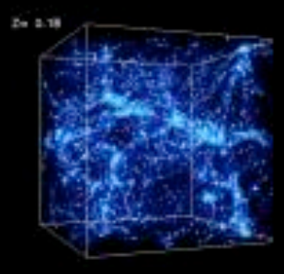

Extra Videos

Many relevant videos can be found at this URL:
http://new-universe.org/zenphoto/Chapter3/Videos/

Particle number in cosmological N-body simulations vs. pub date

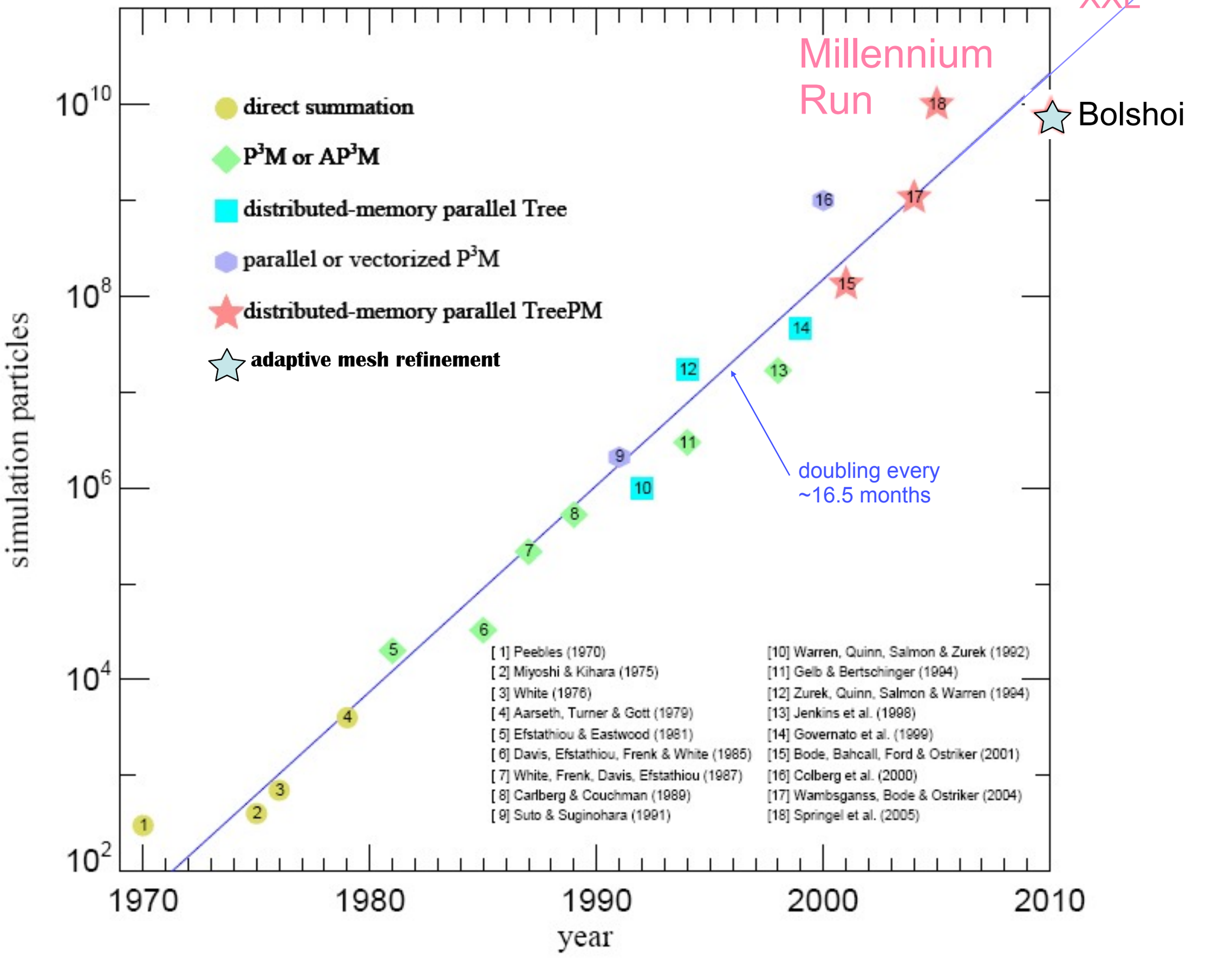

WMAP-only Determination of σ_8 and Ω_M

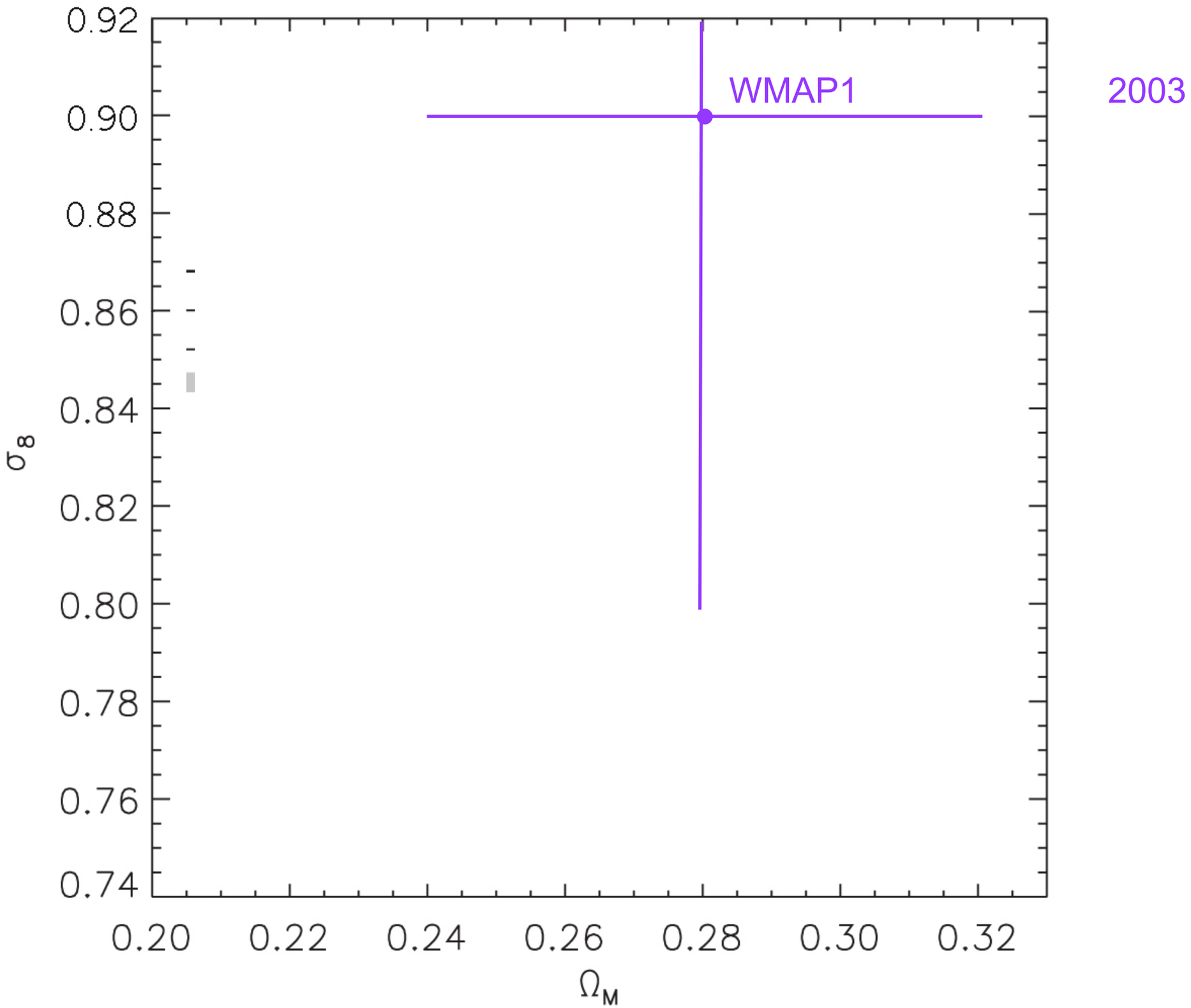

The Millennium Run

- **properties of halos** (radial profile, concentration, shapes)
- **evolution of the number density of halos**, essential for normalization of Press-Schechter-type models
- **evolution of the distribution and clustering of halos** in real and redshift space, for comparison with observations
- **accretion history of halos**, assembly bias (variation of large-scale clustering with as- sembly history), and correlation with halo properties including angular momenta and shapes
- **halo statistics** including the mass and velocity functions, angular momentum and shapes, subhalo numbers and distribution, and correlation with environment

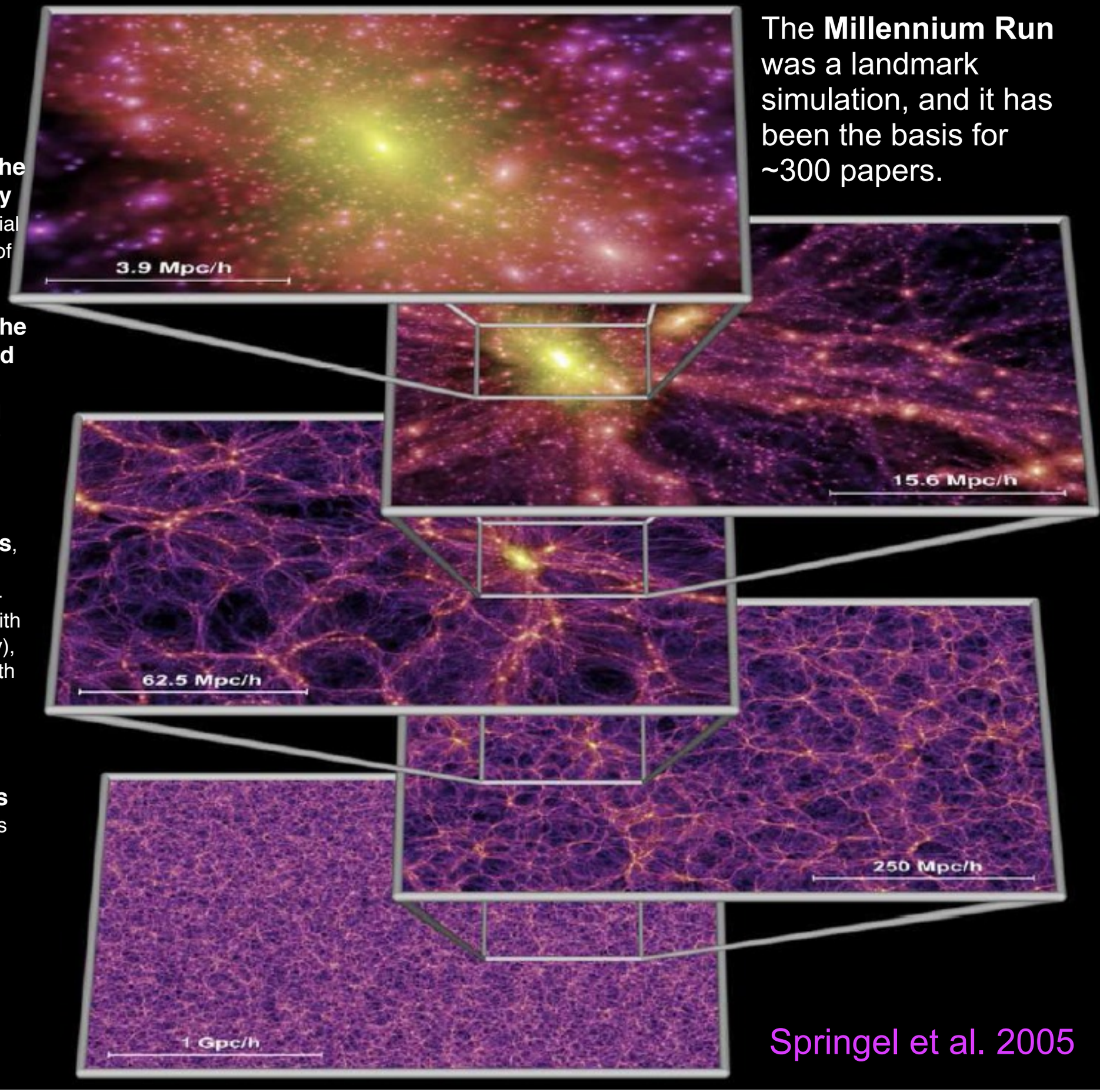

The **Millennium Run** was a landmark simulation, and it has been the basis for ~300 papers.

Springel et al. 2005

- **void statistics**, including sizes and shapes and their evolution, and the orientation of halo spins around voids
- quantitative descriptions of the evolving **cosmic web**, including applications to weak gravitational lensing
- preparation of **mock catalogs**, essential for analyzing SDSS and other survey data, and for preparing for new large surveys for dark energy etc.
- **merger trees**, essential for **semi-analytic modeling** of the evolving galaxy population, including models for the galaxy merger rate, the history of star formation and galaxy colors and morphology, the evolving AGN luminosity function, stellar and AGN feedback, recycling of gas and metals, etc.

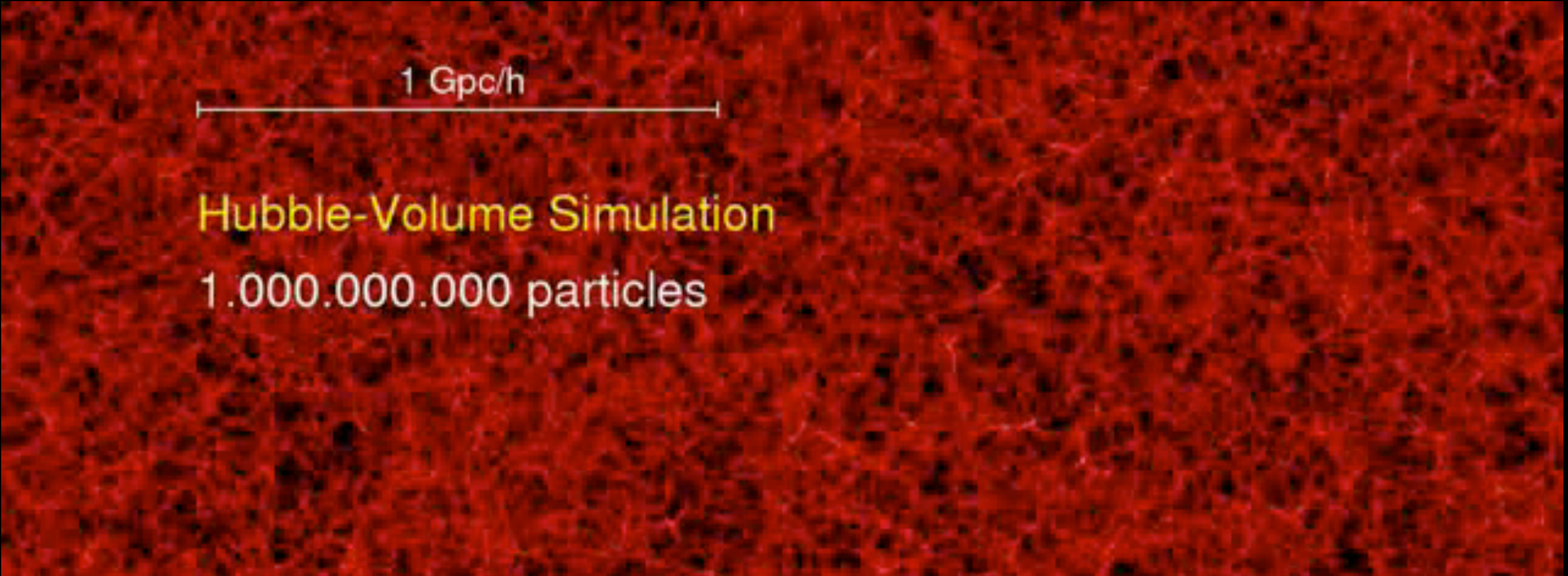
1 Gpc/h
Hubble-Volume Simulation
1.000.000.000 particles
Music: Bach, Partita No. 3
Arthur Grumiaux, violin

Environment of a ‘first quasar candidate’ at high and low redshifts. The two panels on the left show the projected dark matter distribution in a cube of comoving sidelength $10h^{-1}$Mpc, colourcoded according to density and local dark matter velocity dispersion. The panels on the right show the galaxies of the **semi-analytic model (SAM)** overlayed on a gray-scale image of the dark matter density.

The volume of the sphere representing each galaxy is proportional to its stellar mass, and the chosen colours encode the restframe stellar $B-V$ colour index. While at $z = 6.2$ (top) all galaxies appear blue due to ongoing star formation, many of the galaxies that have fallen into the rich cluster at $z = 0$ (bottom) have turned red.

Springel et al. 2005

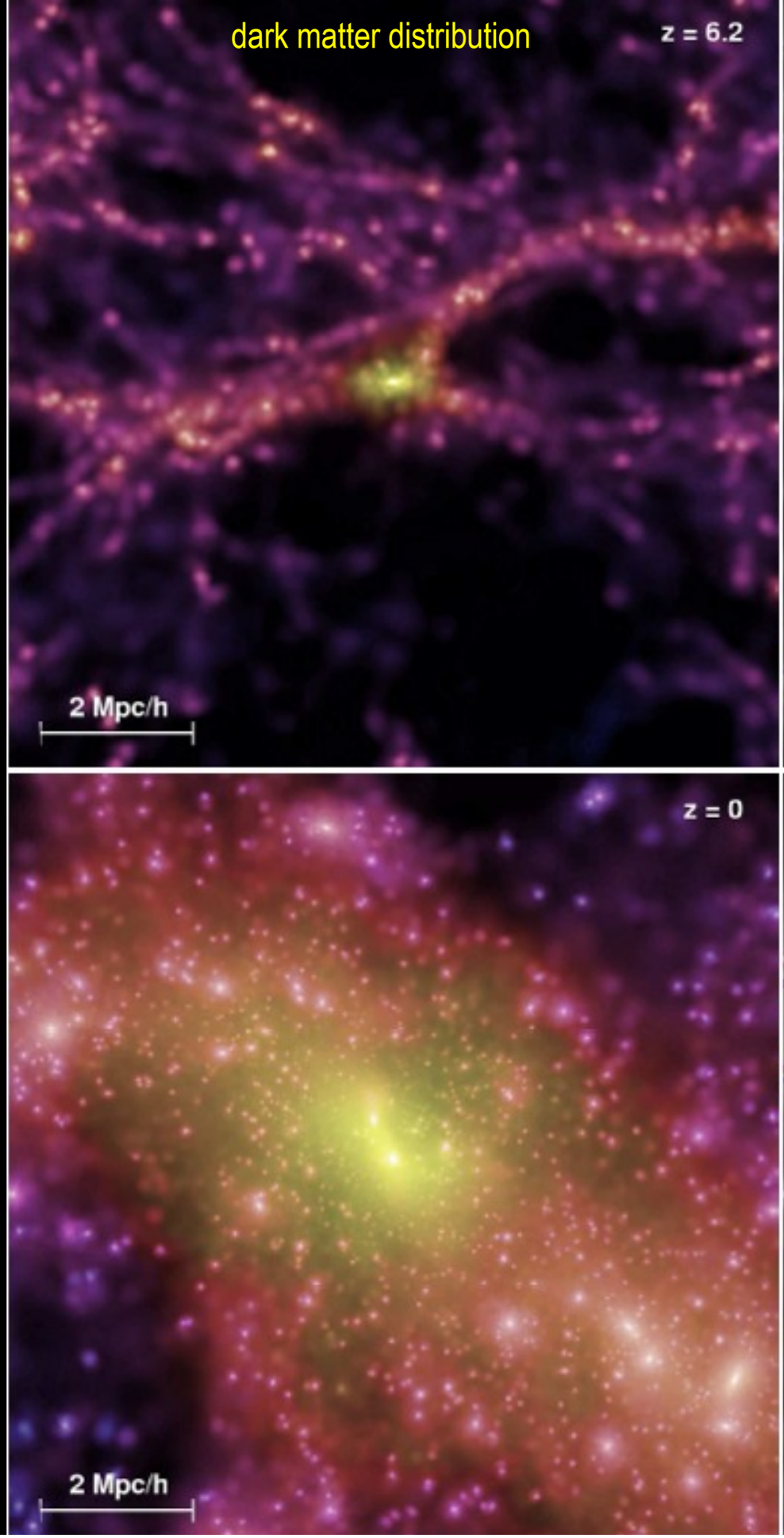

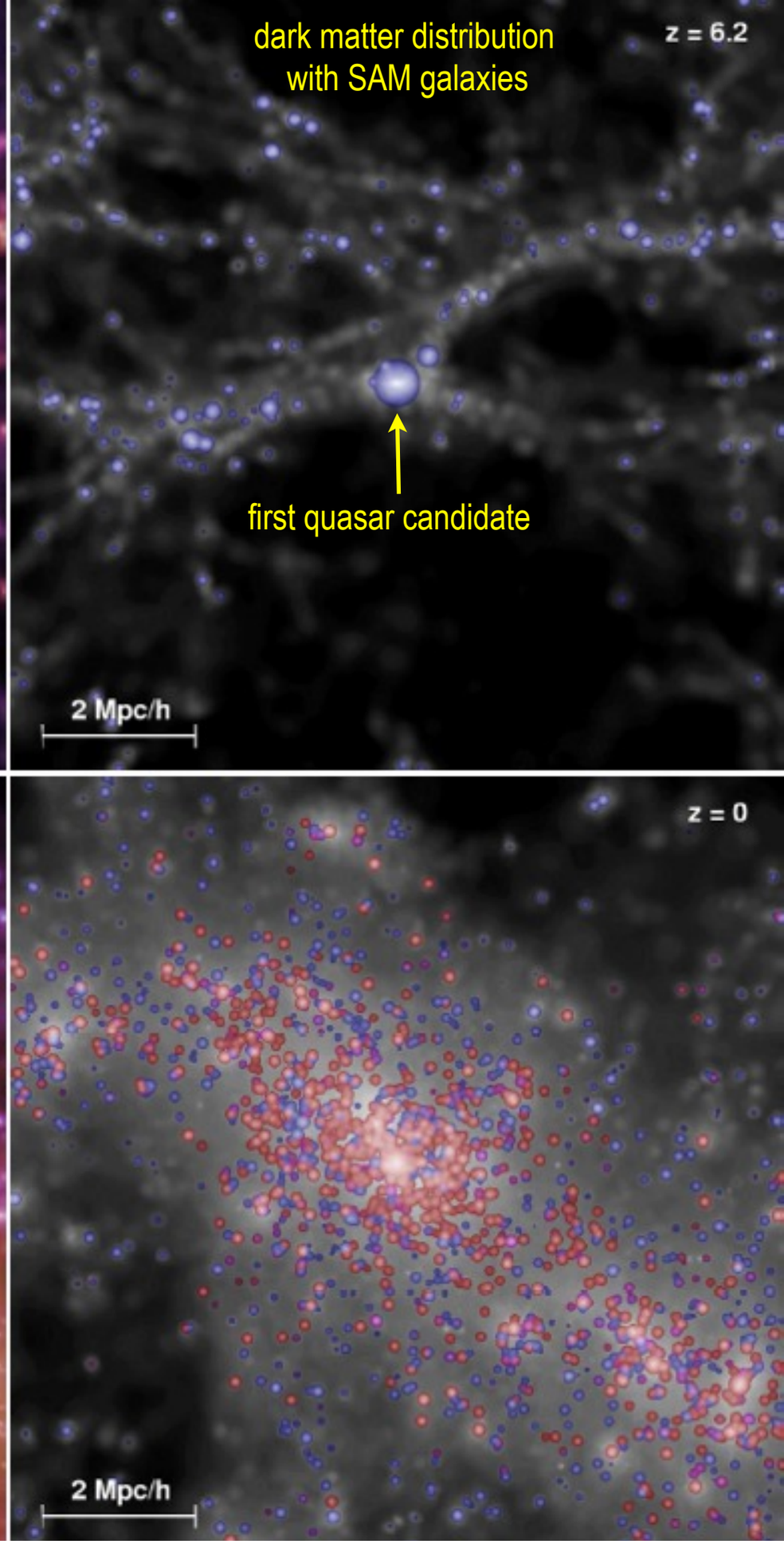

WMAP-only Determination of σ_8 and Ω_M

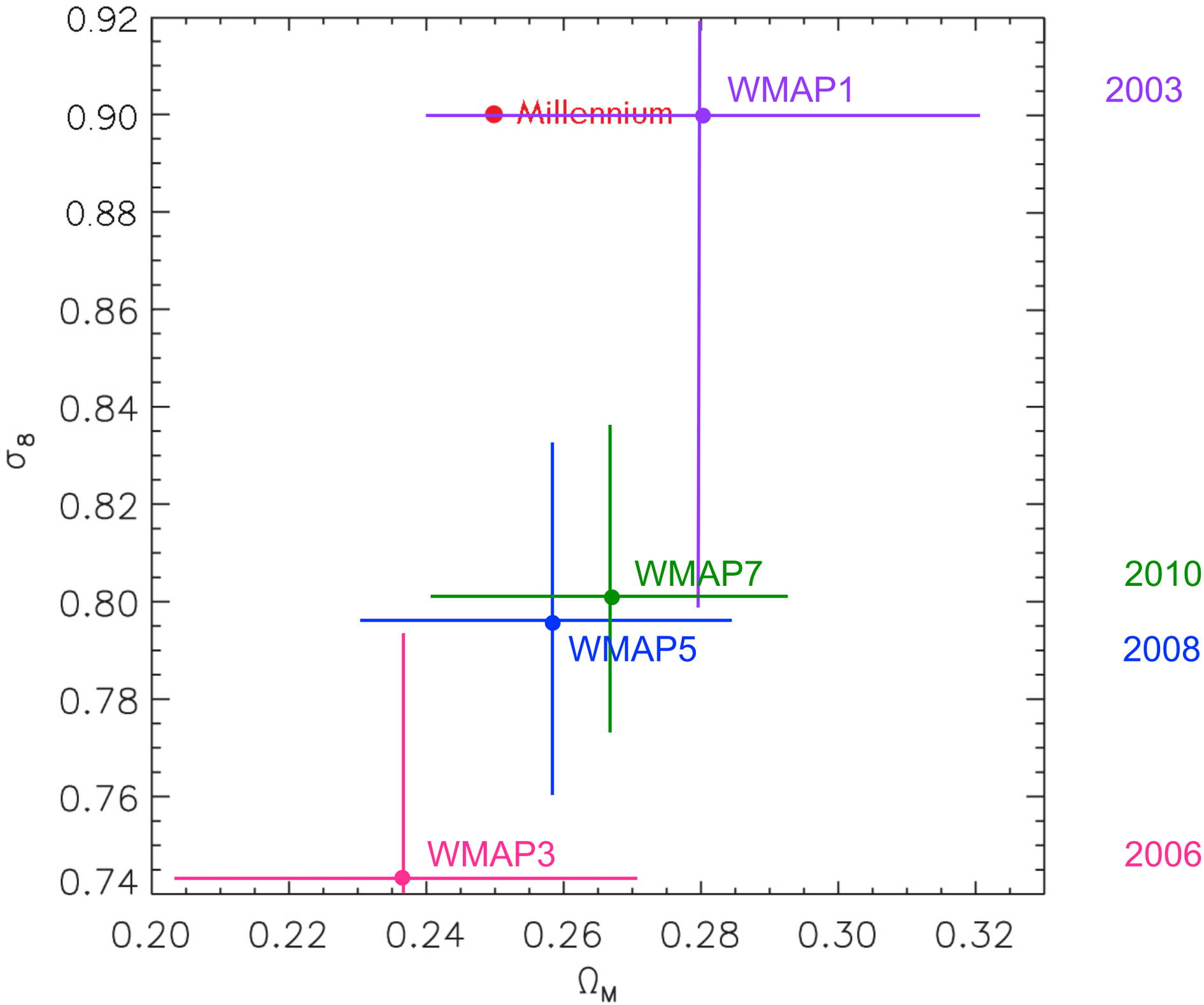

WMAP+SN+Clusters Determination of σ_8 and Ω_M

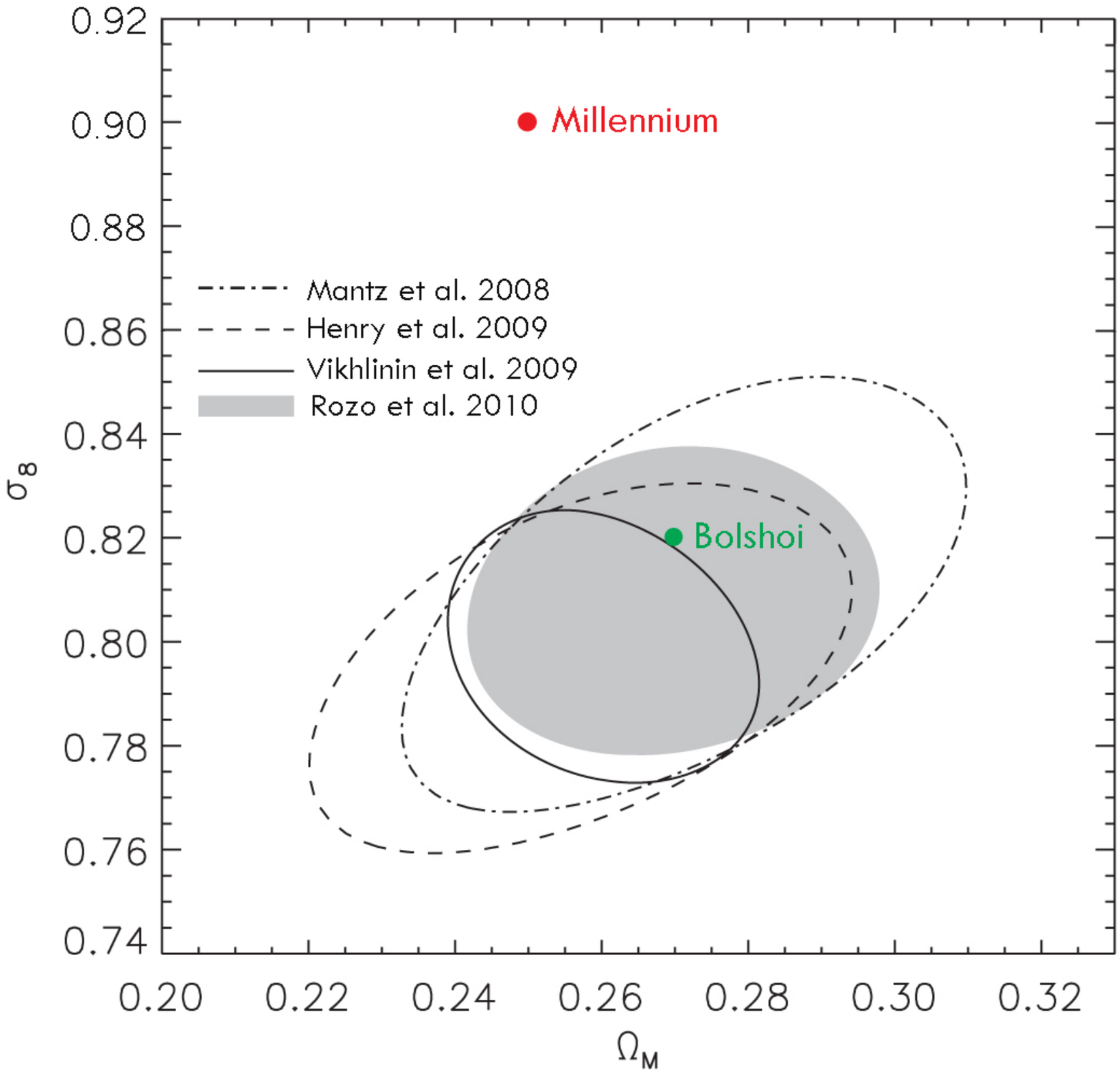

WMAP+SN+Clusters Determination of σ_8 and Ω_M

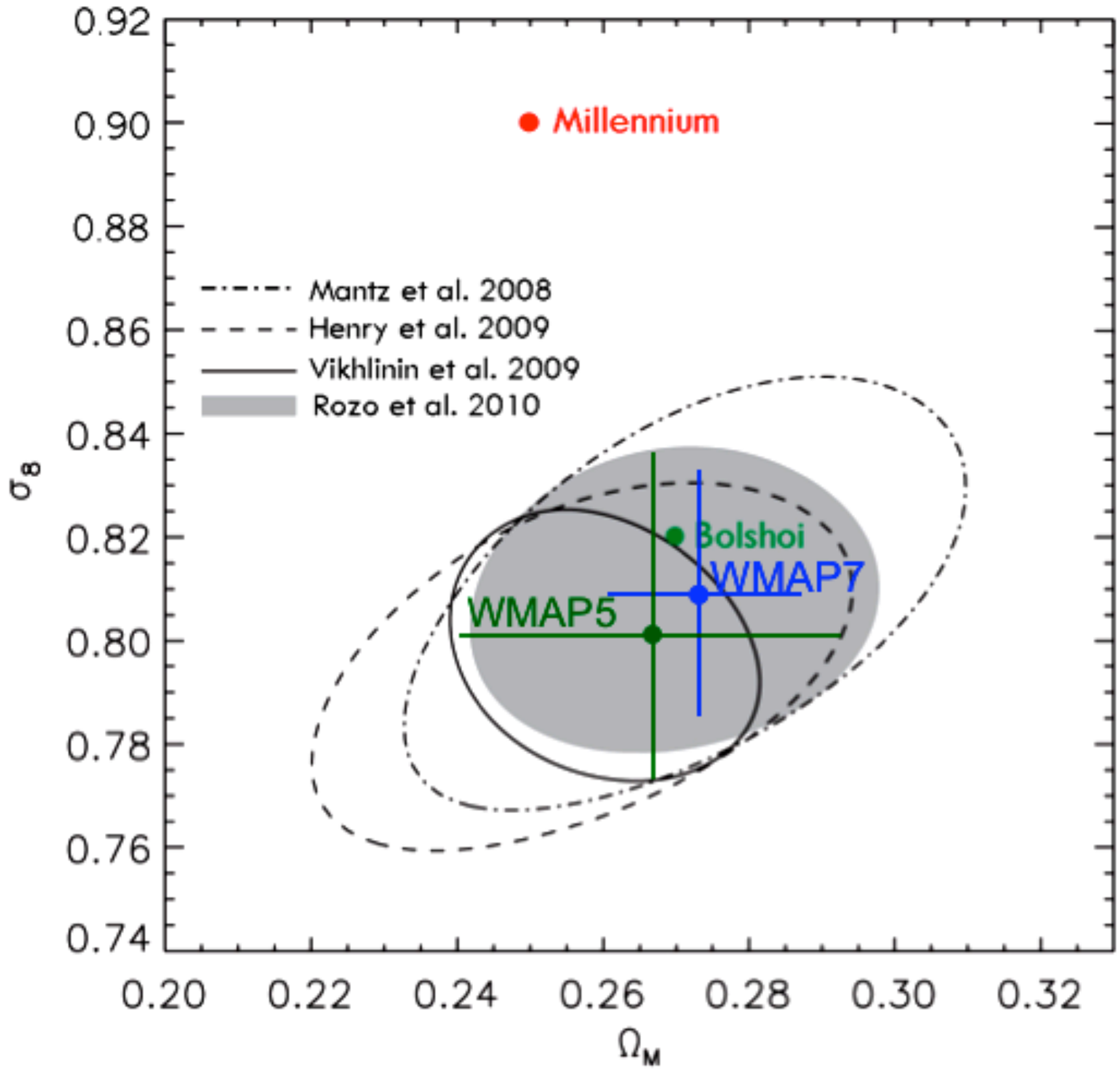

The Bolshoi simulation

ART code

250Mpc/h Box
LCDM

σ_8 = 0.82
h = 0.70

8G particles
1kpc/h force resolution
1e8 Msun/h mass res

dynamical range 262,000
time-steps = 400,000

NASA AMES
supercomputing center
Pleiades computer
13824 cores
12TB RAM
75TB disk storage
6M cpu hrs
18 days wall-clock time

Cosmological parameters are consistent with the latest observations

Force and Mass Resolution are nearly an order of magnitude better than Millennium-I

Force resolution is the same as Millennium-II, in a volume 16x larger

Halo finding is complete to $V_{circ} > 50$ km/s, using both BDM and ROCKSTAR halo finders

Bolshoi and MultiDark halo catalogs were released in September 2011 at Astro Inst Potsdam; Merger Trees will soon be available

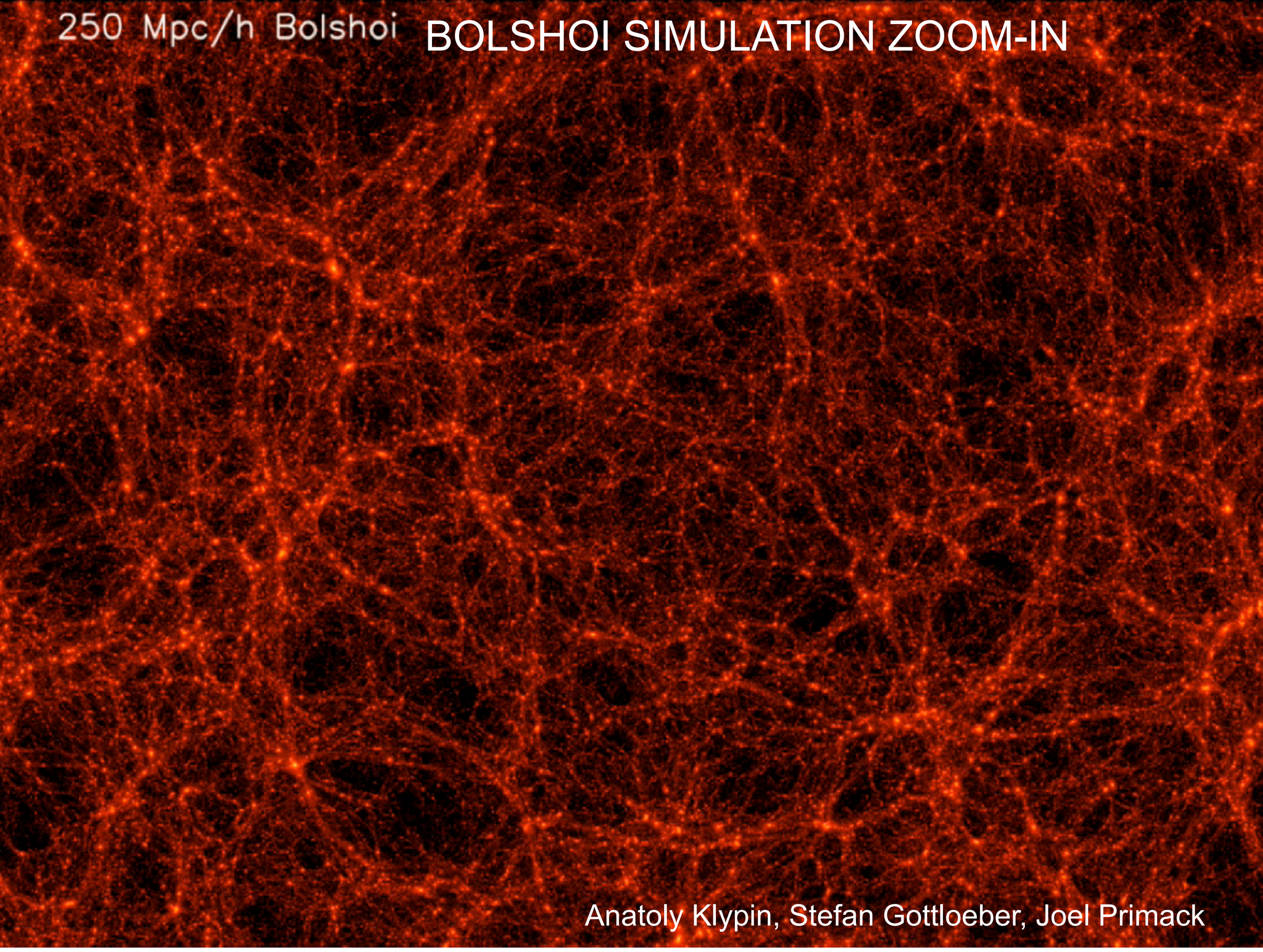
250 Mpc/h Bolshoi
BOLSHOI SIMULATION ZOOM-IN
Anatoly Klypin, Stefan Gottloeber, Joel Primack

Halos and galaxies: results from the Bolshoi simulation

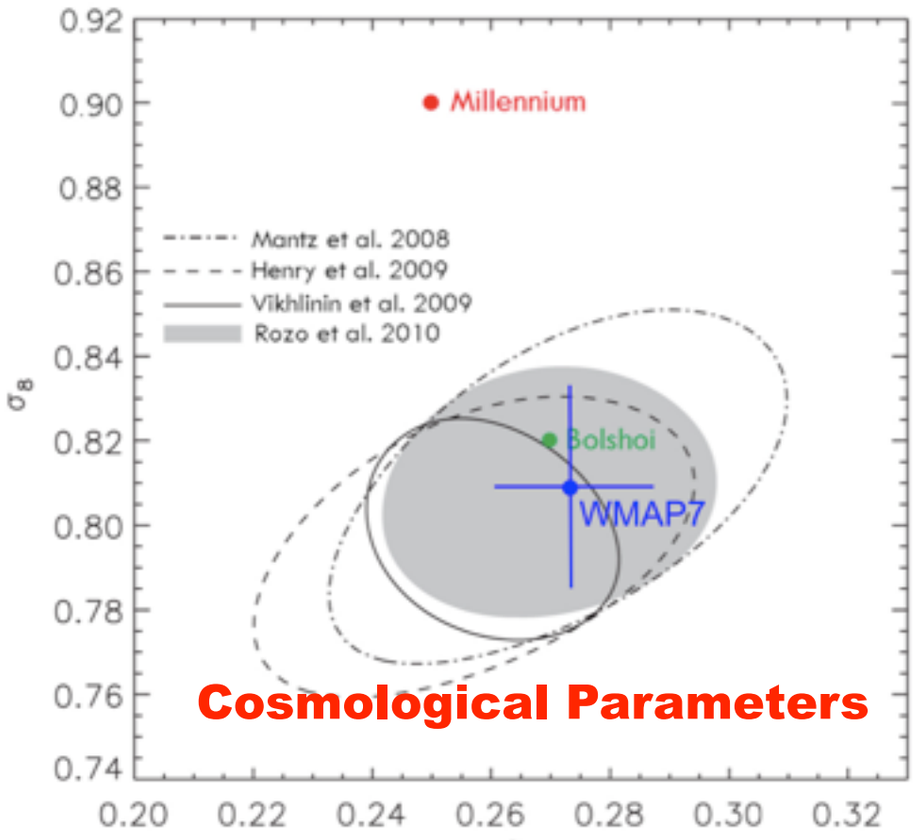

Cosmological Parameters

The Millennium Run (Springel+05) was a landmark simulation, and it has been the basis for ~300 papers. However, it and the new Millennium-II simulations were run using WMAP1 (2003) parameters, and the Millennium-I resolution was inadequate to see many subhalos. The new Bolshoi simulation (Klypin, Trujillo & Primack 2010) used the WMAP5 parameters (consistent with WMAP7) and has nearly an order of magnitude better mass and force resolution than Millennium-I. We have now found halos in all 180 stored timesteps, and we have complete merger trees based on Bolshoi.

Klypin, Trujillo-Gomez, & Primack, arXiv:1002.3660 ApJ in press

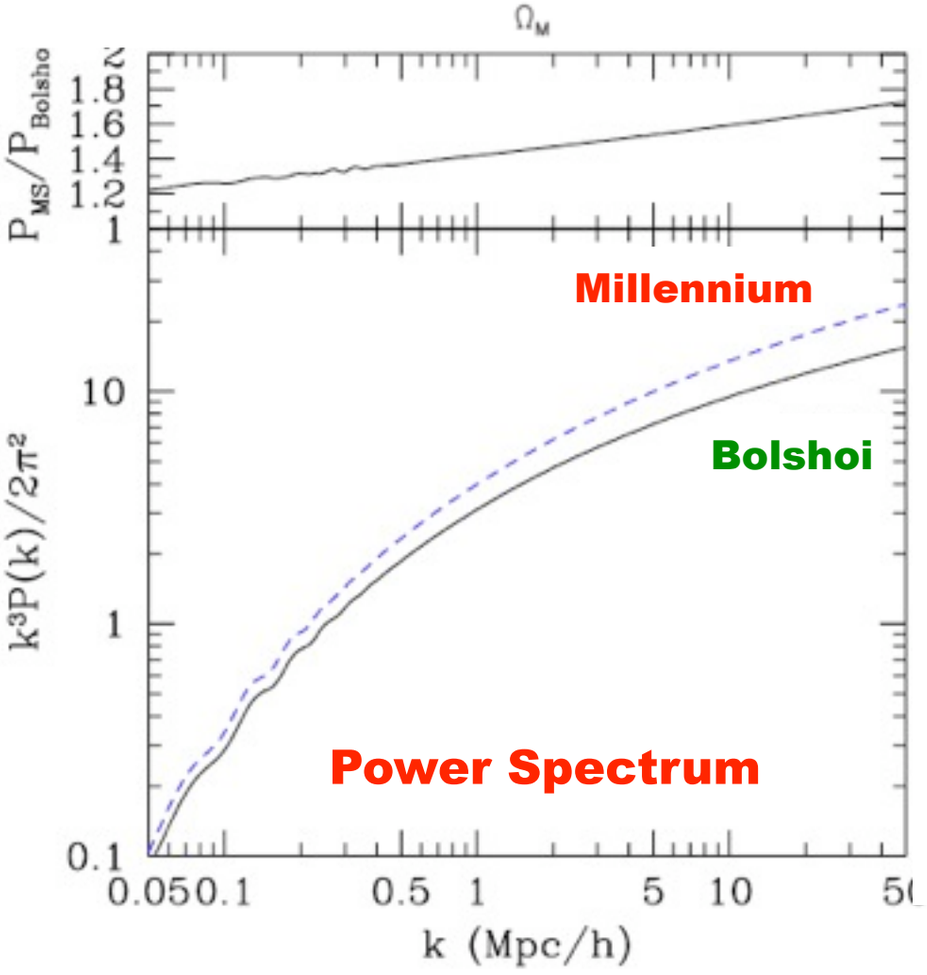

Power Spectrum

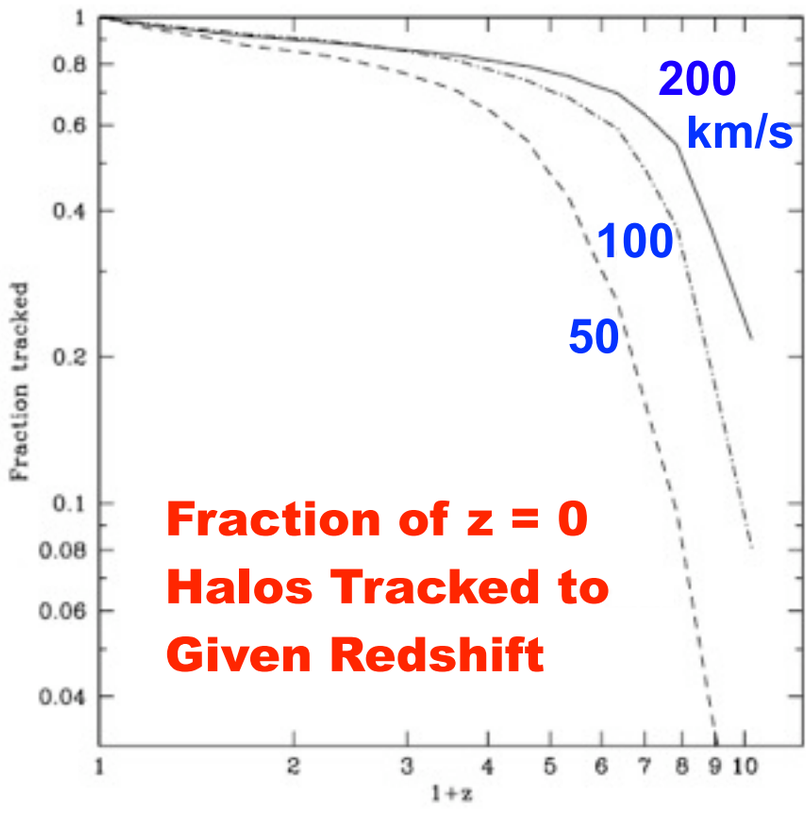

Fraction of z = 0 Halos Tracked to Given Redshift

Subhalos follow the dark matter distribution

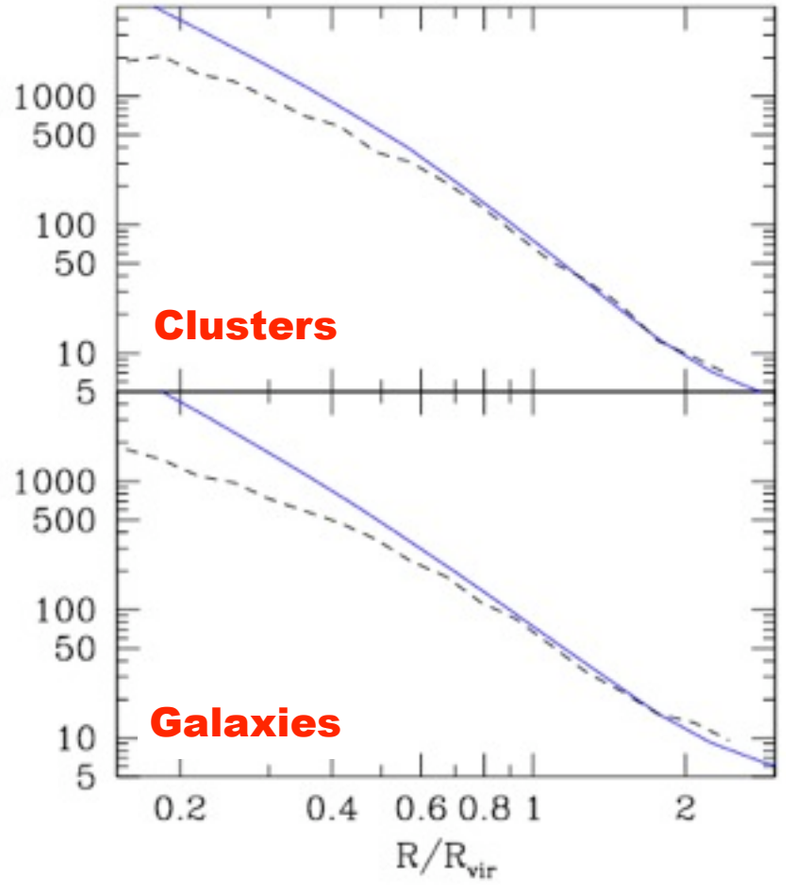

Aquarius Simulation

Milky Way
100,000 Light Years

Milky Way Dark Matter Halo
1,500,000 Light Years

Bolshoi Cosmological Simulation

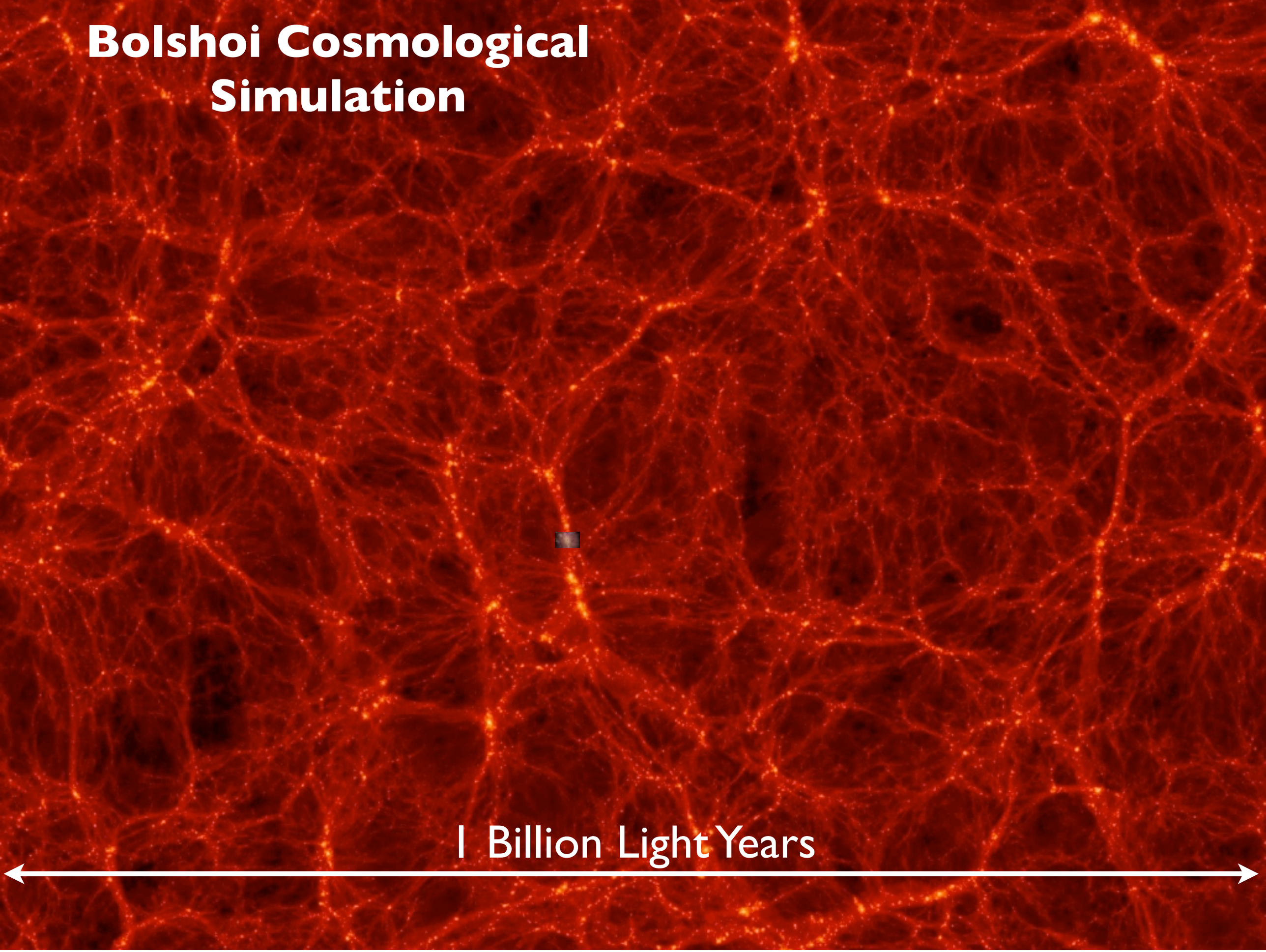

Bolshoi Cosmological Simulation

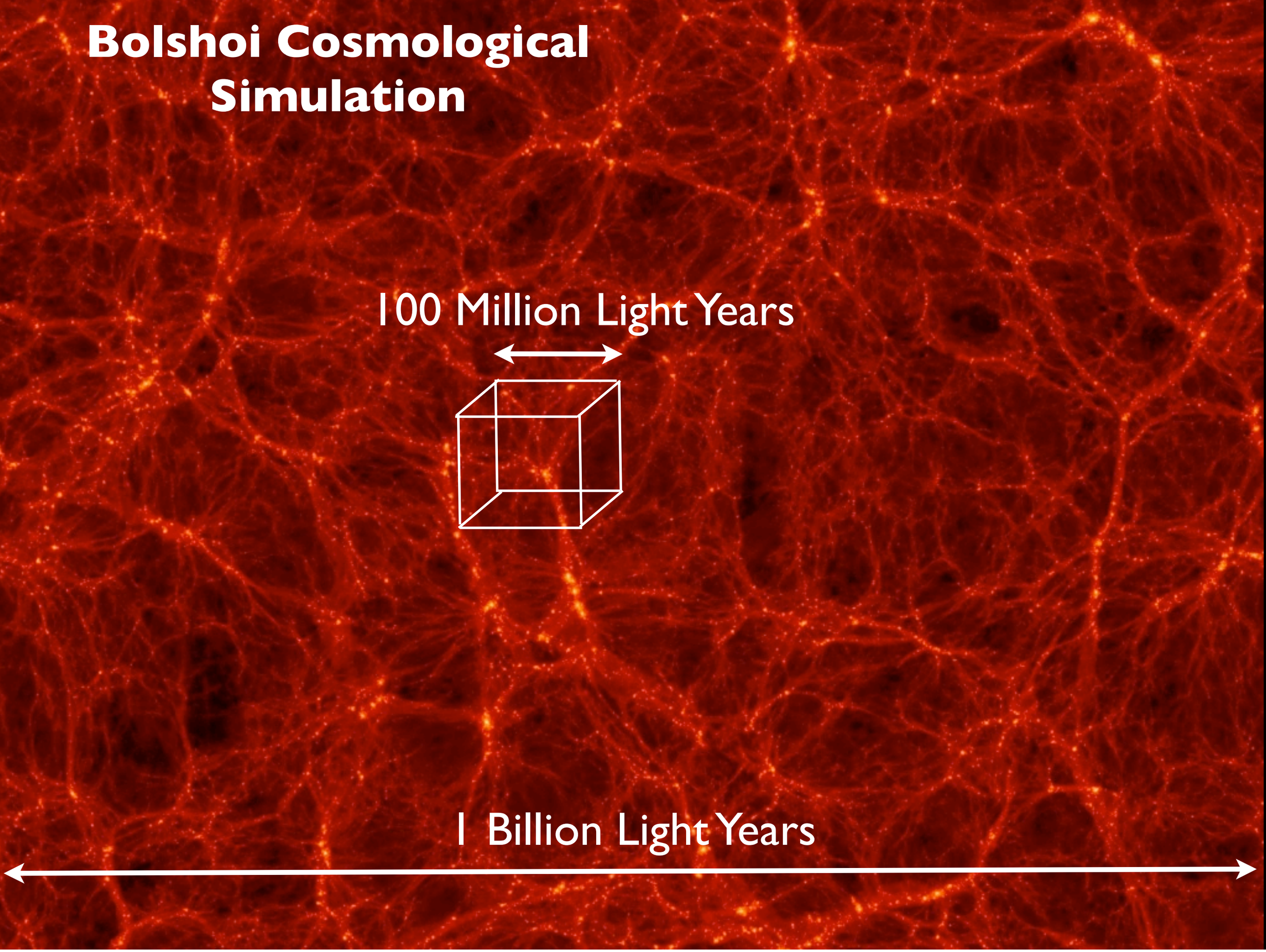

BOLSHOI SIMULATION FLY-THROUGH

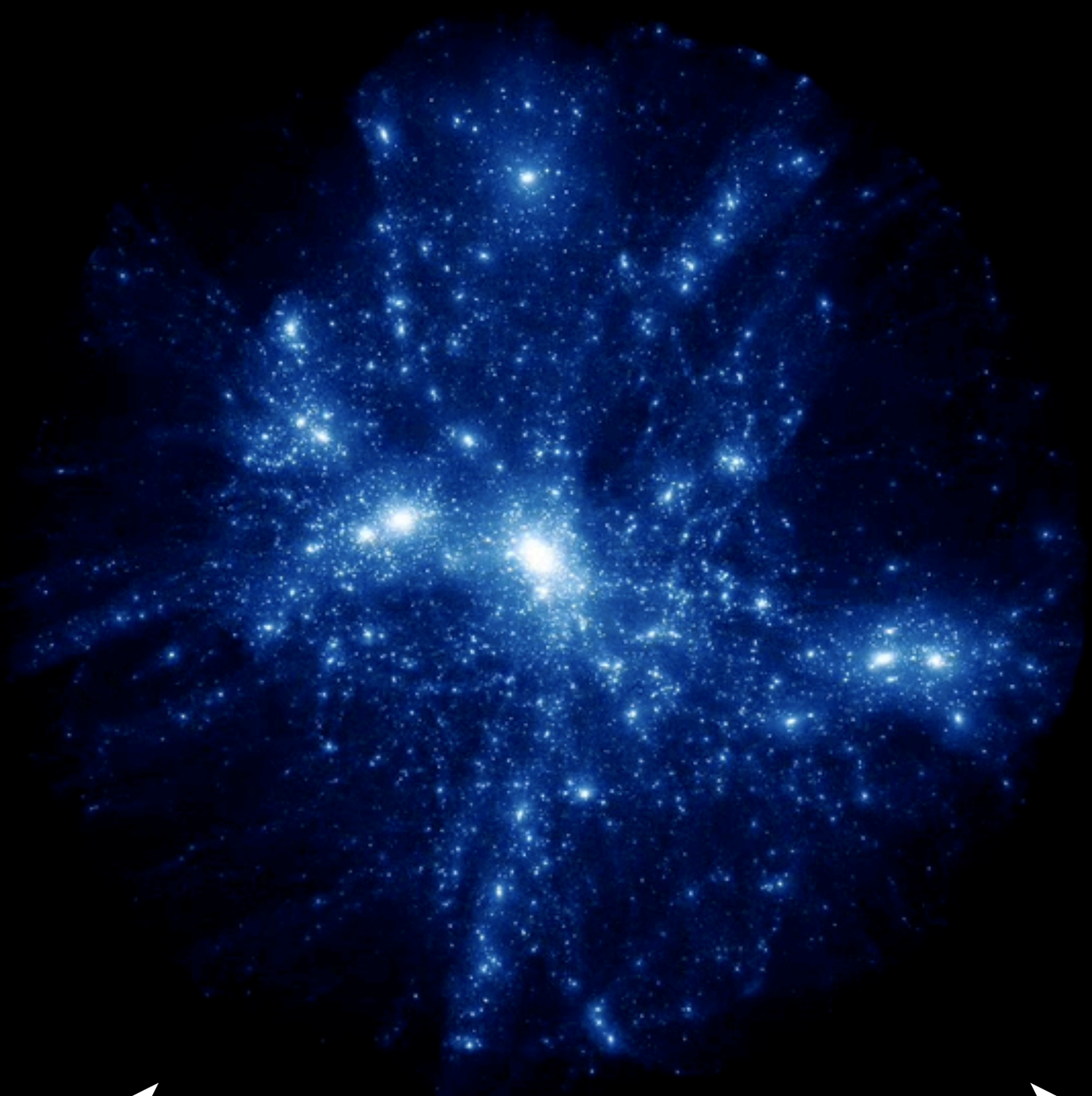

$<10^{-3}$ of the Bolshoi Simulation Volume

100 million light years

Bjork "Dark Matter"

Biophilia